

COMPARATIVE STUDIES OF FUNGAL DIMORPHISM IN DIKARYA

by

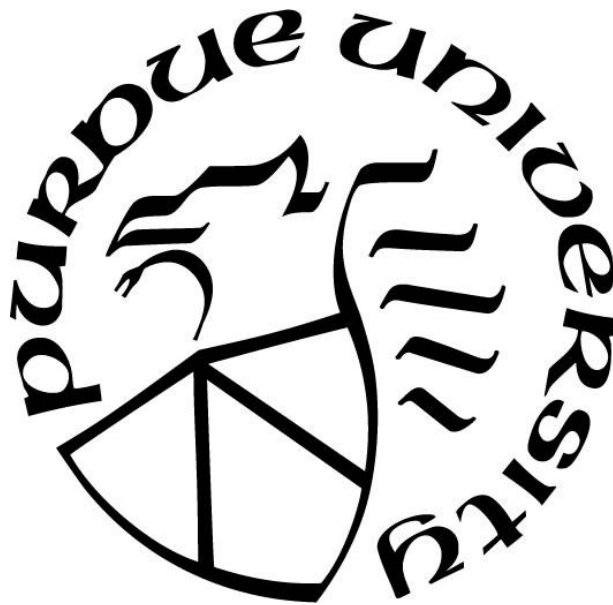
Teeratas Kijpornyongpan

A Dissertation

Submitted to the Faculty of Purdue University

In Partial Fulfillment of the Requirements for the degree of

Doctor of Philosophy



Department of Botany & Plant Pathology

West Lafayette, Indiana

December 2019

**THE PURDUE UNIVERSITY GRADUATE SCHOOL
STATEMENT OF COMMITTEE APPROVAL**

Dr. M. Catherine Aime, Chair

Department of Botany and Plant Pathology

Dr. Stephen B. Goodwin

Department of Botany and Plant Pathology

Dr. Jo Ann Banks

Department of Botany and Plant Pathology

Dr. Michael R. Gribskov

Department of Biological Sciences

Approved by:

Dr. Christopher J. Staiger

Head of the Graduate Program

For anybody who appreciates the beauty of fungi

ACKNOWLEDGMENTS

First and foremost, I would like to express my gratitude to my advisor Dr. Cathie Aime. I feel thankful that she accepted me as a graduate student six years ago, when I had no idea how to conduct research in fungi. She started training me from the beginning and allowed me to explore diverse areas in Fungal Biology. Once I finished my M.S. degree in 2015, she did not hesitate to continue supporting me as a Ph.D. advisor. Although there are several times of academic and financial difficulties throughout my graduate program, she never leaves me behind and always stands by me. Every experience obtained from her has made me become a good researcher up until now.

Dr. Michael Gribskov is another person who has provided substantial guidance for my research projects. I arrived at Purdue in 2013 with a zero background in Computational Biology and Bioinformatics. I have gained lots of knowledge and hands-on experiences from courses I took with him. Being a very busy professor, it is challenging to get in touch with him. However, once meeting with him, he is always helpful and gives useful advices that contribute to my research ideas. Dr. Gribskov is also a wise and enchanting person to have a discussion on life philosophy.

Dr. Jody Banks and Dr. Stephen Goodwin are the other two lovely committee members. My conversation with each of them is usually filled with energy and joy. Both give me not only academic suggestions, but also suggestions for my professional career and personal life. In addition, a few more people on campus are supportive when I am in need: Dr. Gordon McNickle from Department of Botany and Plant Pathology, Dr. Pete Pascuzzi from Purdue Libraries and Dr. Nadia Atallah Lanman from Purdue University Center for Cancer Research. These people are willing to advise me on data analyses, as well as provide moral supports to make me feel confident on what I am doing. I also acknowledge Dr. Phillip SanMiguel and all staff from the Purdue Genomics Core Facility for assistance on preparing samples and post-sequencing analyses for transcriptomic studies.

I would like to thank all 'Aime lab' members for all supports and encouragements throughout the years I have been in the lab. Special thanks to all former lab managers—John F. Klimek, Elena

Karlsen-Ayala and Dr. Rachel A. Koch—to make sure everything in the lab, including my requests, runs smoothly. Stories shared with the lab are invaluable for me. I acknowledge friends and staff in the Botany and Plant Pathology department for every bit of help and fun you have for me. My compatriots are another big part of my life here at Purdue. These Thai people in particular generously provide significant mental and spiritual supports for me—Dr. Nutwadee Chintakovid, Dr. Jiraphan Junjorn, Dr. Nathee Athigakunagorn, Dr. Amnat Eamvijarn, Dr. Matthanawee Sangkao, Dr. Atsadang Boonmee, Dr. Krittikarn Chanpaisaeng, Supattra Singnisai, Sariya Udayachalerm and Nitjaree Maneerat. I want to thank Purdue University Thai Student Association (PUTSA) for a great community in West Lafayette that has fulfilled my life outside the lab throughout the years. Many long-term Thai folks across different regions around the world also give me a big help every time I need.

Without all financial supports, I would not have had a chance to study at this prestigious institution. I would like to express my deep gratitude to the past King Bhumibol Adulyadej Rama IX, the founder of the Anandamahidol Foundation. The foundation scholarship serves as my primary funding source for five years. I also thank the previous department head Dr. Peter Goldsbrough for offering a financial supplement in addition to my scholarship. My last semester at Purdue was supported by the Bilsland Dissertation Fellowship from the Purdue Graduate School. I acknowledge the Mycological Society of America for several grants I received to conduct my research, as well as to present my work in conferences. Other sources of travel funding were from the departmental travel award, the departmental graduate student organization and the Purdue University Graduate Student Government.

Last, but not least, I would like to thank my family, especially my mother, my aunt and my brothers, for their continuous supports for many years. Although they are curious why it takes me so long to pursue the degree, I always feel their love and care, as well as everlasting long-distance supports. They are major sources of energy to keep me persevering for my goal. Finally, I truly appreciate everyone I have known in the past up until now. They all play a role in shaping up myself to be who I am today.

TABLE OF CONTENTS

LIST OF TABLES	9
LIST OF FIGURES	10
ABSTRACT	11
CHAPTER 1. LITERATURE REVIEW	13
1.1 Fungal growth and development.....	13
1.1.1 Filamentous/hyphal growth	13
1.1.2 Yeast growth.....	16
1.2 Dimorphic fungi.....	19
1.3 Smut fungi (Ustilaginomycotina)	22
1.4 Mechanisms for fungal dimorphism	23
1.4.1 Physiological factors that trigger dimorphic transition	24
1.4.2 Signal transduction mechanisms.....	25
1.4.2.1 cAMP-PKA pathway	29
1.4.2.2 MAPK pathway	30
1.4.2.3 Alternative pathways	32
1.4.2.4 Upstream and downstream molecular players.....	33
1.5 Comparative studies.....	35
1.6 Thesis statement and objectives.....	36
CHAPTER 2. EFFECTS OF ENVIRONMENTAL FACTORS ON FUNGAL DIMORPHISM OF USTILAGINOMYCOTINA.....	38
2.1 Introduction.....	38
2.2 Hypotheses.....	39
2.3 Methods.....	39
2.3.1 Taxon sampling	39
2.3.2 Culturing experiments	40
2.3.3 Determination of growth forms and statistical analyses.....	41
2.4 Results.....	42
2.4.1 Pilot experiments on physiological studies of <i>U. maydis</i>	42

2.4.2	Effects of different carbon sources on fungal dimorphism of several Ustilaginomycotina species.....	42
2.4.3	Effects of temperature on fungal dimorphism of several Ustilaginomycotina species	46
2.5	Discussion.....	47
CHAPTER 3. COMPARATIVE TRANSCRIPTOMICS OF YEAST AND FILAMENTOUS GROWTH FORMS ACROSS FOUR DIMORPHIC PLANT-ASSOCIATED FUNGI		51
3.1	Introduction.....	51
3.2	Hypotheses.....	52
3.3	Materials and Methods.....	53
3.3.1	Taxon sampling	53
3.3.2	Orthology assessment and functional annotation	53
3.3.3	Experimental design, RNA isolation and data collection.....	54
3.3.4	Differential gene expression analyses	55
3.3.5	Comparative transcriptomics and functional analyses	55
3.4	Results.....	57
3.4.1	Orthology assessment	57
3.4.2	Dimorphic transition under lipid condition	57
3.4.3	Transcriptomic analyses of individual species	59
3.4.4	Comparative transcriptomics.....	61
3.4.5	Functional analyses.....	67
3.5	Discussion.....	73
CHAPTER 4. INVESTIGATING AN ASSOCIATION BETWEEN GENOMIC PROFILES AND GROWTH FORMS OF FUNGI IN DIKARYA		79
4.1	Introduction.....	79
4.2	Hypotheses.....	80
4.3	Materials and Methods.....	80
4.3.1	Data collection	80
4.3.2	Analytical platform.....	82
4.3.3	Multivariate analyses of genome statistics	82

4.3.4 Multivariate analyses of gene composition	82
4.4 Results.....	83
4.5 Discussion.....	94
CHAPTER 5. CONCLUSION AND FUTURE DIRECTIONS.....	97
APPENDIX A. SUPPLEMENTARY FIGURES AND TABLES	100
APPENDIX B. LIST OF SUPPLEMENTARY MATERIALS	121
REFERENCES	122
VITA.....	159
PUBLICATIONS.....	160

LIST OF TABLES

Table 1.1 Examples of dimorphic fungi, life strategies, and environmental cues for morphological transition.....	21
Table 1.2 A list of known fungal dimorphism genes from the <i>U. maydis</i> literature	27
Table 3.1 Summary statistics of transcriptomic sequencing and read count transformation.....	59
Table 3.2 Summarized numbers of differentially expressed genes in each species	60
Table 3.3 Enrichment analyses of KOG classifications for differentially expressed genes in <i>M. miltonrushii</i> and <i>T. washingtonensis</i>	64
Table 3.4 Enrichment analyses of KOG classifications for differentially expressed genes among Ustilaginomycotina.	65
Table 3.5 Enrichment analyses of KOG classifications for differentially expressed genes among Dikarya.	66
Table 3.6 List of concordantly differentially expressed genes in all studied species	68
Table 3.7 List of some interesting discordant genes in four species.	70
Table 3.8 Gene expression patterns of known dimorphism genes from <i>U. maydis</i> literature and respective orthologs.....	72
Table 4.1 Numbers of genomes included in this study	81
Table 4.2 Indicator genes, identified by fuNOG IDs, that are associated with types of growth form in both Ascomycota and Basidiomycota.	88
Table 4.3 Indicator genes, identified by fuNOG IDs, that are associated with types of growth form in both Ascomycota and Basidiomycota.	91

LIST OF FIGURES

Figure 1.1 The Fungal Tree of Life depicting yeast-like lineages.....	17
Figure 1.2 Overview of the regulatory network for fungal dimorphism in <i>U. maydis</i>	26
Figure 2.1. The pilot experiments on fungal dimorphism of <i>U. maydis</i>	43
Figure 2.2. Effects of carbon source and temperature on fungal dimorphism of Ustilaginomycotina	44
Figure 2.3. Quantification of growth forms of Ustilaginomycotina under types of carbon source and high temperature.	45
Figure 2.4. The effect of natural lipids on growth forms of some Ustilaginomycotina species. ..	46
Figure 2.5 Growth forms of <i>Moesziomyces aphidis</i> under high temperature.	47
Figure 3.1 A designed bioinformatic pipeline for multispecies transcriptomic analyses.	57
Figure 3.2 Dimorphic transition of <i>Meira miltonrushii</i> and <i>Tilletiopsis washingtonensis</i>	58
Figure 3.3 Principal component analyses (PCA) of gene expression data.	60
Figure 3.4 MVA plots for differential gene expression analyses of four studied species.	61
Figure 3.5 Summarized numbers of differentially expressed genes from comparative transcriptomics.....	63
Figure 4.1 NMDS plots of genome statistics of 190 fungal genomes.	84
Figure 4.2 Logistic regression analyses of predictive variables for types of growth form.....	86
Figure 4.3 Analyses of indicator genes derived from six functional classes.	89
Figure 4.4 Analyses of indicator genes derived from multicellularity-associated genes recently published in a previous study.....	92
Figure 4.5 Presence-absence matrices of indicator genes shared in both Ascomycota and Basidiomycota datasets.	93

ABSTRACT

Author: Kijpornyongpan, Teeratas. PhD
Institution: Purdue University
Degree Received: December 2019
Title: Comparative Studies of Fungal Dimorphism in Dikarya
Committee Chair: Dr. M. Catherine Aime

Fungi display diverse growth forms. Some grow as unicellular yeasts, some grow as multicellular hyphae, while others switch between these two growth forms, i.e., the dimorphic fungi. Dimorphism is found in many pathogenic fungi, and it is thought to be a strategy to maximize their fitness during different stages of life cycles. The corn smut fungus *Ustilago maydis* serves as a renowned model organism for studying fungal dimorphism and its role in pathogenesis. However, knowledge only from the model species may not be expanded to other species unless multispecies studies have been demonstrated. In this dissertation, I performed comparative analyses to examine if knowledge from *U. maydis* is translational to other dimorphic fungi. First, a physiological study was conducted to find what can serve as a common signal for dimorphic transition of several Ustilaginomycotina species. I found that the lipid serves as a potential common cue for yeast-to-hyphal transition in most dimorphic species, while alternate types of energy-source carbohydrate do not affect fungal dimorphism. In addition, pectin and high temperature can also trigger filamentous growth in some Ustilaginomycotina species. Second, I performed comparative transcriptomics to determine if a mechanism for yeast-to-hyphal dimorphic transition is conserved across multiple dimorphic species. Three species of Ustilaginomycotina (*U. maydis*, *Tilletiopsis washingtonensis* and *Meira miltonrushii*) plus one species from Ascomycota (*Ophiostoma novo-ulmi*) were included in the analyses. I found that the similarity of transcriptomic alteration is not dependent on phylogenetic relatedness. Genes in amino acid transport and metabolism, energy production and conversion and cytoskeleton are commonly altered during the dimorphic transition of all studied species. Moreover, I discovered several core genes which can play a conserved role in transducing signals for the dimorphic transition. Finally, I performed comparative analyses of 190 fungal genomes to determine genomic properties that are associated with types of fungal growth form. I found that small genome size is a characteristic for yeast-like fungi. Few indicator genes, such as genes encoding proteins in the NADPH oxidase complex and cytoskeletons, which

are predominantly lost in yeast-like fungi in both Ascomycota and Basidiomycota. However, many other genes are associated with types of growth form in a lineage-specific manner. Findings from this dissertation will serve as fundamentals for future research in fungal cell biology, especially in fungal dimorphism. Additionally, results from this study suggest cautions when extrapolating results from model species onto non-model species.

CHAPTER 1. LITERATURE REVIEW

1.1 Fungal growth and development

Fungi is one of the most diverse eukaryotic kingdoms with a recently estimated species number of 5.1 million (1). Collectively the fungi utilize a variety of habitats, nutritional modes and strategies for survival and reproduction. In terms of growth and development, fungal growth varies from basic to very complex structures. Many fungi produce visible spore-bearing structures called fruiting bodies, which can be macroscopic to hundreds of thousands of cubic centimeters in size, such as produced by *Phellinus ellipsoideus* (2). One group, rust fungi in Pucciniomycotina (3), evolves five types of spores throughout their life cycle. Others produce vegetative structures that extend for kilometers in soils. An example is *Armillaria bulbosa*, which serves as the largest individual on the planet with a vegetative structure covering over 15 hectares (4). On the other hand, many fungi lack structural complexity. Some of these appear single cells and have not been observed to produce spores for reproduction. Some others, like microsporidians, have single cells with reduced forms of mitochondria and membranous organelles, and are obligately parasitic inside host cells (5). Despite this variation, the majority of members of the fungal kingdom display one of two common types of growth: filamentous growth and yeast growth.

1.1.1 Filamentous/hyphal growth

Most known fungi have an ability to grow as a tube-like and filamentous structure termed a hypha. The hypha contains multiple cells that may or may not have cross walls (termed 'septa') as a border between them. Hyphae can be branched to increase reticulation and growth direction of a colony. The hypha serves as a basic unit for complex multicellular structures such as a vegetative mycelium covering on a substrate, a dormant structure like sclerotia, an asexual spore-bearing structure or even a fruiting body that bears sexual spores (6). These developmental processes require many physio-chemical interactions between a fungus and an environment, as well as intercellular communications among cells in the hypha.

A hyphal tip is an active area that has indeterminate apical growth. This area contains numerous machineries for building new cell wall and plasma membrane. One of the most conspicuous structures observed from microscopy is a dense aggregation of vesicular bodies called the

Spitzenkörper. It was first discovered in the mushroom-forming fungus *Coprinus* (7), and later found in many fungi having polarized growth such as *Neurospora crassa*, *Aspergillus nidulans*, *Magnaporthe oryzae*, *Colletotrichum graminicola*, *Rhizoctonia solani* and *Ustilago maydis* (8,9). In the model filamentous fungus *N. crassa*, the Spitzenkörper comprises two types of vesicle based on size. Macrovesicles contain glucan synthases, while microvesicles (also known as chitosomes) contain chitin synthases—these two enzymes produce major macromolecules for fungal cell walls (10). Other components near the hyphal tip include ribosomes and mitochondria, wires of actin filaments and microtubules, and endomembranous structures like endosomes, Golgi body, tubular endoplasmic reticulum and vacuoles.

Establishment of polarity and vesicular transport are two major processes during hyphal extension. First, there must be positional markers that are consistently retained at the hyphal tip to indicate the direction of the polarized growth. These markers, bound to sterol-rich lipid rafts at hyphal tip membranes, are crucial for recruitment of other molecules to establish a polarity. One of them includes Cdc42 GTPase, which subsequently recruits formin and other proteins for nucleating actin filaments (11–13). A dense mass of actin filaments at the hyphal tip (termed actin cables) serves as a track for accumulation of secretory vesicles at the Spitzenkörper, as well as for exocytosis of the vesicles from the Spitzenkörper (14). In addition to the actin cables, the actin filaments are formed at the subapical region as actin patches. This actin structure, accompanied by other proteins such as fimbrin, coronin and Arp2/3 complex (15,16), is involved in endocytosis of the subapical region membrane. Endocytosis is proposed to be important for maintaining polarized growth in a few ways—to retract plasma membranes from excess exocytosis, to recycle positional markers and to degrade undesired membrane proteins (6,17).

While the actin filaments play a critical role in vesicular transport at the hyphal tip, the microtubule serves as a railroad for long-distance transport. In addition to cell wall and membrane biogenesis machineries, vesicles transported through microtubules may be coupled with other cargos. Examples are endosome-mediated mRNA trafficking in *U. maydis* and endosome-coupled peroxisome transport in *A. nidulans* (18,19). Growing microtubules also help deliver positional markers of *A. nidulans* and *Schizosaccharomyces pombe* to the hyphal tip (20,21). Microtubules can be formed near a nuclear envelope, at a septum or even the hyphal tip, depending on where a

multiprotein complex called the microtubule-organizing center (MTOC) is assembled (22,23). Finally, vesicular transport requires many motor proteins that act as connectors between vesicles and cytoskeletons, both microtubules and actin filaments (24).

In addition to vesicles and cytoskeletons, other components can play a role in hyphal growth. However, this area is much less studied. Veses et al. (25) summarized how a vacuole contributes to hyphal growth. For instance, *U. maydis* forms highly vacuolated compartments at a distal region instead of undergoing mitotic cell division (26). This is to maintain filamentous growth under limited resources as doubling of nucleus and cytoplasm is more costly than vacuole biogenesis. In *N. crassa*, the vacuole serves as a reservoir for chitin synthases before they are delivered to the Spitzenkörper, suggesting an alternative route of transporting secreted proteins (27). Mitochondria are also found near the hyphal tip, but their role in hyphal growth is poorly understood. Levina and Lew (2006) demonstrated that tip-localized mitochondria in *N. crassa* do not produce ATP through oxidative phosphorylation, but they sequester calcium ions. This maintained high Ca^{2+} concentration may contribute to constant hyphal growth as Ca^{2+} is involved in actin assembly and exocytosis (29,30). Finally, although the importance of tip-localized ribosomes is not empirically tested, an evidence of long-distance mRNA transport in *U. maydis* suggests their role in local translation of proteins required for hyphal formation (18).

As the hypha grows longer, a new compartment is created to make a new daughter cell that remains active for apical growth, while the penultimate cell becomes the intact mother cell. Septum formation is a final step to complete cell division in most filamentous fungi. It requires the assembly of a contractile actomyosin ring at a cytoplasmic division site (14). The contractile ring causes membrane invagination, which occurs simultaneously with chitinous cell wall synthesis to create a septum. GTP-binding family proteins called septins are also assembled, through Cdc42 signaling in *S. cerevisiae*, as a ring at a site where the septum will be formed (31). Several studies have shown that the septins do not only play a role in septum formation, but also establish cell polarity and morphogenesis in several filamentous fungi (32–36). It is still unclear how septins are associated with machineries for septum formation and polarized growth. However, a current model is that septin assembly at a plasma membrane serves as a physical barrier for membrane diffusion, and that generates membrane asymmetry that leads to polarity establishment (31).

Many yeast-like fungi can display filamentous growth under certain conditions. Some of them, like *Candida albicans*, produce true hyphae that are morphologically similar to filamentous fungi (37). However, many others have filamentous growth as a chain of yeast cells, termed pseudohypha (38). Pseudohyphae differ from true hyphae by a few properties. First, pseudohyphae consist of multiple yeast cells that have incompletely separated. For budding yeasts, pseudohyphal growth is easy to recognize by a constriction at the septum. In addition, unlike true hyphae, pseudohyphae are not slender and tube-like. Lateral walls of each pseudohyphal cell are convex or curved, resembling the morphology of a solitary yeast cell. Finally, while hyphal growth occurs by continual polarized growth at the hyphal tip, pseudohyphal growth is a consequence from an oscillation of polarized growth (to form a bud site) and isotropic growth (to expand a yeast cell) (39). Despite these differences, pseudohyphae are still counted as filamentous growth by three points—each cell in a filament is more elongated, the direction of growth is polarized and cell-to-cell adhesion is enhanced (40). Moreover, many molecular machineries that control pseudohyphal growth in the budding yeast *S. cerevisiae* turn out to control hyphal growth in many filamentous fungi (40).

1.1.2 Yeast growth

Yeast is a collective term used to describe unicellular fungi that divide through budding or fission and do not enclose their sexual stages within a fruiting body (38). In other words, yeast can survive, grow and reproduce as a solitary cell. Traditionally, there are two major yeast groups belonging to Ascomycota: budding yeasts in Saccharomycotina and fission yeasts in Taphrinomycotina. Yeasts are also prevalent in certain lineages of Basidiomycota such as Tremellomycetes, Ustilaginomycotina and Pucciniomycotina (3,41,42). Other fungi may have a yeast-like strategy (i.e., they have at least one stage of their life cycles as a unicellular yeast). Exemplars are thermally dimorphic fungi in Eurotiomycetes (43). Figure 1.1 summarizes major lineages in the kingdom Fungi that harbor yeast-like species. The current hypothesis is that yeast-like growth has independently evolved in several lineages from ancestral filamentous fungi (44,45).

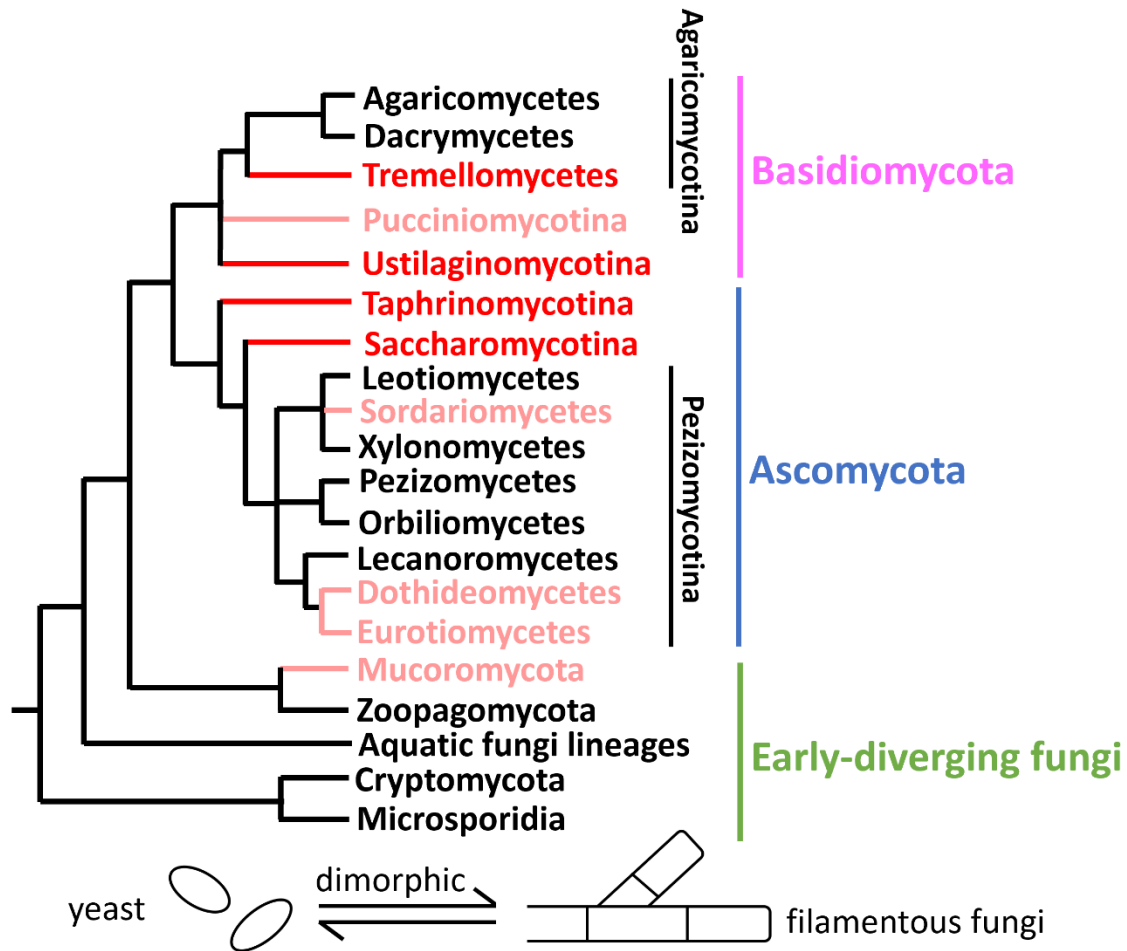


Figure 1.1 The Fungal Tree of Life depicting yeast-like lineages.

The tree is partially modified from a recent study (44). Note that yeast-like fungi refer to fungi having at least one stage of the life cycle as a unicellular yeast. The yeast-like fungi lineages are shown in red color. Pale red lineages have a majority of members as filamentous fungi, but a few members appear as yeast-like fungi.

There are several aspects that make yeast growth different from hyphal growth. In terms of cell wall composition, yeast cell walls have less chitin content than filamentous fungi (2-3% compared to 15% of cell wall dry weight). Also, there are different polysaccharide components between the cell walls of both (46). The second point is about growth direction. Yeasts do not have consistent polarized growth. Cells of the budding yeast *Saccharomyces cerevisiae* are mostly spherical, indicating that they have growth in every direction, termed as isotropic or symmetrical growth. Meanwhile, the fission yeast *Schizosaccharomyces pombe* has bipolar growth, making cells have a cylindrical shape. It has been shown that the localization of the polarity marker Cdc42 GTPase

determines yeast cell shapes—Cdc42 is oscillated between two opposite tips in *Schizosaccharomyces pombe* whilst being oscillated across different cell areas in *Saccharomyces cerevisiae* (47). This contrasts to filamentous fungi in which Cdc42 is constantly localized at a hyphal tip (6).

Cytokinesis is another aspect that differs between yeast and filamentous growth. After reaching a critical cell size, yeasts undergo cell division to produce new cells. They have a complete separation of cell wall and plasma membrane between two daughter cells, whereas many filamentous fungi have interconnected plasma membranes or at least have shared cross walls. In the budding yeast models *Saccharomyces cerevisiae* and *Candida albicans*, there are two stages of septum formation (37,48). A primary septum (aka. a ‘shared’ cross wall) is formed during actomyosin ring contraction. After plasma membranes of two daughter cells are completely separated, both cells build their own secondary septa. Finally, the primary septum is degraded by enzymes to separate daughter cells apart. This cytokinesis mechanism is also conserved in the fission yeast *Schizosaccharomyces pombe* (49), except that fission yields two equal-sized daughter cells while budding yields unequal daughter cells. While the septin ring indicates where to form the septum in fission yeasts and filamentous fungi, it indicates a site of bud formation in *Saccharomyces cerevisiae* (31,48). The budding yeast cell then has an asymmetrical growth towards the bud site prior to nuclear division and cytokinesis.

Although yeasts normally survive and reproduce as a single cell, they have some properties for multicellularity. Many of them can grow as a filamentous form (see below for ‘dimorphic fungi’). Moreover, recent studies have shown that *Saccharomyces cerevisiae* colonies can form two subpopulations based on their spatial locations. The upper layer consists of large cells with low respiration and metabolism under nutrient-limited condition, while the lower layer comprises smaller cells with active catabolism to transfer nutrients to the upper layer (50). Heterogeneous cell types are also found in more complex structures of *Saccharomyces cerevisiae* and *C. albicans* like biofilms and stalk-like colonies (51,52). Hence, these yeast species will continue serving as models to study cell differentiation, as well as how multicellularity is formed.

1.2 Dimorphic fungi

Fungal dimorphism is a phenomenon by which fungi can grow both as a unicellular yeast form and a multicellular filamentous form. Which growth form they display is determined by several factors such as stages in a life cycle, ploidy status, environmental cues and intercellular communication (53). Many yeast-like fungi that can have polarized hyphal growth are considered as dimorphic fungi. However, defining ‘dimorphic fungi’ is often a challenging task, especially for less widely known species. One major reason is a lack of adequate observation. Many mycologists describe species based on their primary growth form observed in nature or in axenic culture. However, as dimorphic fungi may switch to the other growth form only under certain conditions, they may be misidentified as either yeasts or filamentous fungi instead of dimorphic fungi. For example, *Moesziomyces aphidis* was originally described as a yeast species with the presence of elongated cells resembling pseudohyphae (54), but recent studies showed that it can grow as hyphae (55–57). Moreover, distinguishing between true hyphae and pseudohyphae is somewhat difficult unless their cytology is carefully investigated. Hence, an inclusive term ‘filamentous growth’ is often used to avoid any confusion. Finally, the problem comes from the term fluidity. Some researchers include any yeast-like fungi that can undergo filamentous growth as dimorphic fungi (58,59), some consider only yeast-like fungi that can form true hyphae (60), while some others do not provide a clear distinction (53). Moreover, recent literatures have erected the term ‘polymorphic fungi’ for any fungi that can grow as yeasts, pseudohyphae and true hyphae (53,60). In this dissertation, I use the term dimorphic fungi in an inclusive context.

Dimorphic fungi are predominantly found in Dikarya (a subkingdom including Ascomycota and Basidiomycota), although this phenomenon was originally described in the zygomycetes genus *Mucor* (61). Some examples are provided in Table 1.1. In Ascomycota, the most renowned group with high research interest is “thermally dimorphic fungi”—many of which are also known as “black fungi” or “black yeasts” (45). These fungi are typically found as pathogens on humans, and temperature serves as a stimulus for morphological transition (43). Despite this shared character, they are a polyphyletic group. The thermally dimorphic fungi can be found in Sordariomycetes, Eurotiomycetes and Dothideomycetes (Table 1.1). Another renowned dimorphic fungus is *Candida albicans* (Saccharomycotina, Ascomycota), which is an opportunistic human pathogen. For dimorphic plant pathogens, the corn smut fungus *Ustilago maydis* (Ustilaginomycotina,

Basidiomycota) serves as a primary model for research in the field. Other exemplars include *Taphrina deformans* (Taphrinomycotina, Ascomycota) causing peach leaf curl disease, *Ophiostoma ulmi* and *O. novo-ulmi* (Sordariomycetes, Ascomycota) causing Dutch elm disease and *Zymoseptoria tritici* (Dothideomycetes, Ascomycota) causing Septoria tritici blotch on wheat. Recent literature has shown that early-diverging basidiomycetes lineages such as Pucciniomycotina, Ustilaginomycotina and Tremellomycetes comprise many dimorphic fungi (42,62,63). However, they receive minute attention because their members are neither economically important nor detrimentally harmful to humans.

It has been hypothesized that dimorphic fungi utilize different growth forms to maximize fitness in different stages of their life cycle. For instance, filamentous growth in *Saccharomyces cerevisiae*, as a chain of elongated cells under nutrient-limited condition, is considered as a scavenging response to increase a chance of finding nutrients (40). In many dimorphic human pathogens, a unicellular yeast form has a drastic shift of cell wall composition to avoid the recognition of immune cells (60,64). Recent reviews also suggested that the yeast form is beneficial for dissemination through host bloodstream and respiratory tract (60,65). However, the opportunistic pathogen *C. albicans* resides on host's skins and mucosal layers as a commensal yeast, while the hyphal form is used to penetrate host tissues and evade host immunity (37,52). *Metarhizium rileyi* switches to yeast-like growth when reaching the hemolymph of an insect. This helps the fungus spread throughout the host body. Once reaching a threshold critical density, it switches back, possibly by quorum sensing, to hyphal growth to finish colonization and kill the host (66). For dimorphic plant pathogens, filamentous growth is a primary form that penetrates the epidermis and colonizes host tissues (67). Genetic studies in *U. maydis* have shown that mutants with reduced filamentous growth often have attenuated virulence (36,68–71). On the other hand, the yeast form is beneficial for dissemination through plant vascular systems as shown in *Ophiostoma* and *Verticillium* (67). Moreover, it is tempting to propose that the yeast form is more advantageous for passive dispersal through wind, rain or even a vector.

Table 1.1 Examples of dimorphic fungi, life strategies, and environmental cues for morphological transition

Lineages/Species	Life strategy	Environmental cues	References
Ascomycota			
- Saccharomycotina			
<i>Saccharomyces cerevisiae</i>	Saprobe	Nutrient limitation (C, N)	(40)
<i>Candida albicans</i>	Opportunistic human pathogen	Temperature, serum, CO ₂ , pH, farnesol, GlcNAc	(37)
<i>Holleya sinecauda</i>	Plant pathogen	Media solidity	(72)
<i>Yarrowia lipolytica</i>	Saprobe	Nitrogen source, GlcNAc, serum, citrate, pH, anaerobic	(73–75)
- Taphrinomycotina			
<i>Taphrina deformans</i>	Plant pathogen	Unknown cue from host leaves	(76)
<i>Schizosaccharomyces pombe</i>	Saprobe	Nitrogen starvation	(77)
- Eurotiomycetes			
<i>Blastosyces dermatidis</i>	Human pathogen	Temperature, GlcNAc	(43,78)
<i>Coccidioides immitis</i>	Human pathogen	Temperature	(43)
<i>Talaromyces marneffii</i>	Human pathogen	Temperature	(43)
<i>Histoplasma capsulatum</i>	Human pathogen	Temperature, GlcNAc	(43,78,79)
- Sordariomycetes			
<i>Sporothrix schenckii</i>	Human pathogen	Temperature	(43)
<i>Ophiostoma ulmi</i> and <i>O. novo-ulmi</i>	Plant pathogen	Nitrogen source, inoculum density, quorum-sensing	(80,81)
<i>Verticillium albo-atrum</i>	Plant pathogen	Culture agitation, inoculum density	(82)
<i>Metarhizium rileyi</i>	Insect pathogen	Host hemolymph, quorum-sensing	(66)
- Dothideomycetes			
<i>Zymoseptoria tritici</i>	Plant pathogen	Nitrogen starvation	(83)
<i>Aureobasidium pullulans</i>	Saprobe	Nitrogen source, quorum-sensing, Zn ²⁺	(84,85)
<i>Hortaea werneckii</i> *	Saprobe, opportunistic human pathogen	Temperature, CO ₂ , cysteine, inoculum size, agitation	(86,87)
Basidiomycota			
- Ustilaginomycotina			
<i>Ustilago maydis</i>	Plant pathogen	Mating, lipid, hydrophobicity, acidic pH, nitrogen starvation	(88–91)
<i>Malassezia</i> spp.	Opportunistic human pathogen	L-DOPA, lipid on mammal skin, high CO ₂ tension	(92–94)
- Pucciniomycotina			
<i>Microbotryum lychnidis-dioicae</i>	Plant pathogen	Unknown	(95)
- Agaricomycotina			
<i>Cryptococcus neoformans</i>	Human pathogen	Mating, nitrogen starvation, temperature, CO ₂	(96)
<i>Trichosporon cutaneum</i>	Saprobe	Nitrogen source, pH, temperature	(97)
Mucoromycota			
<i>Mucor</i> spp.	Saprobe, opportunistic human pathogen	Carbon source, CO ₂	(98)

*The genus is widely known in literature as *Cladosporium* and *Exophiala*
GlcNAc stands for N-acetyl glucosamine

1.3 Smut fungi (Ustilaginomycotina)

Smut fungi are plant pathogens that produce masses of dusty dark-colored spores called teliospores (99). The pathogens typically infect reproductive parts of plant hosts, but many others are also found to infect vegetative parts such as leaves, stems and roots. Some smut fungi also induce the hosts to form a gall, which serves as a nutrient supply for them. Current taxonomic studies reveal that smut fungi are a polyphyletic assemblage. Most smut fungi belong to an early-diverging basidiomycete lineage called Ustilaginomycotina (62). Minorities are anther smut fungi in the genus *Microbotryum* (Microbotryomycetes, Pucciniomycotina), root gall-forming smut fungi in the genus *Entorrhiza* (Entorrhizomycota) and false smut fungi in the genus *Ustilaginoidea* (Sordariomycetes, Ascomycota) (3,100,101)

Currently Ustilaginomycotina has ca. 1,700 described species in 115 genera (62). Most widely known species are smut fungi on grasses belonging to the orders Ustilaginales and Tilletiales. Some representatives include the corn smut fungus *Ustilago maydis*, the wheat stinking smut fungi *Tilletia* spp. and the sugarcane smut fungus *Sporisorium scitamineum*. In addition, other smut fungi in Ustilaginomycotina, defined by the characteristic teliospores, infect other types of host like dicots, pines or even ferns (62,102). A recent study suggested that a smut pathogenic ancestry has originated at the emergence of the subphylum (41); however, not all members of this clade are considered as smut fungi. Some of these are known as non-smut phytopathogens such as *Pseudomicrostroma juglandis* and *Microstroma album* causing downy leaf spots on walnut and oak trees (103), *Exobasidium* spp. causing leaf and fruit spots on blueberries and cranberries (104), and *Tilletiopsis* spp. causing a white haze syndrome on postharvest apples (105,106). Many others are epiphytic yeast-like fungi commonly isolated from leaf phylloplane (107). Exemplars are genera *Pseudozyma*, *Tilletiopsis*, *Meira* and *Sympodiomyopsis* on various hosts (107), and *Violaceomyces palustris*, which is so far only known to be specific on aquatic ferns *Salvinia* spp. (108). Finally, although the majority of Ustilaginomycotina members are either plant pathogenic or plant-associated fungi, several species are found as animal-associated fungi. A renowned example is the genus *Malassezia*, which comprises lipophilic fungi on mammal skins (109,110). Other representatives are several species of *Moniliella*, *Meira* and *Acaromyces* (111,112).

The corn smut fungus *U. maydis* serves as a model species for several aspects of fungal biology, plant pathology and genetics. Historically, it was a pioneer system to study DNA recombination and gene conversion (113,114). Due to an ease for genetic manipulation, *U. maydis* is a good model to study molecular genetics of host-pathogen interaction and biotrophic development (88,115). The pace of research in this area has been expedited thanks to the completion of the *U. maydis* reference genome in 2006 (116). In terms of life strategy, *U. maydis* has a complicated life cycle that switches between saprobic and pathogenic phases (62). During a haploid stage (n), after teliospore germination and meiosis, the pathogen survives as a saprobic yeast and asexually reproduces by budding. This phase can be grown in axenic culture, but it is rarely detected in nature (62). When two compatible yeasts come close to each other, they form a conjugation tube, through pheromone signaling and responses (117), to undergo cytoplasmic fusion (termed 'plasmogamy'). After that, the fungus in a dikaryotic stage (n+n) switches to a pathogenic filamentous phase. It has polarized hyphal growth with a cell cycle arrest at a G2 stage (118), and the fungus forms retraction septa to separate a viable compartment at an apical region from highly vacuolated compartments at a distal region (26). When the pathogen perceives triggering signals from the host, like hydroxy-fatty acids and hydrophobicity (89,119), it forms an appressorium to penetrate a plant epidermis. After it grows and colonizes plant tissues, its hyphae become fragmented and transformed into teliospores (120), where two nuclei are fertilized to a diploid stage (termed 'karyogamy'). The teliospores are dispersed and dormant until a favorable condition induces their germination to begin a next cycle. From this elaborated life cycle, *U. maydis* also serves as one of the primary models to understand the role of fungal dimorphism in pathogenesis (67,121).

1.4 Mechanisms for fungal dimorphism

As dimorphic fungi perceive signals from surroundings to determine their growth forms, it is important to investigate what signals affect dimorphism, as well as how signal transduction mechanisms trigger morphogenesis. Knowledge in this area is translational especially for dimorphic pathogens. It can lead to the design of chemicals/inhibitors that either block signal perception or disrupt downstream signaling pathways. These could prevent disease progression due to unsuccessful morphological switch, which consequently makes the pathogens unable to survive and overcome host defenses.

1.4.1 Physiological factors that trigger dimorphic transition

Thanks to most dimorphic fungi that can grow under axenic cultures, cumulative physiological studies have provided an overview of what culturing conditions trigger dimorphic transition (Table 1.1). Nitrogen starvation is widely known to trigger yeast-to-hyphal switch in several species such as *Saccharomyces cerevisiae*, *Schizosaccharomyces pombe*, *Candida albicans*, *Cryptococcus neoformans*, *Ustilago maydis* and *Zymoseptoria tritici* (37,40,77,83,90,96). In contrast, *Trichosporon cutaneum* and *Yarrowia lipolytica* represent an exception by which high nitrogen source promotes filamentous growth (75,97). Types of nitrogen source also impact types of growth form in several dimorphic species (73,81,85,97), albeit a general conclusion is hard to be drawn. In addition, the effect of carbon sources on fungal dimorphism has been reported in the literature, but with less attention. Fermentable hexoses have been shown to promote yeast growth in several *Mucor* species (98), while *S. cerevisiae* undergoes invasive filamentous growth when culturing without fermentable sugars (122). The sugar derivative N-acetyl glucosamine (GlcNAc) is found to be an elicitor for filamentous growth of *C. albicans*, *Y. lipolytica*, *H. capsulatum* and *B. dermatidis* (37,74,78).

Rather than nutrient condition, other environmental factors can impact dimorphic switching. For example, acidic pH induces filamentous growth in two basidiomycetes dimorphic fungi—*U. maydis* and *T. cutaneum* (91,97). On the other hand, *Y. lipolytica* and *C. albicans* display yeast growth under the same condition, and they form hyphae under alkaline pH (73,123). Anaerobic condition, or high CO₂ tension, was historically known for triggering yeast growth of several *Mucor* species (98). However, it was later recognized to promote hyphal growth in at least two ascomycetes dimorphic fungi *C. albicans* and *Y. lipolytica* (37,73). Interestingly, there is a single report showing an effect of Zn²⁺ on promoting filamentous growth in *Aureobasidium pullulans* (84). Finally, physical properties while culturing like temperature, media solidity and agitation can affect growth forms in some dimorphic fungi (72,82,97).

Intercellular communication is another critical factor for determining growth forms in dimorphic fungi. Inoculum density plays a major role in dimorphism of several ascomycetes species like *Ophiostoma ulmi* and *O. novo-ulmi*, *Verticillium albo-atrum*, *Metarhizium rileyi* and *A. pullulans* (80,82,85), suggesting quorum-sensing activity in these fungi. Farnesol, as a renowned quorum-

sensing molecule, is secreted by *C. albicans* to suppress filamentous growth and biofilm formation (37). Other quorum-sensing molecules involved in fungal growth and development are discussed in a recent review (124). Although quorum sensing is poorly known in basidiomycetous fungi, mating is associated with dimorphism in a few model species. Yeast cells of *Ustilago maydis* perceive a farnesylated pheromone lipopeptide to initiate conjugation tube formation (117). After plasmogamy, a dikaryotic cell undergoes hyphal growth. The post-mating filamentous growth is also found in *Cryptococcus neoformans* (96), but it can revert back to yeast growth once it becomes a diploid stage through karyogamy.

To become successful in infection and colonization, dimorphic pathogens utilize signals from their hosts for morphological switching. Temperature serves as a primary factor that triggers dimorphic transition in many human pathogenic fungi (Table 1.1). Most of these are adapted to grow as yeasts at 37 °C (human body temperature), and as hyphae in cooler environmental temperatures (43,87,96). High CO₂ tension, which is presumably found in human tissues, can also promote yeast growth in some dimorphic pathogens that cause systemic infection (87,96,98). However, human body temperature, high CO₂ and blood serum are factors that promote filamentous growth in *C. albicans* (37). The commensal and opportunistic fungus *Malassezia* likely requires signals on mammal skins for filamentous growth, which is enhanced under microaerophilic environment (65,94). While signals involved in fungal dimorphism have been extensively studied in human pathogens, knowledge in plant pathogens remains scarce. The only well-studied dimorphic plant pathogen to date is *U. maydis*. Acid pH, lipid and hydrophobicity have been shown to promote filamentous growth of *U. maydis* (89,91,119). These cues are commonly found on a plant host surface (125), indicating that the pathogen perceives the host for dimorphic transition. The peach leaf curl pathogen *Taphrina deformans* is obligately filamentous only when it colonizes a host, possibly after perceiving an unknown signal. While temperature plays a major role in dimorphic transition of human pathogens, whether there is a common cue for dimorphic plant pathogens remains unknown.

1.4.2 Signal transduction mechanisms

After signal perception, dimorphic fungi require an elaborated system of signal transduction, gene regulation and biomolecular localization prior to morphogenetic reprogramming. Upstream

signaling pathways are the most intensively studied since they are widely conserved throughout the fungal kingdom. In Fungi, there are two major conserved pathways—the cAMP/Protein kinase A (PKA) pathway and the mitogen-activated kinase (MAPK) pathway (126,127). In this review, I will provide a comprehensive overview of these signaling pathways, as well as any upstream and downstream molecular players, using *U. maydis* as a model (summarized in Figure 1.2). Any remarkable difference in other dimorphic fungi may be reviewed and discussed.

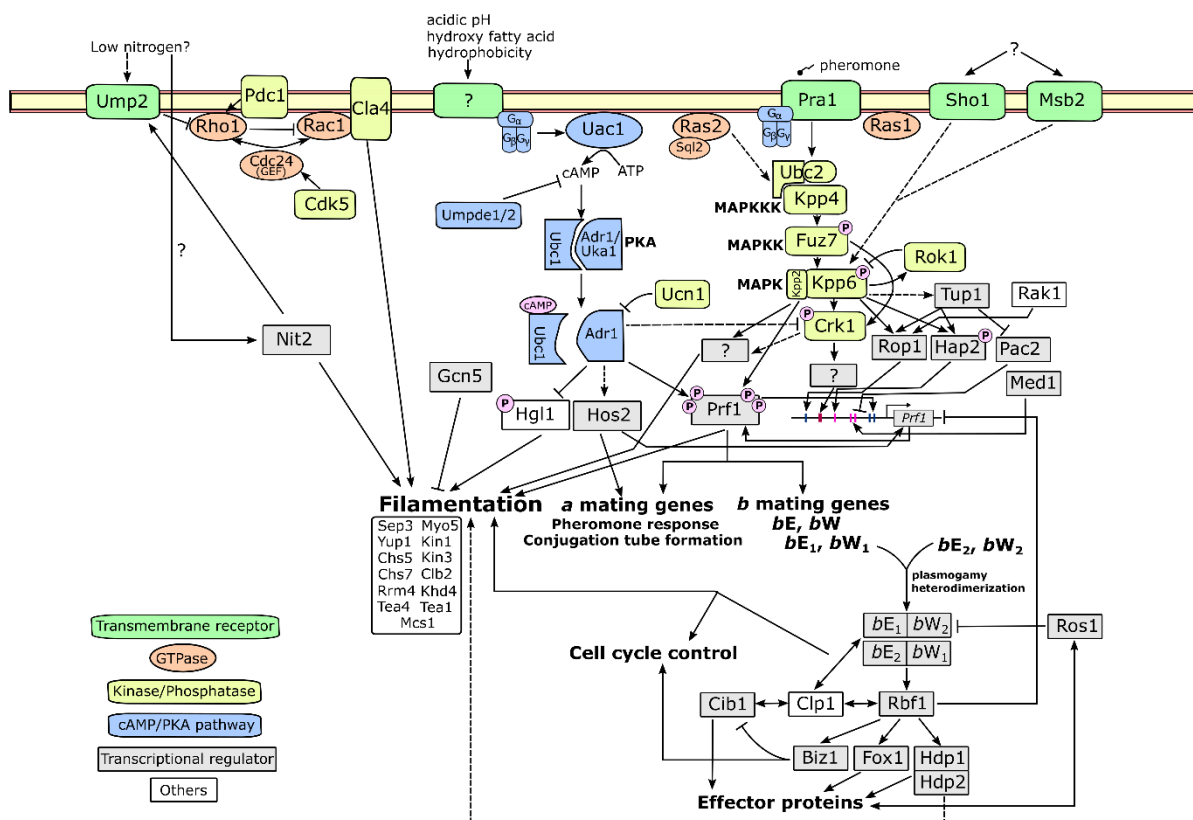


Figure 1.2 Overview of the regulatory network for fungal dimorphism in *U. maydis*. Filamentous growth of *U. maydis* can be triggered through a few pathways: the cAMP/PKA pathway, the MAPK pathway and the GTPase-mediated signaling pathways. These signal transductions are followed by the alteration of the transcriptional network that activates downstream effectors for morphogenesis. Details of molecular players in the figure can be found in Table 1.2.

Table 1.2 A list of known fungal dimorphism genes from the *U. maydis* literature

Categories	Gene name	Function	References
Receptors	<i>Pra1</i>	Pheromone receptor	(128)
	<i>Msb2</i>	Transmembrane mucin, multicopy suppressor of a budding defect	(119)
	<i>Sho1</i>	Osmosensor transmembrane protein	(119)
	<i>Ump2</i>	Ammonium transporter	(129)
cAMP/PKA pathway	<i>Gpa3</i>	G protein alpha subunit	(130)
	<i>Bpp1</i>	G protein beta subunit	(131)
	<i>Uac1</i>	Adenylate cyclase	(132)
	<i>Ubc1</i>	Regulatory subunit of cAMP-dependent protein kinase A	(132,133)
	<i>Adr1</i>	Catalytic subunit of cAMP-dependent protein kinase A	(134)
	<i>Uka1</i>	cAMP-dependent protein kinase A	(134)
	<i>Umpde1/2</i>	Phosphodiesterases	(135)
MAPK pathway	<i>Ucn1</i>	Antagonist phosphatase of PKA	(136)
	<i>Ubc2</i>	Pheromone-responsive SH3 domain protein	(137,138)
	<i>Kpp2/Ubc3</i>	MAP kinase	(139,140)
	<i>Kpp4/Ubc4</i>	MAP kinase kinase kinase	drew
	<i>Kpp6</i>	MAP kinase	(141)
	<i>Fuz7/Ubc5</i>	MAP kinase kinase	(142,143)
	<i>Rok1</i>	Dual specificity protein phosphatase	(144)
GTPase-mediated signaling	<i>Crk1</i>	MAP kinase	(68)
	<i>Ras1, Ras2</i>	<i>Ras</i> family GTPase	(145,146)
	<i>Sql2</i>	Cdc25-like guanyl nucleotide exchange factor	(146)
	<i>Rho1</i>	<i>Rho</i> family GTPase	(147)
	<i>Pdc1</i>	14-3-3 homolog	(148)
	<i>Cla4</i>	PAK family kinase	(149)
	<i>Rac1</i>	<i>Rho</i> family GTPase	(150)

Table 1.2 continued

Categories	Gene name	Function	References
Transcriptional regulator	<i>Biz1</i>	<i>b</i> locus-dependent Zn finger transcription factor	(151)
	<i>Hap2</i>	CCAAT-box binding protein	(152)
	<i>Rop1</i>	High-mobility-group (HMG) domain transcription factor	(153)
	<i>Prf1</i>	Pheromone response factor functioning as a transcription factor	(71,154)
	<i>Rbf1</i>	<i>b</i> locus-dependent Zn finger transcription factor	(155)
	<i>Cib1</i>	<i>b</i> locus-dependent Zn finger transcription factor	(156)
	<i>Gcn5</i>	Histone acetyltransferase	(157)
	<i>Hos2</i>	Histone deacetylase	(158)
	<i>Tup1</i>	General transcriptional repressor	(159)
	<i>Pac2</i>	WOPR family transcriptional repressor	(159)
	<i>Ros1</i>	WOPR family transcriptional regulator	(160)
	<i>Nit2</i>	GATA transcription factor responsive to low nitrogen	(70)
	<i>Med1</i>	Transcription factor	(161)
Other downstream molecular players	<i>Hgl1</i>	Putative regulatory protein	(162)
	<i>Rak1</i>	Seven-WD40 repeat motif protein	(163)
	<i>Myo5</i>	Class V myosin	(164)
	<i>Kin1, Kin3</i>	Kinesin-1 and 3 required for hyphal growth	(165)
	<i>Rrm4, Khd4</i>	RNA-binding protein for filamentous growth	(166,167)
	<i>Clb2</i>	B-type cyclin 2	(168)
	<i>Chs5</i>	Chitin synthase V	(169)
	<i>Chs7</i>	Chitin synthase	(169)
	<i>Mcs1</i>	Myosin chitin synthase 1	(169)
	<i>Clp1</i>	Function in nuclei distribution during cell division in dikaryon	(156)
	<i>Yup1</i>	<i>t</i> -SNARE protein for vesicular cycling	(9)
	<i>Sep3</i>	Septin 3 as an effector of cAMP/PKA pathway	(36)
		<i>Tea1, Tea4</i>	Cell end markers

1.4.2.1 cAMP-PKA pathway

The cAMP-PKA pathway is a well conserved signaling pathway across eukaryotic organisms (127). The signaling initiates by the perception of an extracellular stimulus through a G protein-coupled receptor (GPCR). Once a ligand binds to the receptor, it interacts with a heterotrimeric G protein complex, which is bound to the receptor, to activate a G_{α} subunit by incorporating a GTP molecule. Then, the active G_{α} subunit dissociates from the G protein complex and subsequently binds and activates an enzyme called adenylate cyclase. This enzyme catalyzes a conversion of ATP to 3'-5' cyclic AMP (cAMP). The cyclic AMP serves as a second messenger inside a cell that amplifies a signal to downstream targets. One of the most important targets is protein kinase A (PKA), a heterotetrameric enzyme constituting two regulatory subunits and two catalytic subunits. The cAMP molecule can bind to the regulatory subunits, causing them to release from the catalytic subunits. The PKA catalytic subunits can then phosphorylate many downstream proteins involved in various cellular responses. Finally, to provide a feedback control, a phosphodiesterase enzyme reduces an intracellular cAMP level by hydrolyzing a phosphodiester bond of cAMP, yielding AMP as a product.

Most components of the cAMP-PKA pathway have been characterized in *U. maydis*. Regenfelder et al. (130) discovered four G_{α} genes (*Gpa1* – *Gpa4*). Only *Gpa3* shows a distinct phenotype; a mutant has a promoted filamentous growth but does not respond to a pheromone. A subsequent discovery of G_{β} (*Bpp1*) reveals a similar biological function to *Gpa3* (131). The gene *Uac1* was identified as an adenylate cyclase in *U. maydis* (132), for which a mutant has constitutively filamentous growth. Although the heterotetrameric structure of PKA is yet to be validated, the regulatory subunit *Ubc1* and the catalytic subunits *Adr1* and *Uka1* were characterized. The *ubc1* mutant has a defect on filamentous growth *in vitro* (132), while during a dikaryotic stage it can colonize a host with a presence of hyphae but not a gall formation (133). The *adr1* mutant is constitutively filamentous during a haploid stage, but its pathogenicity is defective (134). The other PKA catalytic subunit *Uka1* does not show any significant effects on growth form and pathogenicity (134). Finally, Agarwal et al. (135) recently performed functional characterization of two phosphodiesterase genes *Umpde1* and *Umpde2*. The *umpde1* deletion results in significantly reduced pathogenicity. While the *umpde2* deletion mutant has a subtle effect on pathogenicity, its filamentous growth is strongly attenuated.

Overall, several molecular genetic studies have shown that the activation of the cAMP-PKA pathway promotes budding but reduces filamentous growth of *U. maydis in vitro*. The trend is confirmed by the addition of exogenous cAMP, which yields a similar outcome (132,172,173). This morphological response is opposite of *C. albicans* and *S. cerevisiae* by that filamentous growth is a consequence of the pathway activation (37,40). However, defects of several components in the pathway often lead to hampered pathogenic development. These findings suggest that the cAMP-PKA pathway plays a multiple role in both cellular and pathogenic developments. In addition, only dimorphic transition to filamentous growth is not enough for the switching from a saprobic phase to a pathogenic phase.

1.4.2.2 MAPK pathway

The mitogen-activated protein kinase (MAPK) pathway is another extensively studied pathway in many eukaryotic systems. The pathway is activated through a sequential phosphorylation of Ser/Thr/Tyr protein kinases, termed MAPK cascade. There are three major groups of kinases in the MAPK cascade. A MAPK kinase kinase (MAPKKK) is activated by an upstream molecular player such as a G-protein complex, a GTPase or a kinase. The active MAPKKK then phosphorylates a MAPK kinase (MAPKK) to enable its activity. After that, the MAPKK phosphorylates a MAPK to trigger its function as a final step in the cascade. The activated MAPK can either stimulate or inhibit many downstream targets such as protein kinases, protein phosphatases, transcription factors, etc.

Major components of the MAPK cascade have been described in *U. maydis*—*Kpp4/Ubc4* as a MAPKKK gene (143,174), *Fuz7/Ubc5* as a MAPKK gene (142,143) and *Kpp2/Ubc3*, *Kpp6* and *Crk1* as MAPK genes (139–141,175). In addition, two additional genes directly involved in the cascade are identified. The pheromone-responsive adaptor protein Ubc2 physically interacts with Kpp4 (137,138). The other is a dual specificity phosphatase named *Rok1*, which negatively controls Kpp2 and Kpp6 through dephosphorylation (144). In *S. cerevisiae*, there are several gene members in the MAPK family. A recent comparative genomics analysis reveals that almost all of these genes have respective orthologs in *U. maydis* (126), but less than half of which have been characterized.

Currently, most known MAPK genes of *U. maydis* are involved in pheromone response, conjugation tube formation, filamentous growth and pathogenic development (68,139,140,142,143,174,175). An exception is *Kpp6*, of which the mutant has normal morphogenesis but attenuated pathogenicity (141). The *Kpp4-Fuz7-Kpp2* MAPK cascade corresponds to the *Ste11-Ste7-Kss1* cascade in *S. cerevisiae*—it affects the transition to filamentous growth (40,126). A *Kss1* paralog named *Fus3*, another downstream target of *Ste7*, has a separate role in *S. cerevisiae* mating (40). However, in *U. maydis* the mating function is complemented by *Kpp2*, while its paralog *Kpp6* has a single function in pathogenic development. The *U. maydis* *Crk1* is another downstream target of *Fuz7*. *Crk1* function, having a role in filamentous growth, mating and pathogenesis (68,69), can also be regulated through phosphorylation by *Kpp2* and cAMP-mediated mechanism. *Ime2*, an ortholog of *Crk1* in *S. cerevisiae*, is involved in pseudohyphal growth and meiotic progression via the cAMP-mediated pathway, albeit its upstream MAPK counterpart is still unknown (176). These examples demonstrate the functional diversification of the MAPK pathway, as well as its potential crosstalk to the cAMP/PKA pathway. *Saccharomyces cerevisiae* has at least two other MAPK cascades—the *Bck1-MKK1/2-Sit2* cascade involved in cell wall integrity and the *Ste11/Ssk2/Ssk22-Pbs2-Hog1* cascade involved in the high osmolarity pathway (126). None of these have been studied in *U. maydis*. Therefore, it is interesting to investigate the other MAPK members to understand how they affect *U. maydis* growth and development.

The multidomain adaptor protein *Ubc2* provides another example of functional diversification within a single molecule. Klosterman et al. (137) showed that the SAM and RA domains at the N-terminus region of *Ubc2* are essential for *U. maydis* filamentous growth. A direct interaction of the SAM domain and *Kpp4* is suggested as an underlying mechanism to activate the MAPK cascade. Meanwhile, the C-terminal SH3 domains of *Ubc2* are dispensable for filamentous growth, but instead required for pathogenesis (137). Other proteins that interact with *Ubc2* to trigger a different response are yet to be known. To summarize, the *U. maydis* MAPK pathway frequently has a coupled function for both filamentous growth and pathogenic development.

1.4.2.3 Alternative pathways

In addition to the cAMP/PKA and MAPK pathways, GTPases are other important signaling components for filamentous growth. A few families of GTPases are described in *U. maydis*: Ras, Rac and Rho family. There are two genes in the Ras family, *Ras1* and *Ras2*. *Ras2*, acting upstream of the MAPK cascade, contributes to filamentous growth, mating response and pathogenicity (145). A subsequent study showed that the Ras2 function is activated by the guanyl nucleotide exchange factor *Sql2* (146). While *Sql2* overexpression leads to constitutively filamentous growth, its deletion mutant has normal mating but also adversely affects pathogenic development (146). *Ras1*, less studied than *Ras2*, is only known to promote the expression of a pheromone gene (146). Rac is another GTPase family known for polarized growth and cell wall expansion in *U. maydis* (150). Overexpression of *Rac1* causes *U. maydis* to display filamentous growth during its haploid stage, while the overexpression of a hyperactivated form leads to an isotropic cell wall expansion and cell lethality (150). *Rac1* is activated by the guanyl nucleotide exchange factor *Cdc24*, but potentially inhibited by the Rho1 GTPase (147). The only downstream target of *Rac1* currently known is the PAK family kinase *Cla4*, which modulates polarized growth, cell separation and bud neck formation (147,149). The cyclin-dependent kinase *Cdk5* is also involved in cell polarity through modulating *Cdc24* localization at a hyphal tip (177).

There are few other signaling pathways that are related to fungal dimorphism, but not intensively studied in *U. maydis*. One is the two-component signaling system, which is thoroughly investigated in thermally dimorphic fungi (64). The pathway is activated by signal perception through a hybrid histidine kinase, which induces the phosphorylation of its response regulator at a histidine residue. After that, a histidine phosphotransfer protein mobilizes a phosphate group from the response regulator to a downstream target to activate/deactivate its function. Recent studies have shown that the class III hybrid histidine kinase plays a crucial role for dimorphic switching in *Histoplasma capsulatum*, *Talaromyces marneffii* and *Blastomyces dermatidis* (64). Another pathway is the calcium signaling pathway. Upon a signal perception that leads to calcium ion influx, an elevated intracellular Ca^{2+} concentration facilitates a calcium-binding protein called calmodulin to become active. The Ca^{2+} -bound calmodulin then interacts with other downstream proteins to trigger their function. One of these is a Ser/Thr protein phosphatase named calcineurin, which is found to control dimorphic transition in two dimorphic human pathogens *Mucor*

circinelloides and *Paracoccidioides brasiliensis* (178,179). In *M. circinelloides*, calcineurin also contributes to spore size regulation, cell wall integrity and antifungal drug resistance (180). A single study in *U. maydis* identified the catalytic subunit of calcineurin Ucn1 as an antagonist of PKA, which consequently activates post-mating filamentation and pathogenicity (136).

1.4.2.4 Upstream and downstream molecular players

Among researches in signal transduction, signal perception is one of the least studied areas due to a couple of reasons. One is because most receptors are transmembrane proteins, which are difficult for studying protein structures and interactions. Another reason is the exhaustiveness of matching which ligands bind to which receptors. In *U. maydis*, the only confirmed ligand-receptor interaction is a lipoprotein pheromone and a seven-transmembrane pheromone receptor (117). The binding of the pheromone to the receptor results in the activation of a MAPK signaling cascade (138,143,174). The high-affinity ammonium transporter Ump2 has recently been described as affecting *U. maydis* filamentous growth under a low-ammonium condition (90,181). A physical interaction between Ump2 and the Rho1 GTPase suggests a mechanism for filamentous growth via the Rho1-Rac1 signaling pathway. Thus, it is tempting to hypothesize that Ump2 serves as a receptor for nitrogen starvation in addition to a transporter function. Sho1 and Msb2 are two other characterized transmembrane proteins found to interact with the MAPK cascade (119). These two proteins affect stress response and pseudohyphal growth in *S. cerevisiae*, whereas their orthologs in *U. maydis* play a role in appressoria formation but not filamentous growth (119). Other signals, like acidic pH and lipids, are involved in *U. maydis* filamentous growth. However, their corresponding receptors are yet to be discovered.

The pheromone response factor 1 (Prf1) is a master transcription factor that controls the mating process, filamentous growth and pathogenic development of *U. maydis* (88,121). Primarily, it turns on genes—*a* and *b*—in the *MAT* loci. Genes at the *a* locus function in pheromone production, pheromone response and conjugation tube formation, while the *b* locus encodes two transcription factors (*bE* and *bW*) that become active through heterodimerization with their counterparts after plasmogamy (182). Considered as a key regulator in cellular and pathogenic development, many studies have investigated how *Prf1* itself is regulated. The promoter region of *Prf1* is relatively long with a length of at least 2 kilobases (153). *Prf1* can autoactivate itself by binding to its

promoter to initiate transcription (153,154). The promoter region is also subjected to several transcription factors such as Rop1, Pac2, Hap2 and Med1 (153,159,161), and the regulation network of these genes has been investigated (159,163). A recent study reveals that the histone deacetylase Hos2 facilitates Prf1 transcription through unwinding the Prf1 open-reading frame region from histone molecules (158). In addition to transcriptional control, the Prf1 activity is also regulated via post-translational phosphorylation. Prf1 has multiple Serine/Threonine sites that are subjected to phosphorylation by PKA and Kpp2 (183). The PKA phosphorylation sites are required to induce gene expression in both *a* and *b* loci, while the MAPK phosphorylation sites are essential for only *b* locus expression. Therefore, Prf1 represents one of a few known molecules that integrate signaling from different pathways and fine-tune downstream cellular responses.

Once a dikaryotic stage is formed, through activities of *MAT a* genes, the homeodomain transcription factors encoded by the *MAT b* locus of each nucleus become functional in a heterodimerized form. The bE/bW heterodimer can transcriptionally regulate dozens of genes (184). However, Heimel et al. (155) revealed that the bE/bW heterodimer may not directly regulate these downstream targets, but instead functions through another master regulator called Rbf1. Several genes in pathogenesis and cell cycle regulation have been identified as targets of Rbf1 (155). Considering this, the bE/bW regulatory cascade is crucial for filamentation and pathogenic development during the dikaryotic stage. After *U. maydis* fully colonizes the host, it undergoes a transition from vegetative growth to teliospore formation. A recent study has identified the WOPR family transcriptional factor Ros1 as a primary regulator for this switching (160). One of the Ros1 functions includes a feedback inhibition of the bE/bW regulatory cascade.

Although Prf1 serves as a central regulator for dimorphic transition, there are a few cases where *U. maydis* undergoes filamentous growth in a Prf1-independent manner. For instance, Lee and Kronstad (145) demonstrated that the hyperactivated Ras2 leads to constitutively filamentous growth in a *prf1* mutant. The *prf1* mutant can also form hyphae under an induction by acidic pH or lipids (173,185). According to these, there must be other alternate downstream molecular players that need to be discovered. Hgl1, a direct phosphorylation target of PKA (162), is so far not known to be linked to Prf1. The GATA transcription factor Nit2 is recently identified as a response factor for filamentous growth under nitrogen catabolite repression (70). The *nit2* deletion

mutant does not have altered expression of *Prf1* and its upstream genes, suggesting that *Nit2* is either downstream or independent of *Prf1*. The gene encoding histone acetyltransferase *Gcn5* also contributes to *U. maydis* dimorphism (157), but whether its function is Prf1-dependent remains unknown. To sum up, there are several alternative pathways inducing dimorphic transition in *U. maydis*. However, the Prf1-mediated regulatory pathway is still crucial for pathogenic development of *U. maydis* as it leads to mating, dikaryotization and the establishment of the bE/bW heterodimer, which turns on many downstream targets including effectors and pathogenesis proteins. Empirical evidence to support this argument is the construction of the solopathogenic strain SG200 (186). The strain contains *bW2* and *bE1* genes, making it form the bE/bW heterodimer by itself and it is pathogenic even in a haploid stage.

After sequences of signal transduction and transcriptional regulation, target genes for cellular structures and morphogenesis are ultimately activated. Some of these characterized in *U. maydis* include cytoskeletal motors such as the class V myosin gene *Myo5* and the kinesin genes *Kin1* and *Kin3* (26,164,165). Chitin synthases are another group of genes that affect fungal dimorphism. Weber et al. (169) found that the polar chitin synthases *Chs5* and *Chs7* are required for conjugation tube formation, dikaryotic hyphae formation and pathogenicity, while the Myosin V chitin synthase *Mcs1* only influences polarized growth once entering into plant tissues. In addition, cell division genes like the B-type cyclin *Clb2*, the nuclei distribution gene *Clp1*, and the septin gene *Sep3* are involved in *U. maydis* filamentous growth (36,168,187). *Yup1* encodes an endosomal *t*-SNARE protein that is important for exocytosis and endocytosis; this is found to be critical for polarized growth (9). The cell end markers *Tea1* and *Tea4*, indicating a site for polarized growth, have been recently characterized in *U. maydis* (170,171). Finally, the RNA-binding proteins *Khd4* and *Rrm4* have been shown to control regular filamentous growth (166,167). They function in long-distance mRNA transport so that transcripts involved in polarized growth can be expressed at a precise location in a cell (121).

1.5 Comparative studies

Rather than differences in morphological appearance of two growth forms, how yeasts differ from filamentous fungi remains one of the fundamental questions in fungal biology. Thanks to advancements in DNA sequencing technologies, hundreds of fungal genomes have been generated

over the past decade, and they can be used in comparative studies (188,189). Nagy et al. (44) suggested that yeast-like fungi have independently evolved multiple times in several lineages of Dikarya. The commonality of emerging yeast-like clades includes massive gene loss and the diversification of genetic toolkits, like Zn-cluster transcription factors, to regulate yeast growth (44). More recently, Nguyen et al. (190) generated the reference genome of *Neolecta irregularis*. Despite belonging to the yeast-like clade Taphrinomycotina, this fungus appears to lose the ability to grow as yeasts, and instead produces hyphae and complex fruiting bodies. Their comparative genomics analyses reveal numerous candidate genes conserved in *Neolecta* and other ascomycetes filamentous fungi; many of these are either absent or divergent in Saccharomycotina and Taphrinomycotina (190). Although these two studies list potential genes that explain a difference between yeasts and filamentous fungi, representatives in each yeast-like clade were not extensively sampled—some of which have only 1–2 species. Analyses derived from incomplete taxon sampling may not reflect the biology of the whole fungal clades of interest.

Dimorphic fungi also serve as a good system to understand the difference between yeast growth and filamentous growth. One interesting aspect is how dimorphic fungi perceive stimuli to undergo morphological switching. Although it is widely known in dimorphic human pathogens that temperature serves as a primary stimulus for dimorphic transition, little is known in dimorphic plant pathogens, as well as dimorphic plant-associated fungi. Another aspect is to investigate the gene expression profiles of yeast growth versus filamentous growth. This has been widely examined in some model species such as *Candida albicans*, *Histoplasma capsulatum* and *Ustilago maydis* (191–196). Recent researches have expanded transcriptomic studies to other non-model species (197,198). Nigg and Bernier (197,199) are the first group that performs multispecies comparison, which is based on the collection of results from multiple studies. However, their comparison only covers gene ontology, which is quite broad and not specific. In addition, they did not incorporate any bioinformatic analyses to discover any common core genes involved in each growth form among several dimorphic species.

1.6 Thesis statement and objectives

In this dissertation, I attempt to utilize multiple approaches, ranging from physiology to genomics and transcriptomics to understand the molecular bases of yeast and filamentous growth. Smut fungi

and allied members in Ustilaginomycotina are selected as a primary group of interest. Three main objectives of the dissertation are as follows:

1. To determine potential factor(s) that trigger dimorphic transition of Ustilaginomycotina species.
2. To discover potential 'core' genes that are involved in each type of growth form (yeast versus filamentous growth) through multispecies transcriptomic analyses.
3. To determine if genomic profiles can distinguish yeast-like fungi from filamentous fungi, as well as to discover candidate genes associated with fungal growth forms

CHAPTER 2. EFFECTS OF ENVIRONMENTAL FACTORS ON FUNGAL DIMORPHISM OF USTILAGINOMYCOTINA

2.1 Introduction

Fungal dimorphism is a phenomenon by which fungi can grow both as unicellular yeasts and as multicellular hyphae. Each growth form is displayed at different stages of a life cycle to maximize survival and fitness of the fungus. Good examples are dimorphic fungi that parasitize plants and animals (60). In general, a yeast phase is beneficial for dissemination through the bloodstream and vasculature of hosts, while a filamentous phase is essential for primary infection and penetration through host tissues (60,67).

Previous studies have investigated the physiology of fungal dimorphism both in industrially important and pathogenic fungi. In the widely-known genetic model *Saccharomyces cerevisiae*, pseudohyphal growth is promoted by nitrogen starvation, high osmolarity and ploidy status (200,201). Meanwhile, types of nitrogen sources, pH and temperature are major factors for determining growth forms in the biotechnologically important basidiomycete fungus *Trichosporon cutaneum* (97). In several human pathogenic fungi, temperature change is a primary factor to trigger dimorphic transition (60,64). While increased temperature to 37 °C results in hyphal-to-yeast transition in most dimorphic human pathogens (64,65), some opportunistic pathogens such as *Candida albicans* and *Trichosporon* spp. primarily grow as hyphae during human infection (37,65). Dimorphic fungi that are entomopathogenic undergo transition from hyphal growth to yeast-like growth after exposing to hemolymph inside insect bodies (66,202,203). In dimorphic plant pathogens, several factors have been shown to be involved in dimorphic transition such as nutrient starvation, types of nitrogen sources, inoculum density, high osmolarity and hydrophobicity (60,67). However, unlike dimorphic human pathogens that utilize temperature as a common cue, it is unknown if plant pathogenic fungi share any common signals for dimorphic transition.

Smut fungi are a group of dimorphic plant pathogens that cause diseases on several economically important crops. Exemplars are the corn smut fungus *Ustilago maydis*, the wheat smut fungi *Tilletia* spp. and the sugar cane smut fungus *Sporisorium scitamineum*. The smut fungi grow as

free-living yeasts in nature during a haploid stage, and become filamentous and pathogenic after cytoplasmic fertilization between two compatible yeast cells as well as perception of external signals, potentially from plant hosts (65,67). Some signals include nutrient starvation, acidic pH and lipid compounds such as cutin and hydroxy-fatty acid (89,91,185,201). Although the knowledge of fungal dimorphism is currently expanding based on studies of the model organism *U. maydis*, it may not reflect the biology of other smut pathogens. “Smut” fungi are classified in seven orders in Ustilaginomycotina, some of which are not evolutionarily closely related to the others (41). In addition, most members of the subphylum are plant-associated fungi and have dimorphic growth strategy (41,62). This raises a question about whether these fungi share any common signals for growth form transition as temperature is found as a common signal for dimorphic human pathogens.

2.2 Hypotheses

- Since most Ustilaginomycotina species are plant-associated fungi, they may use a common biomolecule from plant hosts for dimorphic transition.
- Lipids, abundantly found on plant surfaces, trigger dimorphic transition in the model species *U. maydis*. As most Ustilaginomycotina species either live on leaf phylloplane or use leaves as a penetration route for infection, lipids can be a promising candidate for the study.

2.3 Methods

2.3.1 Taxon sampling

The following strains were included in the study: *Ustilago maydis* TKC58, *Moesziomyces aphidis* MCA6183 and *Testicularia cyperi* MCA3645 (≡ ATCC MYA-4640) for Ustilaginales; *Violaceomyces palustris* SA807 (≡ CBS 139708) for Violaceomycetales; *Meira miltonrushii* MCA3882 (≡ ATCC-MYA 4883 ≡ CBS 12591), *Meira* sp. MCA4637 and *Acaromyces ingoldii* MCA4198 (≡ CBS 140884) for Exobasidiales; *Tilletiopsis washingtonensis* MCA4186 (≡ NRRL Y-63783) for Entylomatales; *Jaminaea rosea* MCA5214 (≡ CBS 14051) and *Pseudomicrostroma glucosiphilum* MCA4718 (≡ CBS14053) for Microstromatales. We created species abbreviations by using the first three letters from genus names combined with the first two letters from specific

epithets. Therefore, all studied species were abbreviated as Ustma, Moeap, Tescy, Viopa, Meimi, Meisp, Acain, Tilwa, Jamro and Psegl, consecutively.

2.3.2 Culturing experiments

The *Ustilago maydis* strain TKC58 was selected for three pilot experiments, which tested the effects of three factors: carbon source concentration, pH and types of carbon source. We utilized the recipe of the Holliday's minimal liquid medium (204) as the standard medium for the study. The Holliday's minimal liquid medium has the following properties—1% glucose (w/v) as a carbon source, KNO_3 as a nitrogen source, trace elements added in the medium and pH equal to 7.0 under a phosphate buffer. For the pilot experiments, the medium recipe was adjusted according to each testing factor. We varied glucose concentration in three treatments as 0.2%, 1% and 5% for testing the effect of carbon source concentration. For the pH test, two types of media were used: the Holliday's minimal medium (pH 3, 7 and 9) and the Holliday's complete medium (pH 3, 5 and 7). We used 1% glucose (w/v) and 1% Tween40 (w/v) as different types of carbon source. For inoculation, we cultured the fungal strain in yeast malt broth (YMB) at room temperature (25 °C) and the shaking condition of ca. 180 rounds per minute (rpm) for 3 days. After that, cell suspensions were collected by centrifugation and rinsed three times in sterile water. The cell amount of 1×10^6 cells was inoculated into 5 ml of culture media, resulting in 2×10^5 cells/ml as an initial cell concentration. Based on microscopic observation, most cells in the inoculum appeared as yeast growth. There were five replicates for each treatment. The cultures were observed 1, 3 and 5 days after incubation at room temperature and 180 rpm shaking condition.

As the pilot experiment of *U. maydis* suggested that its growth form becomes steady after five days of incubation, we selected this timepoint for data collection in subsequent experiments. The type of carbon source is a primary factor to test types of growth form for ten Ustilaginomycotina species/strains. Carbon sources used in the experiments are the following: glucose as a control carbon source used in the standard Holliday's minimal medium, sucrose as a representative for a mobilized carbon source of plants, soluble starch as a representative for a storage carbon source of plants, pectin as a representative for a structural carbohydrate (e.g., a component of cell wall) of plants and Tween40 as a lipid mimic, representing a hydrophobic surface of plants. Glucose in the Holliday's minimal medium was replaced by different carbon sources under 1% (w/v)

concentration. We also tested the effect of temperature (25°C, 35°C and 37°C) on types of growth form using the Holliday's minimal medium with 1% glucose as a carbon source. For all cultures, we followed the inoculation protocol as described above with five replicates for each treatment. The culture was observed five days after incubation at room temperature (25 °C), with exceptions in the temperature experiment as noted (25°C, 35°C and 37°C), and 180 rpm shaking condition.

We also tested the effect of natural lipids on fungal dimorphism. Because the lipids are insoluble in an aqueous solution, a solid medium was used instead. The Holliday's minimal liquid medium was adjusted to the solid medium by adding 2% agar (w/v). There were two treatments according to types of carbon source: 0.5% glucose (w/v) and 0.5% canola oil (w/v). The starting inoculum of 100,000 cells in 50 µl was added on the agar as a suspension drop. We inoculated four suspension drops of the same strain for each agar plate. The cultures were incubated at room temperature and observed up to 7 days.

2.3.3 Determination of growth forms and statistical analyses

To determine fungal growth forms, cell morphologies of cultures were observed under BH-2 Olympus microscopy (Olympus corp., Tokyo, Japan). We used 20X and 40X objective lens with a phase contrast. We adapted the method for growth form determination described by Manning and Mitchell (205). For each treatment, at least two hundred cells were counted and classified into two categories—yeast cells and filamentous cells. A cell bud was counted as one yeast cell, while an elongated fungal structure longer than two yeast cells without constriction between cells was counted as filamentous cells. For cultures on the solid medium, we utilized the Olympus SZ61 stereomicroscope to visualize colony morphology. The Olympus SC30 camera was used to capture photomicrographs of fungal morphologies through the Olympus cellSens v. 1.8 software.

A percentage of filamentous cells in each experimental unit was used as a proxy for types of growth form. We utilized R version 3.4.1 under RStudio version 1.0.153 for data analyses and visualization. Mean and standard deviation were reported for each treatment as line and bar graphs using the ggplot2 package version 3.1.0 (206). One-way analysis of variance (ANOVA) was used to analyze the difference in types of growth form among treatments. The Levene's test was used to test the homogeneity of variance assumption. The data were log-transformed in case raw data

did not meet the assumption. Finally, the Tukey's HSD test was used as a post-hoc comparison among treatments. P-values less than 0.01 were considered as statistically significant.

2.4 Results

2.4.1 Pilot experiments on physiological studies of *U. maydis*

First, we tested which factors (types of carbon source, pH and glucose concentration) affect types of growth form of the model species *U. maydis*. Clearly, percentages of filamentous cells from all experiments are less than 50%, indicating that a majority of *U. maydis* cell populations still have yeast growth (Figure 2.1). According to our results, *U. maydis* has the highest filamentous growth when using Tween40 as a carbon source; it starts having a significant difference in growth forms after three days of incubation (Figure 2.1A). However, we did not see yeast-to-hyphal dimorphic transition under acidic condition (pH 3), as reported in the previous study of Ruiz-Herrera et al. (91). Furthermore, growth forms under different pH seem dependent on types of media used for culturing (Figure 2.1B and C). Finally, although there is a fluctuation of growth forms across different glucose concentrations, the percentages of filamentous cells under any timepoints are not significantly different across the treatments (Figure 2.1D).

2.4.2 Effects of different carbon sources on fungal dimorphism of several Ustilaginomycotina species

Next, we investigated the effects of different carbon sources on growth forms of several Ustilaginomycotina species (Figure 2.2 and 2.3). Tween40 is a carbon source that promotes filamentous growth of most dimorphic species—*J. rosea*, *Meira miltonrushii*, *Tilletiopsis washingtonensis*, *U. maydis* and *V. palustris*. *Moesziomyces aphidis* and *Testicularia cyperi* are the only two dimorphic species that do not have significant filamentous growth in Tween40. However, *Testicularia cyperi* and *V. palustris* have significantly increased filamentous growth when using pectin as a carbon source. Meanwhile, energy-source carbohydrates such as glucose, sucrose and soluble starch do not trigger filamentous growth in all dimorphic species (Figure 2.2 and 2.3). Finally, three species included in our studies have only one growth form no matter what types of carbon source they are cultured in—*Meira* sp. MCA4637 and *P. glucosiphilum* as constitutive yeasts and *A. ingoldii* as constitutive filamentous fungus.

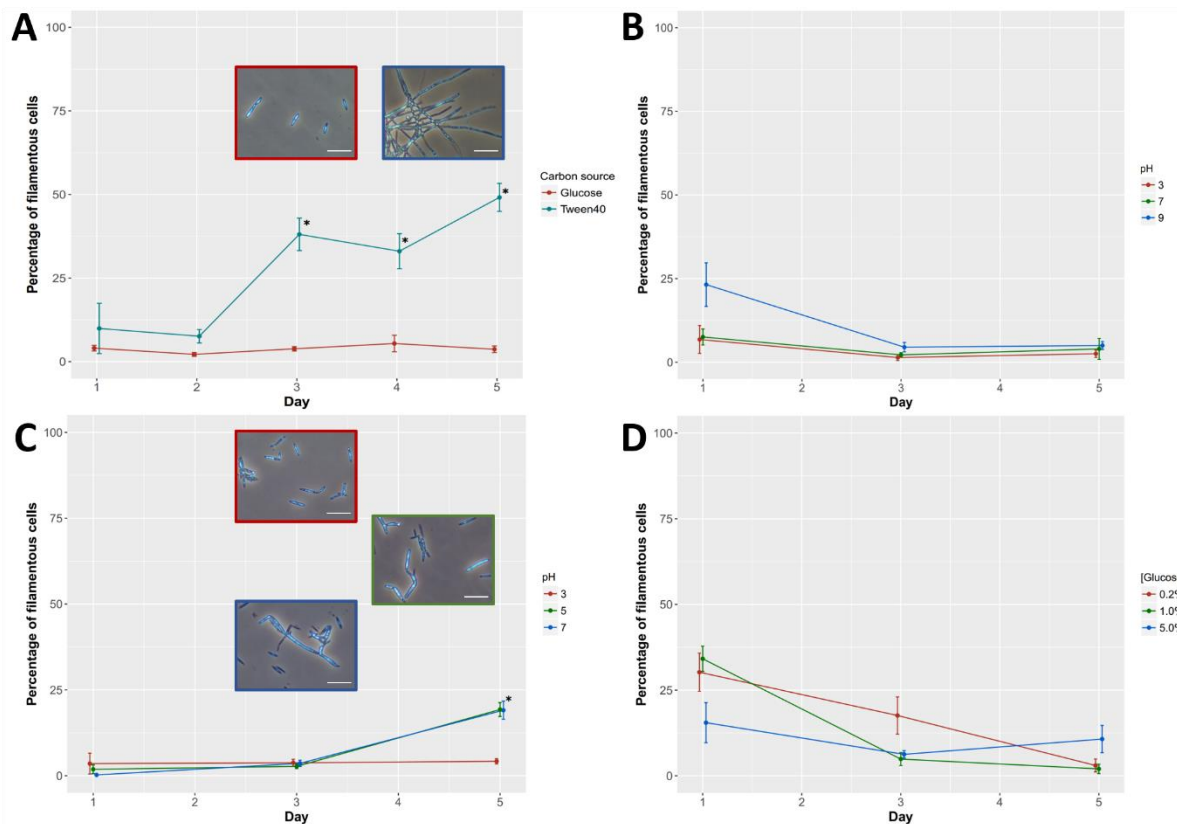


Figure 2.1. The pilot experiments on fungal dimorphism of *U. maydis*.

Culturing experiments were conducted to determine which environmental factor affects dimorphic transition of *U. maydis*. Factors we tested are as follows: (A) Types of carbon source (glucose and Tween40), (B) pH (3, 7, 9) under the Holliday's minimal medium, (C) pH (3, 5, 7) under the Holliday's complete medium and (D) glucose concentration (0.2%, 1% and 5% w/v). The cultures were observed after 1, 3 and 5 days of incubation under room temperature (25 °C).

Growth forms were reported as a percentage of filamentous cells. Asterisks indicate statistical differences between treatments at certain timepoints ($p < 0.01$). Photomicrographs of *U. maydis* cell morphologies were shown in panels (A) and (C). Frame colors of photomicrographs correspond to colors of line graphs. Bars: 20 μm .

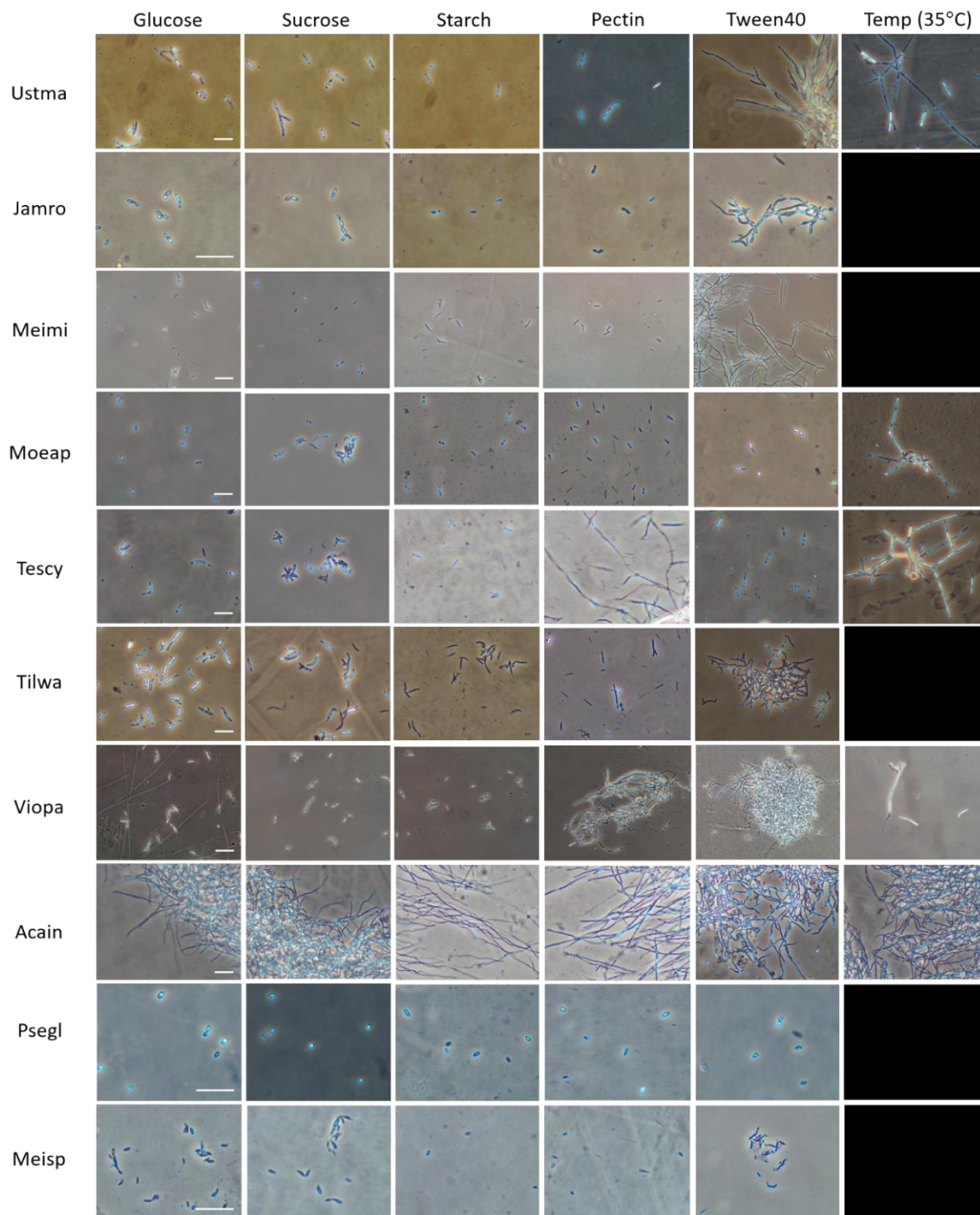


Figure 2.2. Effects of carbon source and temperature on fungal dimorphism of *Ustilaginomycotina*.

Cell morphologies of ten *Ustilaginomycotina* species treated under different types of carbon source (glucose, sucrose, starch, pectin, Tween40) and high temperature (35 °C) with glucose as a carbon source. Most treatments were incubated at 25 °C, otherwise as indicated, for 5 days. The fungal cultures were observed under phase-contrast microscopy. Note that some species do not grow at 35°C (indicated by black panels). Bars: 20 μm.

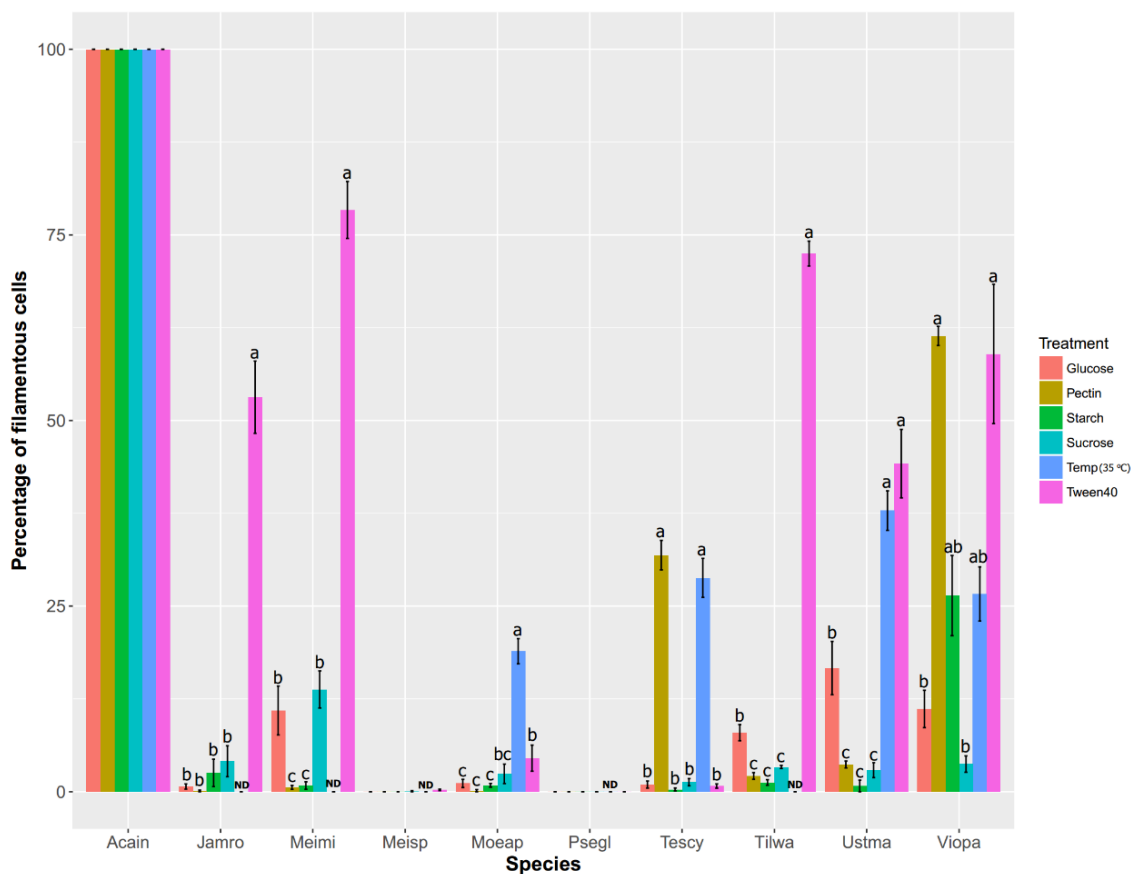


Figure 2.3. Quantification of growth forms of Ustilaginomycotina under types of carbon source and high temperature.

This figure provides statistical representation from Figure 2.2. Growth forms were reported as percentages of filamentous cells. One-way analysis of variance (ANOVA) was used to test differences among treatments for each species. Letters indicate groups inferred from the Tukey HSD post-hoc test. ND: no data, meaning that the fungal species do not grow under a certain condition.

To demonstrate the effect of natural lipids on fungal dimorphism, we inoculated dimorphic species on the Holliday's minimal solid medium amended with either glucose or canola oil as a carbon source. Three of these—*U. maydis*, *V. palustris* and *T. washingtonensis*—underwent filamentous growth at colony edges on the canola oil treatment compared to controls that have glucose as a carbon source (Figure 2.4). None of the other dimorphic species responded to the oil treatment.

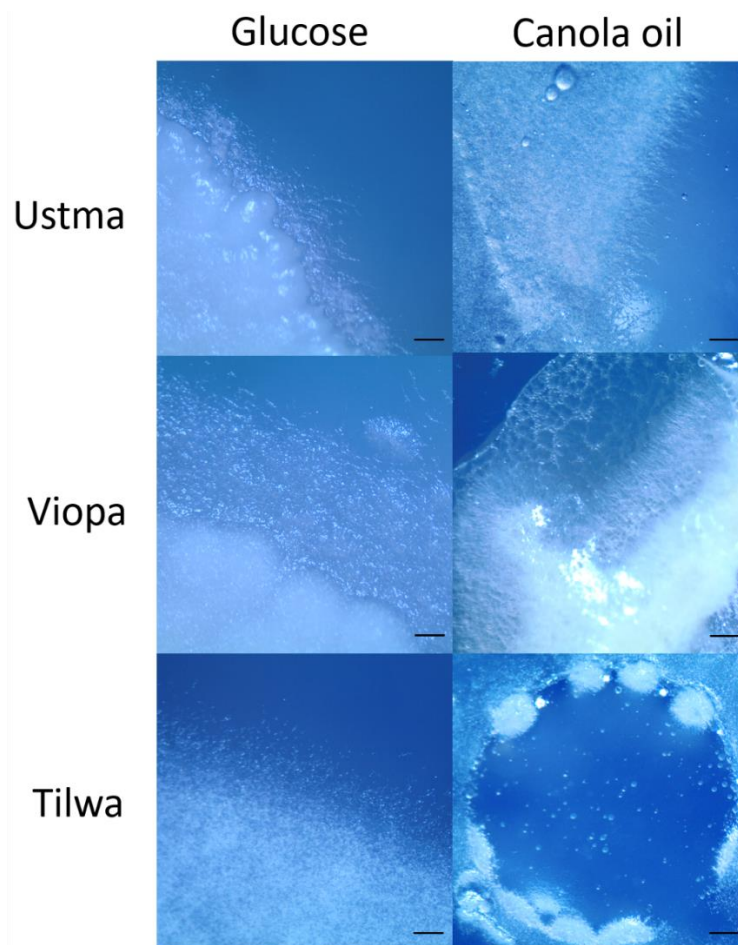


Figure 2.4. The effect of natural lipids on growth forms of some Ustilaginomycotina species. All dimorphic Ustilaginomycotina were cultured on the Holliday's minimal solid medium with either 1% glucose or 1% canola oil as a carbon source. The colony morphologies were observed up to seven days using a stereomicroscope. Three species, *U. maydis*, *V. palustris* and *T. washingtonensis*, display different growth forms at colony edges—the cultures on canola oil have filamentous margins while the ones on glucose do not. Bars: 200 μ m.

2.4.3 Effects of temperature on fungal dimorphism of several Ustilaginomycotina species

Finally, all Ustilaginomycotina species were challenged under high temperature. Several species failed to grow at 35°C, including *J. rosea*, *M. miltonrushii*, *Meira* sp. MCA4637, *P. glucosiphilum* and *T. washingtonensis*. Filamentous growth was promoted at 35°C for *U. maydis*, *M. aphidis*, *T. cyperi* and *V. palustris* (Figure 2.2 and 2.3). Three of the latter four species that were capable of growth at 35°C failed to grow at 37 °C, i.e., human body temperature. Only *M. aphidis* grew at human body temperature with high proportion of filamentous cells, while it grew well as yeasts at 25°C (Figure 2.5).

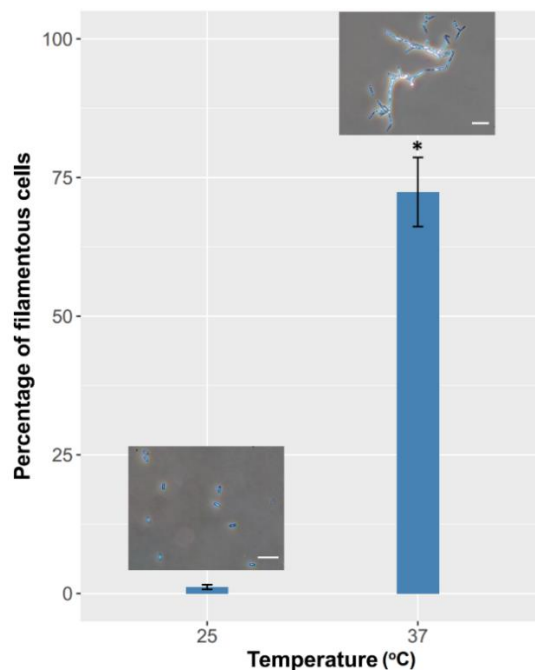


Figure 2.5 Growth forms of *Moesziomyces aphidis* under high temperature. Ustilaginomycotina dimorphic species were cultured in the Holliday’s minimal liquid medium and incubated at 25 °C or 37 °C for five days. Only *M. aphidis* can grow at 37°C with extensive hyphal growth. Photomicrographs of cell morphologies and barplots are shown. An asterisk indicates statistical difference in the percentage of filamentous cells ($p < 0.01$). Bars: 20 μm .

2.5 Discussion

We initiated our study by conducting pilot experiments on *U. maydis*, which serves as a renowned model species on fungal dimorphism and its role in pathogenicity (65,67,88). Our findings are congruent to previous studies (89,185), which found lipids including Tween40 as a cue for filamentous growth of *U. maydis*. However, we found that the dimorphic transition is not an all-or-none response—the percentage of filamentous cells only increases to 50% under the Tween40 treatment (Figure 2.1A). It has to be noted that several studies only reported a few photomicrographs as a representation of growth form (97,185,202). As the growth forms of dimorphic fungi are dynamic both in terms of cell population and time (66,97,207), we strongly encourage to use a quantitative approach, combined with statistical analyses, to support the findings as well as to determine the strength of biological phenomena. Moreover, protocols used to distinguish between yeast and filamentous cells should be clearly defined in the studies, as these can be critical for result interpretation. Detailed methods have described in systems like *Candida albicans* and *Ophiostoma* (80,205,208).

The previous study from Ruiz-Herrera et al. (91) showed that acidic pH can trigger yeast-to-hyphal transition in *U. maydis*. They also illustrated that the response is dependent on types of nitrogen source used in the media. Our results suggest an interaction effect between pH and types of media that consist of different nitrogen sources (Figure 2.1B and C). However, we do not find hyphal growth under acidic conditions (pH 3) in any settings. Due to this conflict, we decided not to proceed testing the pH effect in multispecies experiments.

Our study shows that Tween40, as a lipid mimic, triggers dimorphic transition in most dimorphic Ustilaginomycotina species tested (Figure 2.2 and 2.3). Canola oil, as a natural lipid, also promotes filamentous growth of some species on solid media (Figure 2.4). These confirm findings from the previous study of Klose et al. (185), showing that plant oils, fatty acids and Tween40 promote filamentous growth of *U. maydis*. More recent studies also revealed the effect of hydroxy-fatty acids and a hydrophobic surface on promoting hyphal growth of the *U. maydis* solopathogenic strain SG200 (89). As an external layer of plants (i.e. cuticle) is rich in lipid compounds (125), it is possible that plant-associated fungi utilize these biomolecules as signals upon their arrival on the host surface. Among species included in this study, *J. rosea* and *M. miltonrushii* are described as phylloplane fungi (209,210). Although *T. washingtonensis* is a common yeast-like fungus on leaf phylloplanes, it has recently been found producing extensive hyphal growth on apple skins, causing the postharvest disorder ‘white haze’ syndrome (105,106). *Violaceomyces palustris* is found as a phylloplane, and possibly endophytic, yeast of aquatic ferns in the genus *Salvinia* (108). In addition, hydrophobicity and lipid compounds are involved in morphogenesis in other plant pathogenic fungi, such as appressoria formation in the rice blast fungus *Magnaporthe oryzae* and the powdery mildew pathogen *Blumeria graminis* (211,212) and yeast-to-hyphal transition in the Dutch Elm disease pathogens *O. ulmi* and *O. novo-ulmi* (207,208). Even though all abovementioned fungi interact with a variety of plant hosts, they share similar types of signals to trigger their morphological transition.

However, the lipid compounds do not promote hyphal growth in some other species such as the smut fungus *T. cyperi* and the epiphytic yeast-like fungus *M. aphidis* (Figure 2.2 and 2.3). It may be because they do not rely on hosts for growth and development. This is unlikely to be our case, as *T. cyperi* is a pathogen of the sedge *Rhynchospora*. Alternatively, different fungi may sense

different signal molecules from plants. For example, *Magnaporthe oryzae* can sense surface hydrophobicity, cutin monomers or leaf waxes to trigger appressoria formation as a same output (211). Since an environment on plant surfaces is rich in lipids but poor in nitrogen compounds (125), some plant-associated fungi such as *Saccharomyces cerevisiae* and *Zyoseptoria tritici* may perceive nitrogen starvation as a signal that they arrive at host surfaces (83,201). Whereas, others may perceive other biomolecules inside plant hosts. To our knowledge, this is the first report that pectin triggers growth form transition in dimorphic fungi—*V. palustris* and *T. cyperi* (Figure 2.2 and 2.3).

Temperature has been widely known as a cue for dimorphic transition in human pathogenic fungi (60,64). Intriguingly, our study has found that temperature can be a trigger for dimorphic transition in some Ustilaginomycotina species—*U. maydis*, *M. aphidis*, *T. cyperi* and *V. palustris* (Figure 2.2 and 2.3). Among these, only *M. aphidis* is able to grow under 37 °C with extensive hyphal growth (Figure 2.5). Recent reports found *Moesziomyces aphidis* as an opportunistic pathogen, growing as a hyphal form inside the tissues of immunocompromised patients (56,213). Its developmental response is similar to *Candida albicans* once entering human tissues (37). However, most human-pathogenic dimorphic fungi switch to yeast growth at 37 °C. In terms of human pathogenicity, yeast growth is advantageous for evasion from host immunity and thermotolerance, whereas the benefit of hyphal growth in human tissues remains skeptical (37,60,64). As *M. aphidis* belongs to the smut fungi clade Ustilaginaceae, the transition from plant-associated fungi to opportunistic pathogens on humans is very notable. However, another *M. aphidis* strain has filamentous growth when culturing in soybean oil (57), while our study does not see a similar result. This indicates intraspecific variation at the level of fungal growth and development, which is rarely noticed in the literature.

In summary, our studies support that an environment from a host plays a crucial role for determining growth forms of dimorphic fungi. Temperature is a general cue for dimorphic transition in human pathogenic fungi, both aggressive and opportunistic ones. We suspect lipid compounds, as found on plant surfaces, can trigger yeast-to-hyphal transition in many plant-associated dimorphic fungi no matter whether they are true pathogens. However, the difference in triggering cues may depend on signal perception mechanisms and life strategies. It is notable that

none of the energy-source carbohydrates significantly promotes filamentous growth in our studied dimorphic species. Finally, although most Ustilaginomycotina members are considered as having a dimorphic life strategy (41,62), some others, like *A. ingoldii* and *P. glucosiphilum*, can display either only yeast growth or only hyphal growth. The inclusion of non-model but phylogenetically related species into future studies will lead to better understanding of fungal dimorphism in an evolutionary context.

CHAPTER 3. COMPARATIVE TRANSCRIPTOMICS OF YEAST AND FILAMENTOUS GROWTH FORMS ACROSS FOUR DIMORPHIC PLANT-ASSOCIATED FUNGI

3.1 Introduction

Dimorphic fungi have an ability to display both unicellular yeast growth and multicellular filamentous growth. This strategy is prevalent in many pathogenic fungi as it maximizes the fitness in different stages of their life cycles (60). In dimorphic plant pathogens, a yeast phase is thought to be predominant for passive dispersal in an environment and dissemination through host vasculature, while a filamentous phase is crucial for initial stages of penetration and colonization (60,67). Therefore, studying how these fungi switch from yeast growth to hyphal growth is important since it could lead to disease management strategies.

The corn smut fungus *Ustilago maydis* serves as a primary model to understand fungal dimorphism and its role in plant pathogenesis (88,121). Yeast-to-hyphal dimorphic transition of *U. maydis* involves multiple steps of pheromone sensing, mating and perception of host signals. These are regulated under complex intracellular processes—including activation of signaling pathways, alteration of transcriptional networks and recruitment of machineries for polarized filamentous growth (reviewed in Chapter 1). Researchers in the field are continuously discovering novel genes involved in fungal dimorphism. However, this type of study is so far limited to data from the model species, and only in *U. maydis* among dimorphic plant pathogens. Research derived from multiple species would be beneficial to determine if, for instance, the dimorphic mechanism is conserved. This can lead to the design of chemicals or inhibitors that target core molecular players to block development of dimorphic fungi, especially the pathogenic ones.

Recently, transcriptomic sequencing has been a powerful tool to examine what types of genes have altered expression under different growth stages of dimorphic fungi (199). This high-throughput technique allows researchers to not only focus on primary genetic models, but also expand to other non-model species. However, current studies have been focusing on transcriptomic analyses of individual species. Comparative transcriptomics is an emerging strategy to discover common genes that affect the same trait across different species. For example, Krizsán et al. (214) performed

comparative transcriptomics across six mushroom species to determine common genes for complex multicellularity in Fungi. Nigg et al. (197) compared transcriptomic profiles between yeast growth and filamentous growth of three dimorphic fungi—*Ophiostoma novo-ulmi*, *Candida albicans* and *Histoplasma capsulatum*. They concluded that there is a poor conservation of global gene expression profiles across the studied species. More recently, Nigg and Bernier (199) reviewed multiple transcriptomic studies to find common biological processes associated with each growth form across several dimorphic fungi. However, these two studies did not intensively conduct bioinformatic analyses to find out whether there are any common genes, as well as any biological processes, involved in different types of growth form across multiple species.

To address the abovementioned knowledge gap, we performed transcriptomic analyses across four dimorphic fungi that are associated with plants. Two Ustilaginomycotina species, *Meira miltonrushii* and *Tilletiopsis washingtonensis*, were selected as non-model species for transcriptomic sequencing. We also incorporated gene expression datasets from the model species *Ustilago maydis*, plus one non-model ascomycetous species (*Ophiostoma novo-ulmi*), for our study. We examined if the conservation of gene expression profiles is linked to phylogenetic relatedness. Finally, known *U. maydis* dimorphism genes were used to determine whether there is any common trend of altered gene expression across multiple species.

3.2 Hypotheses

- There are some common biological processes that regulate the transition from yeast to filamentous forms across multiple dimorphic fungi. These may be genes involved in cytoskeleton, signal transduction or cell division.
- Being the most distantly related species in a phylogenetic context, the transcriptomic profile of *O. novo-ulmi* is the least similar to the other three Ustilaginomycotina species.
- Known dimorphism genes from *U. maydis* have conserved functions, as well as conserved regulatory processes for expression, across different dimorphic species. Considering this, we expect similar expression patterns for these genes.

3.3 Materials and Methods

3.3.1 Taxon sampling

Four dimorphic species were selected for this study. *Meira miltonrushii* and *Tilletiopsis washingtonensis* represent non-model species in the “smut” subphylum Ustilaginomycotina, Basidiomycota. *Meira miltonrushii* (Exobasidiales) is described as a phylloplane epiphyte isolated from a magnolia leaf (209). *Tilletiopsis washingtonensis* (Entylomatales) is an epiphytic species commonly isolated from plant leaves (215), but it was recently found to colonize postharvest apples in Europe (105,106). *Ustilago maydis* (Ustilaginales) is a smut pathogen on maize and serves as a primary genetic model in this subphylum (88). We sampled another species from a different phylum, Ascomycota, to examine the conservation of transcriptional alteration in yeast growth versus filamentous growth when comparing to basidiomycetes species. *Ophiostoma novo-ulmi*, a causal agent of the Dutch Elm disease on elm trees (216), was selected for this study.

3.3.2 Orthology assessment and functional annotation

Prior to comparative transcriptomic analyses, we need to determine which genes are phylogenetically equivalent across four species. To achieve this, the reference genomes, gene models and protein models of all studied species were downloaded from the DOE-JGI MycoCosm portal (189). Reference genomes we utilized are as follows: *M. miltonrushii* CBS12591 version 1.0 and *T. washingtonensis* NRRL Y-63783 version 1.0 (41), *U. maydis* strain 521 version 2.0 (116) and *O. novo-ulmi* version 1.0 (217). We ran orthology assessment through OrthoFinder version 2.1.2 (218) using the protein models as an input. Only single-copy orthogroups were retained. In case any orthogroups have paralogs, we inspected a gene tree phylogeny generated from the OrthoFinder to determine when a gene duplication happens. If there is a subtree which contains only one paralog per species, we assigned gene members in the subtree as a new orthogroup. Three sets of orthogroups were retained for subsequent analyses: orthogroups between *M. miltonrushii* and *T. washingtonensis*, orthogroups among Ustilaginomycotina (*M. miltonrushii*, *T. washingtonensis* and *U. maydis*), and orthogroups among all four species.

Because all four fungal genomes may be annotated in different, we performed functional annotation of all protein models by eggNOG version 4.5 (219). The software provided different annotation properties such as eukaryotic clusters of orthogroups (KOG) ID number, KOG

functional class, gene ontology (GO) term ID and brief description for potential function. Finally, a list of genes involved in fungal dimorphism of *U. maydis* was retrieved from the literature (see Table 1.2 in Chapter 1). We used the results from OrthoFinder to determine respective orthologs in other species. In this case any potential paralogs were also included into the analyses.

3.3.3 Experimental design, RNA isolation and data collection

We did set up an experiment for yeast-to-hyphal dimorphic transition of *M. miltonrushii* MCA 3882 (\equiv CBS 12591) and *T. washingtonensis* MCA 4186 (\equiv NRRL Y-63783). Each fungal strain was cultured in the Holliday's minimal liquid medium (204). There were two treatments for types of carbon source in the medium: glucose and Tween40. We set up three and four replicates for *M. miltonrushii* and *T. washingtonensis*, respectively. Our results from previous experiments showed that these two species have yeast growth in glucose and filamentous growth in Tween40 (see Chapter 2). A total number of 5×10^6 cells were used as a starting inoculum in 5 ml of the liquid medium. The cultures were incubated at room temperature for three days under the shaking condition of 180 rpm. After that, we observed micromorphology under a phase-contrast microscope to confirm that the growth forms were as expected before RNA harvest.

To harvest RNA, the fungal cultures were centrifuged at 15,000x g and rinsed with sterile water for three times. After that, they were ground in liquid nitrogen using plastic homogenizers and stored at -80 °C until used. RNA samples were extracted from the frozen tissues using the Omega Fungal RNA kit (Omega Bio-Tek Corp., Norcross, GA). RNA quality was determined by Nanodrop spectrophotometry and 1% agarose gel electrophoresis. Finally, the RNA samples were sent to the Purdue Genomics Core Facility for transcriptomic sequencing. Briefly, poly A+ libraries were prepared using Illumina's TruSeq mRNA Library Prep Kit (Illumina Inc., San Diego, CA). The cDNA libraries were sequenced under the NovaSeq S2 platform through 50-bp paired-end reads (2x50). Approximately 30 million and 15 million reads were generated for each sample of *T. washingtonensis* MCA 4186 and *M. miltonrushii* MCA 3882, respectively. Summaries of read statistics were shown in Table 3.1.

For *U. maydis* and *O. novo-ulmi*, we utilized published datasets from previous studies (196,198). Nigg and Bernier (198) performed time-lapse transcriptomic sequencing during yeast-to-hyphal

transition of *O. novo-ulmi* when transferring the cultures from the minimal medium to the complete medium. The Illumina reads were downloaded from the NCBI Sequence Read Archive (SRA) database: SRX1958716, SRX1958730 and SRX1958720 for three replicates of *O. novo-ulmi* displaying yeast growth (0 hr after media transfer) and SRX1958729, SRX1958719 and SRX1958725 for three replicates of *O. novo-ulmi* displaying filamentous growth (27 hrs after media transfer). Meanwhile, Lanver et al. (196) performed microarray analysis to examine transcriptional profiles of *U. maydis* under yeast-to-hyphal transition on hydrophobic surfaces. The normalized microarray data were downloaded from the NCBI GEO database (accession number GSE53947). We selected the expression data of two treatments—wild-type growing on glass plates (displaying yeast growth) and wild-type growing on hydrophobic surfaces (displaying filamentous growth)—for differential gene expression analyses. The microarray probes, under the AffyMatrix platform GPL3681, were converted to *U. maydis* gene IDs prior to transcriptomic comparison (Supplementary Material 1).

3.3.4 Differential gene expression analyses

We started processing Illumina sequencing data by trimming adapters and low-quality bases through Cutadapt version 1.13 (220) and Trimmomatic version 0.36 (221). Quality check after read cleaning was performed using fastqc version 0.11.7 (222). Then, the clean reads were mapped to the reference genomic sequences through TopHat version 2.1.1 (223). BAM alignments were transformed into gene read counts using htseq version 0.7.0 (224). Finally, we performed differential gene expression analyses for each species using the DESeq2 package version 1.20.0 (225), performed under R version 3.5.0 and RStudio version 1.1.463. For the normalized microarray data of *U. maydis*, we performed the differential gene expression analysis using the limma package version 3.36.5 in the R platform (226). The log₂ fold change value was calculated as the ratio of the gene expression level from the treatment displaying filamentous growth against the treatment displaying yeast growth. The log₂ fold change and adjusted p-value were further used for comparative transcriptomic analyses.

3.3.5 Comparative transcriptomics and functional analyses

First, we compared differential gene expression results between *M. miltonrushii* and *T. washingtonensis*. Genes having adjusted p-value less than 0.01 were considered as differentially

expressed. Only genes having single-copy orthogroups in both species were examined. For orthogroups that are differentially expressed in both species, we checked expression patterns whether they were concordant (upregulated or downregulated in both species) or discordant (upregulated in one species but downregulated in the other). Numbers of orthogroups having different expression patterns were summarized as a Venn diagram. We used Chi-square (χ^2) goodness of fit to test whether the concordant/discordant patterns occur randomly. Finally, the enrichment of KOG functional classes was determined by hypergeometric test (227). After that, we repeated the analyses for Ustilaginomycotina species (*M. miltonrushii*, *T. washingtonensis* and *U. maydis*) and all four species. As including multiple datasets may decrease the chance of getting genes that are differentially expressed in all species, we relaxed the critical p-value to 0.05 to make the call for differentially expressed genes more inclusive.

Among differentially expressed genes in each species, we also determined whether the set of known dimorphism genes was enriched through the hypergeometric test. Finally, several genes were selected for exploring potential functions and hypothesizing how they are involved in fungal dimorphism. The selection criteria were such as genes having concordant expression patterns across all studied species, genes assigned in enriched KOG functional class and genes having functional annotation related to growth and development like genes in cell wall/membrane biogenesis, vesicular transport, cytoskeleton, transcriptional regulation and signal transduction. A bioinformatic pipeline was summarized in Figure 3.1. Data and scripts used in the bioinformatic analyses were provided in Supplementary Materials 2–11.

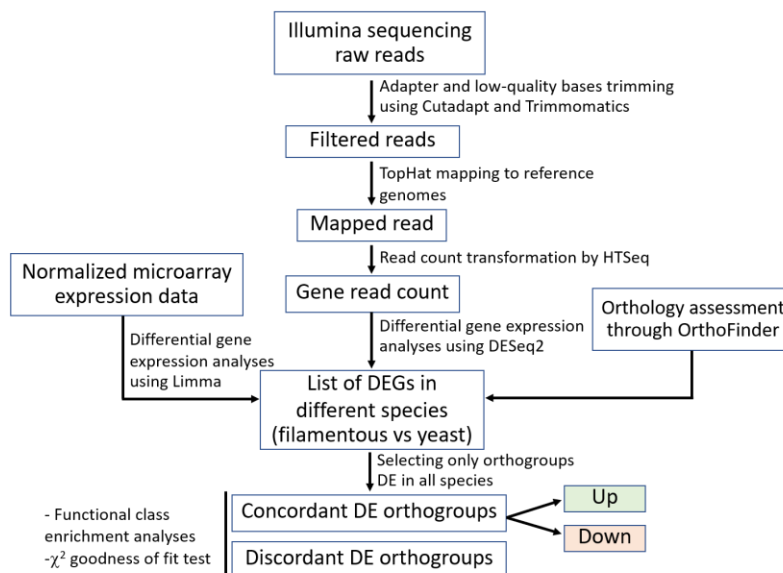


Figure 3.1 A designed bioinformatic pipeline for multispecies transcriptomic analyses.

3.4 Results

3.4.1 Orthology assessment

We found 2,653, 2,527 and 2,502 single-copy orthogroups among *M. miltonrushii* and *T. washingtonensis*, among Ustilaginomycotina, and among all four species, respectively (Supplementary Material 12). However, genes in some orthogroups do not have available expression data and that results in the final numbers of 2,227 and 2,205 among Ustilaginomycotina and all four species, respectively. There were 56 described dimorphism genes of *U. maydis* from the literature. These genes are classified into six categories (see Chapter 1): receptor genes, the cAMP/PKA signaling pathway, the MAPK signaling pathway, GTPase-mediated signaling, transcriptional regulators and genes involved in other downstream processes.

3.4.2 Dimorphic transition under lipid condition

Two Ustilaginomycotina species, *M. miltonrushii* and *T. washingtonensis*, were cultured under two conditions. The cultures in the glucose treatment display unicellular yeast growth, while the ones in the Tween40 treatment display multicellular hyphal growth (Figure 3.2A). We harvested the cultures after three days of incubation since it is the earliest timepoint they had distinct growth forms between two treatments (see Chapter 2). The proportion of filamentous cells for each treatment prior to RNA extraction was shown in Figure 3.2B.

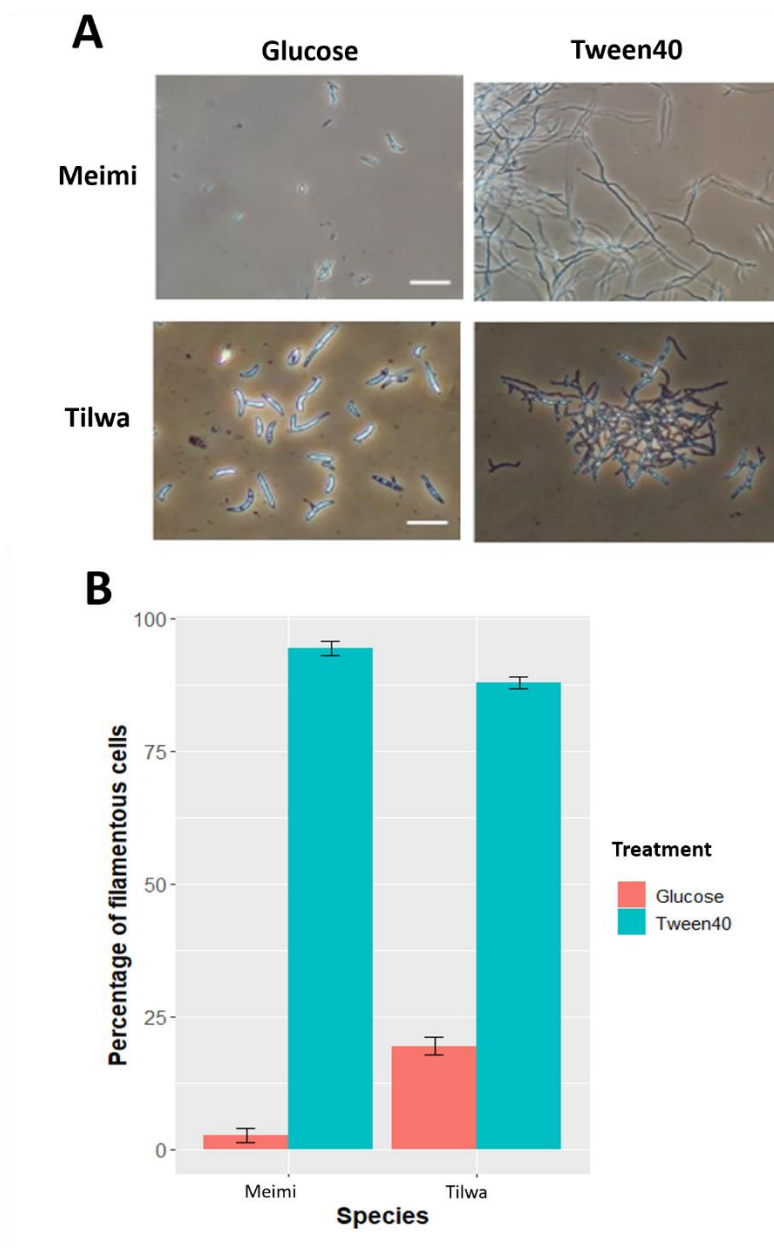


Figure 3.2 Dimorphic transition of *Meira miltonrushii* and *Tilletiopsis washingtonensis*. The two species have dimorphic transition from yeast to filamentous growths after culturing with Tween40 as a carbon source for 3 days. They retain yeast growth when using glucose as a carbon source. (A) Photographs of cell morphologies. Bars = 20 μ m and (B) Proportion filamentous cells. At least 200 cells were counted to determine growth forms. The two species were abbreviated as follows: Meimi for *Meira miltonrushii* and Tilwa for *Tilletiopsis washingtonensis*. Numbers of replicates are three for Meimi and four for Tilwa.

3.4.3 Transcriptomic analyses of individual species

Illumina sequencing data of *M. miltonrushii*, *T. washingtonensis* and *O. novo-ulmi* were used to determine gene expression level. Summary statistics can be found in Table 3.1. Briefly, there are ca. 80% of sequencing reads of *M. miltonrushii* and *T. washingtonensis* that are transformed into gene read count data, except for the *T. washingtonensis* Glucose replicate 3 sample, which has a significant level of rRNA contamination. For *O. novo-ulmi*, however, only half of the total raw reads were uniquely mapped to the reference genome. This may indicate either potential contamination during the library preparation or incompleteness of the reference genome.

In terms of differential gene expression analyses for each species, the transcriptomic profiles across samples are clustered based on treatments (Figure 3.3), indicating that the within-group variation is much less than between-group variation as expected. On average, around half of protein-encoding genes are differentially expressed (Figure 3.4 and Table 3.2). The MA plot of *U. maydis* appears different from the other species due to the nature of data (microarray hybridization data compared to high-throughput sequencing data).

Table 3.1 Summary statistics of transcriptomic sequencing and read count transformation

Species	Sample name	Number of raw reads	Number of reads mapped to reference genomes	Number of reads transformed into gene read count
<i>Meira miltonrushii</i>	Glucose rep1	20,598,574	20,050,912 (97.3%)	17,149,878 (83.3%)
	Glucose rep2	13,807,724	13,425,090 (97.2%)	11,528,300 (83.5%)
	Glucose rep3	13,820,124	13,462,382 (97.4%)	11,581,147 (83.8%)
	Tween40 rep1	8,844,964	8,591,376 (97.1%)	7,291,731 (82.4%)
	Tween40 rep2	19,389,616	18,750,634 (96.7%)	15,777,920 (81.4%)
	Tween40 rep3	11,274,474	11,000,424 (97.5%)	9,356,865 (83.0%)
<i>Tilletiopsis washingtonensis</i>	Glucose rep1	31,020,318	27,041,444 (87.2%)	23,844,503 (76.9%)
	Glucose rep2	27,998,824	25,096,946 (89.6%)	22,081,357 (78.9%)
	Glucose rep3	34,902,106	23,823,352 (68.3%)	21,282,911 (61.0%)
	Glucose rep4	38,816,072	34,307,588 (88.4%)	29,961,102 (77.2%)
	Tween40 rep1	36,987,660	33,971,316 (91.8%)	29,419,048 (79.5%)
	Tween40 rep2	37,490,828	35,061,240 (93.5%)	30,315,719 (80.9%)
	Tween40 rep3	34,836,746	32,062,658 (92.0%)	27,963,072 (80.3%)
	Tween40 rep4	15,744,164	14,358,930 (91.2%)	12,317,966 (78.2%)
<i>Ophiostoma novo-ulmi</i>	0 hr rep 1	12,558,694	6,745,116 (53.7%)	6,098,740 (48.6%)
	0 hr rep 2	7,702,036	3,645,220 (47.3%)	3,389,323 (44.0%)
	0 hr rep 3	12,521,615	7,009,633 (62.5%)	6,385,574 (51.0%)
	27 hr rep 1	9,609,094	5,145,382 (53.5%)	4,536,259 (47.2%)
	27 hr rep 2	7,708,972	3,550,559 (46.1%)	3,052,262 (39.6%)
	27 hr rep 3	8,383,075	4,533,933 (54.1%)	4,046,773 (48.3%)

Table 3.2 Summarized numbers of differentially expressed genes in each species
(adjusted p-value < 0.01)

Species	Total number of protein-encoding genes	Genes included in the analyses	Differentially expressed genes	Upregulated genes	Downregulated genes
<i>Meira miltonrushii</i>	7,452	7,400	3,981 (53.8%)	2,011 (27.2%)	1,970 (26.6%)
<i>Tilletiopsis washingtonensis</i>	7,011	6,999	3,702 (52.9%)	1,838 (26.3%)	1,864 (26.6%)
<i>Ophiostoma novo-ulmi</i>	8,640	8,393	4,112 (49.0%)	1,950 (23.2%)	2,162 (25.8%)
<i>Ustilago maydis</i>	6,785	5,639	2,834 (50.3%)	1,339 (23.7%)	1,495 (26.5%)

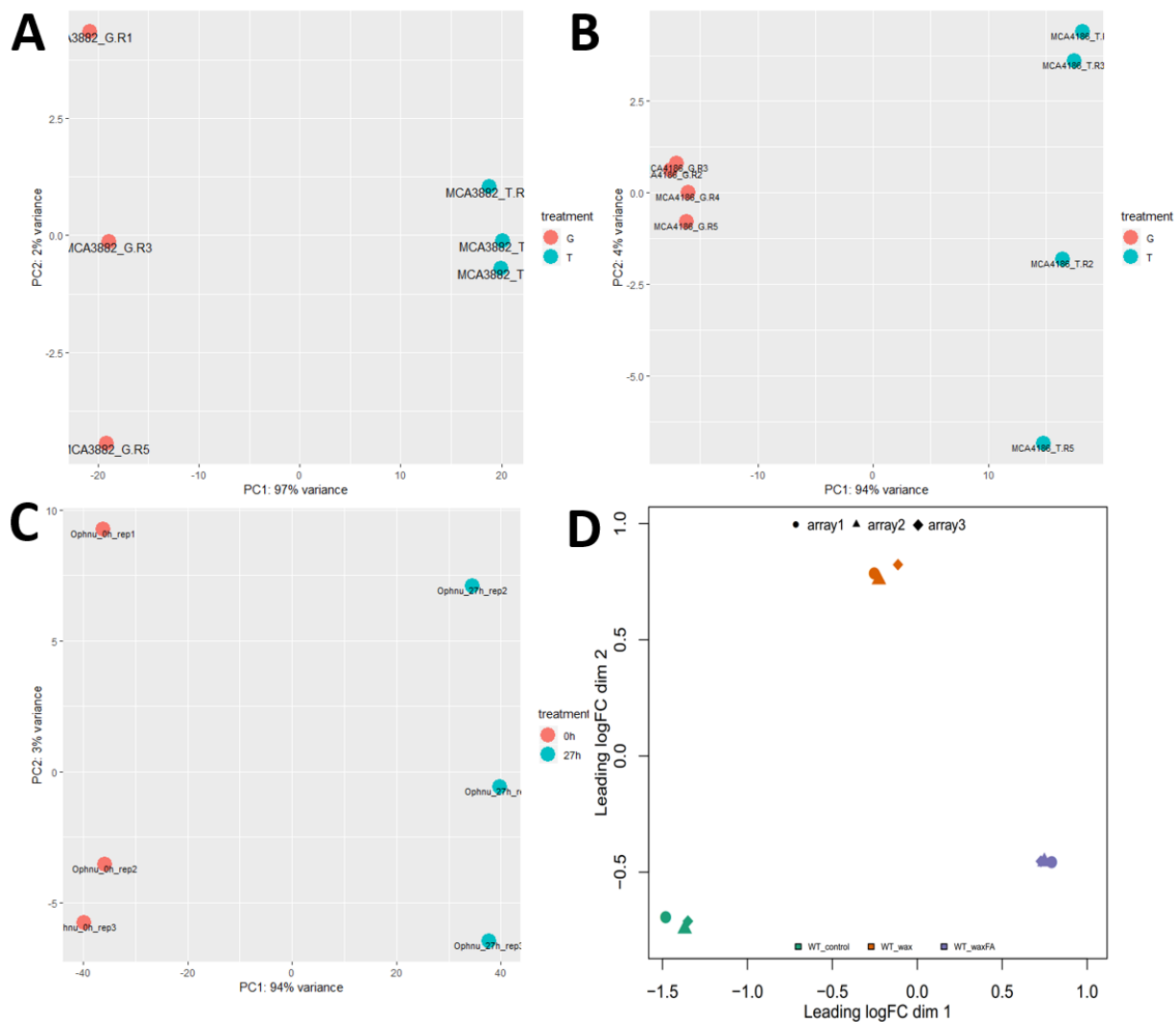


Figure 3.3 Principal component analyses (PCA) of gene expression data.

(A) – (C) PCA plots of transformed read counts for (A) *Meira miltonrushii* MCA3882, (B) *Tilletiopsis washingtonensis* MCA4186 and (C) *Ophiostoma novo-ulmi*. Most variability falls into the first PC axis. The plots show a clear separation between two treatments, which represent yeast growth and filamentous growth. (D) PCA plot of microarray expression data for *U. maydis*. Data points are clustered according to treatments.

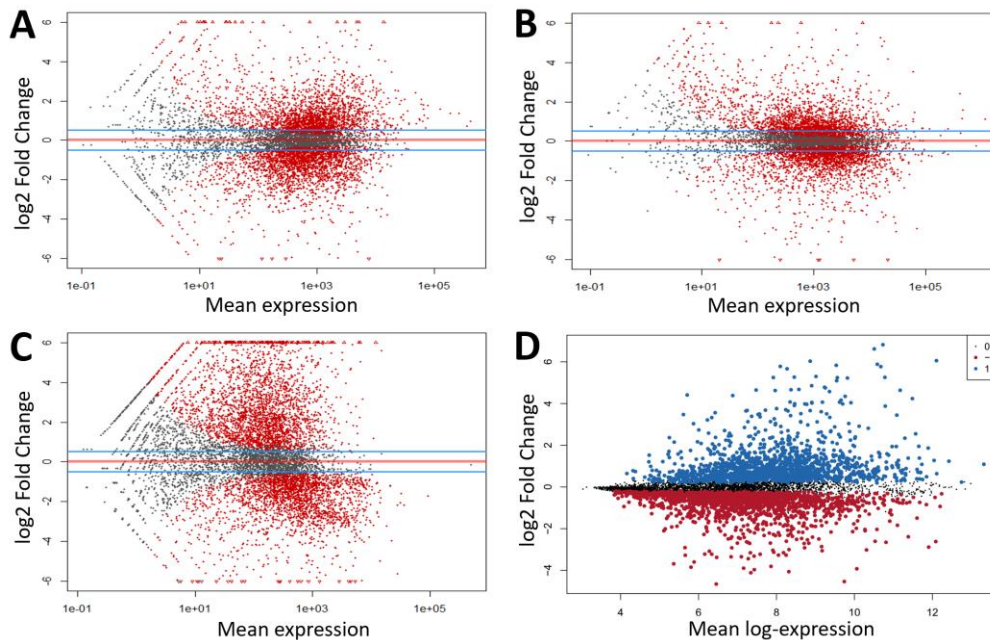


Figure 3.4 MVA plots for differential gene expression analyses of four studied species. (A) *M. miltonrushii* (B) *T. washingtonensis* (C) *O. novo-ulmi* and (D) *U. maydis*. The log₂ fold change was calculated as a proportion of the expression level in filamentous growth against yeast growth. For the (A) – (C) plots, red dots indicate differentially expressed genes. For the (D) plot, blue and red dots indicate differentially upregulated and downregulated genes, respectively.

3.4.4 Comparative transcriptomics

Among 2,653 orthogroups between *M. miltonrushii* and *T. washingtonensis*, we found 831 orthogroups that are differentially expressed in both species—338 and 493 of these have concordant and discordant expression patterns, respectively (Figure 3.5A and D). A larger number of discordant patterns do occur by chance ($\chi^2 = 28.911$, $df = 1$, $p\text{-value} = 7.78 \times 10^{-8}$). Among the 831 differentially expressed orthogroups, KOG functional classes in amino acid transport and metabolism (class E) and translation, ribosomal structure and biogenesis (class J) are significantly enriched (Table 3.3). The functional class in cell wall and membrane biogenesis (class M) has the second highest representation of differentially expressed genes with the odd ratio of 1.811, but is not significantly enriched based on the hypergeometric test.

There are 565 out of 2,227 orthogroups that are differentially expressed in Ustilaginomycotina species under yeast-to-hyphal transition (Figure 3.5B). Of this number, there are 43 commonly upregulated orthogroups, 100 commonly downregulated orthogroups and 422 discordant

orthogroups (Figure 3.5E). Notably, the discordant pattern between *T. washingtonensis* and the other two species is more prevalent than the other scenarios ($\chi^2 = 82.172$, $df = 3$, $p\text{-value} < 2.2 \times 10^{-16}$). Among the 143 concordant orthogroups, KOG functional classes in energy production and conversion (class C), amino acid transport and metabolism (class E) and cytoskeleton (class Z) are significantly enriched (Table 3.4). Class M is not significantly enriched from the analyses despite having a high odd ratio of 1.984.

When combining all four species into the analyses, only 49 out of 2,205 orthogroups have concordant expression patterns—16 and 33 of which are upregulated and downregulated during yeast-to-hyphal transition (Figure 3.5C and F). We found the discordant patterns of 328 orthogroups are not randomly distributed ($\chi^2 = 65.249$, $df = 7$, $p\text{-value} = 1.34 \times 10^{-11}$). The most prevalent discordant patterns are found between *T. washingtonensis* and the other three species, and between *T. washingtonensis* + *O. novo-ulmi* and *M. miltonrushii* + *U. maydis* (Figure 3.5F). Functional enrichment analyses reveal that genes in the classes C, E and Z are significantly enriched among orthogroups that are differentially expressed in all species (Table 3.5). The class M also has a high odd ratio of 1.623, but is not statistically significant.

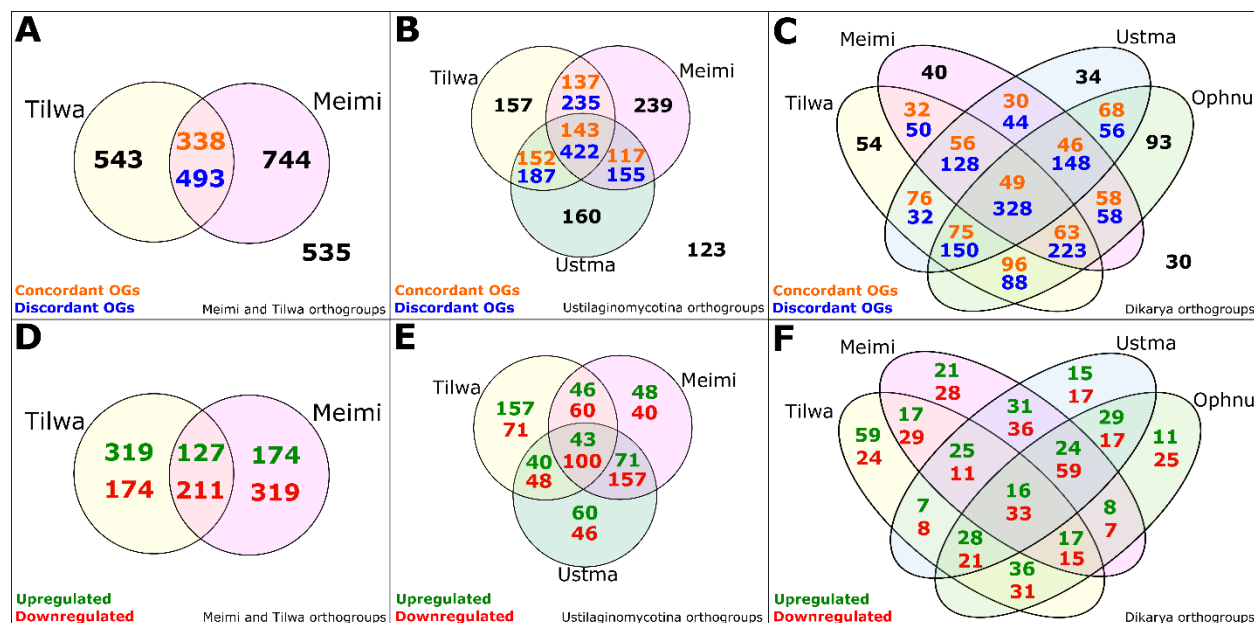


Figure 3.5 Summarized numbers of differentially expressed genes from comparative transcriptomics.

The comparisons are among two species (Meimi and Tilwa; A and D), three species (plus Ustma; B and E) and four species (plus Ophnu; C and F). (A) – (C) Venn diagrams depicting numbers of differentially expressed genes in each species. For overlapping regions, differentially expressed genes are classified into two categories. Genes that have concordant expression patterns (either upregulated or downregulated in every species) are labelled in orange, while genes that have discordant patterns (with at least one species having a conflicting pattern) are labelled in blue.

The total numbers of genes in each comparison are based on the number of orthogroups discovered from OrthoFinder: 2,653 genes for (A), 2,227 genes for (B) and 2,205 for (C).

(D) – (F) Venn diagrams depicting numbers of upregulated/downregulated genes among differentially expressed genes in all species. Numbers of the center regions in (A) – (C) were enumerated for possible scenarios of concordant/discordant patterns. Abbreviations are as follows: Meimi, *Meira miltonrushii*; Tilwa, *Tilletiopsis washingtonensis*; Ustma, *Ustilago maydis*; and Ophnu, *Ophiostoma novo-ulmi*.

Table 3.3 Enrichment analyses of KOG classifications for differentially expressed genes in *M. miltonrushii* and *T. washingtonensis*.

There are 831 out of 2,653 orthogroups that are differentially expressed in both species.

KOG classification	Total number of orthogroups	Number of differentially expressed orthogroups	Odd ratio	p-value
A - RNA processing and modification	192	44	0.649	0.995
B - Chromatin structure and dynamics	49	12	0.712	0.882
C -Energy production and conversion	141	51	1.295	0.091
D - Cell cycle control, cell division, chromosome partitioning	81	21	0.771	0.874
E - Amino acid transport and metabolism	108	51	2.083 [#]	< 0.001*
F- Nucleotide transport and metabolism	61	18	0.925	0.655
G- Carbohydrate transport and metabolism	86	28	1.077	0.416
H- Coenzyme transport and metabolism	64	23	1.252	0.234
I- Lipid transport and metabolism	76	24	1.026	0.503
J- Translation, ribosomal structure and biogenesis	270	101	1.436	0.004*
K- Transcription	153	35	0.648	0.991
L- Replication, recombination and repair	124	32	0.767	0.916
M- Cell wall/membrane/envelope biogenesis	20	9	1.811 [#]	0.138
O- Posttranslational modification, protein turnover, chaperones	256	90	1.277	0.045
P- Inorganic ion transport and metabolism	43	14	1.068	0.478
Q- Secondary metabolites biosynthesis, transport and catabolism	20	5	0.731	0.799
S- Unknown function	388	116	0.994	0.543
T- Signal transduction mechanisms	168	46	0.839	0.859
U- Intracellular trafficking, secretion, and vesicular transport	242	77	1.073	0.337
V- Defense mechanisms	9	2	0.626	0.827
Y- Nuclear structure	14	4	0.878	0.683
Z- Cytoskeleton	68	23	1.139	0.352

*Significant (p-value < 0.01)

[#]Odd ration > 1.5

Table 3.4 Enrichment analyses of KOG classifications for differentially expressed genes among *Ustilaginomycotina*.

Of 2,227 orthogroups shared among *M. miltonrushii*, *T. washingtonensis* and *U. maydis*, there are 565 orthogroups that are differentially expressed in all species.

KOG classification	Total number of orthogroups	Number of differentially expressed orthogroups	Odd ratio	p-value
A - RNA processing and modification	164	39	0.935	0.669
B - Chromatin structure and dynamics	43	10	0.895	0.677
C -Energy production and conversion	122	50	2.211 [#]	< 0.001*
D - Cell cycle control, cell division, chromosome partitioning	75	19	1.010	0.531
E - Amino acid transport and metabolism	96	49	3.360 [#]	< 0.001*
F- Nucleotide transport and metabolism	51	15	1.243	0.289
G- Carbohydrate transport and metabolism	73	20	1.128	0.370
H- Coenzyme transport and metabolism	49	16	1.453	0.147
I- Lipid transport and metabolism	69	21	1.315	0.185
J- Translation, ribosomal structure and biogenesis	229	35	0.512	1.000
K- Transcription	139	33	0.930	0.671
L- Replication, recombination and repair	109	21	0.700	0.944
M- Cell wall/membrane/envelope biogenesis	20	8	1.984 [#]	0.106
O- Posttranslational modification, protein turnover, chaperones	216	49	0.878	0.801
P- Inorganic ion transport and metabolism	38	12	1.375	0.231
Q- Secondary metabolites biosynthesis, transport and catabolism	17	6	1.616 [#]	0.243
S- Unknown function	323	74	0.900	0.790
T- Signal transduction mechanisms	150	32	0.802	0.881
U- Intracellular trafficking, secretion, and vesicular transport	217	46	0.797	0.920
Y- Nuclear structure	12	2	0.588	0.849
Z- Cytoskeleton	63	23	1.745 [#]	0.028*

*Significant (p-value < 0.05)

[#]Odd ration > 1.5

Table 3.5 Enrichment analyses of KOG classifications for differentially expressed genes among Dikarya.

Of 2,205 orthogroups shared among *M. miltonrushii*, *T. washingtonensis*, *U. maydis* and *O. novo-ulmi*, there are 377 orthogroups that are differentially expressed in all species.

KOG classification	Total number of orthogroups	Number of differentially expressed orthogroups	Odd ratio	p-value
A - RNA processing and modification	164	19	0.623	0.982
B - Chromatin structure and dynamics	43	4	0.493	0.952
C -Energy production and conversion	122	34	1.998 [#]	0.001*
D - Cell cycle control, cell division, chromosome partitioning	75	14	1.126	0.395
E - Amino acid transport and metabolism	93	33	2.878 [#]	< 0.001*
F- Nucleotide transport and metabolism	51	10	1.194	0.365
G- Carbohydrate transport and metabolism	72	11	0.876	0.703
H- Coenzyme transport and metabolism	49	9	1.099	0.460
I- Lipid transport and metabolism	69	13	1.138	0.389
J- Translation, ribosomal structure and biogenesis	229	29	0.691	0.974
K- Transcription	138	13	0.490	0.997
L- Replication, recombination and repair	107	17	0.921	0.661
M- Cell wall/membrane/envelope biogenesis	20	5	1.629 [#]	0.246
O- Posttranslational modification, protein turnover, chaperones	214	34	0.926	0.682
P- Inorganic ion transport and metabolism	38	7	1.101	0.477
Q- Secondary metabolites biosynthesis, transport and catabolism	17	4	1.500 [#]	0.328
S- Unknown function	319	49	0.889	0.783
T- Signal transduction mechanisms	147	21	0.807	0.842
U- Intracellular trafficking, secretion, and vesicular transport	217	34	0.909	0.715
Y- Nuclear structure	12	1	0.440	0.895
Z- Cytoskeleton	63	19	2.174 [#]	0.006*

*Significant p-value (< 0.05)

[#]Odd ration > 1.5

3.4.5 Functional analyses

First, we focused on genes assigned to the enriched functional classes (C, E, and Z). Most differentially expressed genes in class E (12 out of 33) are concordantly downregulated in all four species (Table 3.5). Genes encoding mitochondrial proteins, including receptors, membrane transporters, a ribosomal protein and a redox enzyme, are also concordantly downregulated (Table 3.6). However, there are 17 orthogroups in class C that are upregulated in *T. washingtonensis* but downregulated in the other species. These genes are annotated as components in the electron transport system and ATP synthases (Table 3.7).

For cytoskeletal orthogroups in class Z (Table 3.6), all four species have upregulation of the beta tubulin gene (*UMAG_05828* for *U. maydis*) and the gene encoding a SEY1-like protein (*UMAG_12136*, (228)). Conversely, we found a few notable discordant patterns (Table 3.7). One is the described Septin-3 gene in *U. maydis* (*UMAG_03449*), which is downregulated in *M. miltonrushii* but upregulated in the others. Another is several components of the actin-related protein ARP 2/3 complex—they are upregulated in *T. washingtonensis* and *O. novo-ulmi* but downregulated in the other two species.

Among concordantly upregulated genes in all four species, we detected some remarkable genes in signaling transduction mechanisms (Table 3.6). One is the gene encoding the cell end marker *Tea4* (*UMAG_01012*), which is found at a hyphal tip during polarized growth (170). Other components are orthologs of genes involved in phosphatidylinositol-mediated signaling (229–232) such as the phosphoinositide-4-kinase *Stt4* (*UMAG_06103*), the membrane protein *Efr3* for the assembly of *Stt4* complex (*UMAG_05218*), the phosphatidylinositol-3,4,5-triphosphatase phosphatase *PTEN* (*UMAG_03760*, described as *Ptn1* in *U. maydis*) and the E3 RING-type ubiquitin ligase *Pib1* (*UMAG_12183*).

In addition, we examined the expression patterns of known *U. maydis* dimorphism genes and their orthologs (Table 3.8). Although the whole gene set is not significantly enriched from the hypergeometric test (p-value > 0.05), we detected a few interesting transcriptional alterations. The *U. maydis* kinesin 3 (*Kin3*, *UMAG_06251*) and the cell end marker gene *Tea4* (*UMAG_01012*) are the only two orthogroups that have significant upregulation in all four species. Meanwhile, four

orthogroups are concordantly upregulated in Ustilaginomycotina species—the gene encoding ammonium permease *Ump2* (*UMAG_05889*), the gene encoding the paralog of protein kinase A *Uka1* (*UMAG_11860*), the gene encoding bZIP transcription factor *Cib1* (*UMAG_11782*) and a paralog of the gene encoding guanyl nucleotide exchange factor *Sql2* (*UMAG_11476*). These genes are not differentially expressed in *O. novo-ulmi*. Among discordant orthogroups (Table 3.8), we detected conflicting patterns in several signaling genes such as *Kpp2* (*UMAG_03305*), *Kpp6* (*UMAG_02331*), *Crk1* (*UMAG_11410*), *Rho1* (*UMAG_05734*) and *Cla4* (*UMAG_10145*). These genes are downregulated in *T. washingtonensis* but upregulated in the other species during yeast-to-hyphal transition.

Table 3.6 List of concordantly differentially expressed genes in all studied species

*Patterns (up, down) are based on the expression level in filamentous growth compared to yeast growth.

<i>U. maydis</i> gene id	KOG class	Pattern*	Potential function
<i>UMAG_11268</i>	C	Down	NADPH adrenodoxin oxidoreductase, mitochondrial
<i>UMAG_04530</i>	C	Down	Mitochondrial carrier protein
<i>UMAG_05546</i>	C	Down	Mitochondrial carrier protein
<i>UMAG_00311</i>	E	Down	Asparagine synthetase
<i>UMAG_01402</i>	E	Down	Chorismate synthase
<i>UMAG_10308</i>	E	Down	Catalyzes two activities which are involved in the cyclic version of arginine biosynthesis
<i>UMAG_03537</i>	E	Down	ornithine carbamoyltransferase
<i>UMAG_03974</i>	E	Down	Phosphoribosyl-AMP cyclohydrolase
<i>UMAG_04584</i>	E	Down	tryptophan synthase
<i>UMAG_04429</i>	E	Down	Aminotransferase class I and II
<i>UMAG_04899</i>	E	Down	aspartate-semialdehyde dehydrogenase
<i>UMAG_04939</i>	E	Down	arginase EC 3.5.3.1
<i>UMAG_05671</i>	E	Down	Aminotransferase class-III
<i>UMAG_10681</i>	E	Down	Ketol-acid reductoisomerase
<i>UMAG_11807</i>	E	Down	ATP phosphoribosyltransferase
<i>UMAG_11363</i>	H	Down	Lumazine binding domain
<i>UMAG_03071</i>	I	Down	Enoyl-CoA hydratase/isomerase family
<i>UMAG_00138</i>	J	Down	This protein promotes the GTP-dependent binding of aminoacyl-tRNA to the A-site of ribosomes during protein biosynthesis
<i>UMAG_10154</i>	J	Down	tRNA synthetases class I (E and Q), catalytic domain
<i>UMAG_11095</i>	J	Down	Anticodon-binding domain of tRNA
<i>UMAG_01184</i>	K	Down	Inherit from fuNOG: DNA-directed RNA polymerase I and III
<i>UMAG_04542</i>	O	Down	UBCc
<i>UMAG_05030</i>	O	Down	SPFH domain / Band 7 family
<i>UMAG_01421</i>	S	Down	Cyclin

Table 3.6 continued

<i>UMAG_12200</i>	S	Down	Sodium:solute symporter family
<i>UMAG_11758</i>	S	Down	Protein of unknown function (DUF1014)
<i>UMAG_05890</i>	S	Down	Mitochondrial ribosomal subunit protein
<i>UMAG_12321</i>	S	Down	CTNS
<i>UMAG_00614</i>	U	Down	Eukaryotic porin
<i>UMAG_11168</i>	U	Down	Tim10/DDP family zinc finger, mitochondrial
<i>UMAG_01096</i>	U	Down	Mitochondrial import receptor subunit Tom22
<i>UMAG_11021</i>	U	Down	Tetratricopeptide repeat
<i>UMAG_05496</i>	E, I	Up	cystathionine beta-lyase
<i>UMAG_03593</i>	I	Up	Fatty acid hydroxylase superfamily
<i>UMAG_00798</i>	L	Up	helicase, member of the UBC2 RAD6 epistasis group.
<i>UMAG_12183</i>	M	Up	E3 RING-type ubiquitin ligase with FYVE and PI3K-binding domains
<i>UMAG_00510</i>	O	Up	Holliday junction DNA helicase ruvB N-terminus
<i>UMAG_11751</i>	P	Up	Domain of unknown function (DUF307)
<i>UMAG_05218</i>	S	Up	Membrane protein orthologous to Efr3, a regulatory component for the assembly of phosphoinositide 4-kinase complex
<i>UMAG_05827</i>	S	Up	Inherit from euNOG: filamentation protein (Rhf1)
<i>UMAG_01012</i>	T	Up	SH3 domain protein orthologous to the cell end marker Tea4/Bud14
<i>UMAG_01737</i>	T	Up	Haemolysin-III related protein
<i>UMAG_03760</i>	T	Up	Phosphatidylinositol-3,4,5-trisphosphate 3-phosphatase
<i>UMAG_06103</i>	T	Up	Phosphoinositide 4-kinase
<i>UMAG_10018</i>	U	Up	EXS family orthologous to ER retention protein Erd1
<i>UMAG_11091</i>	U	Up	Pfam:TBC orthologous to GTPase-activating protein Gyp5
<i>UMAG_12136</i>	Z	Up	Cooperates with the reticulon proteins and tubule-shaping DP1 family proteins
<i>UMAG_05828</i>	Z	Up	Beta tubulin

Table 3.7 List of some interesting discordant genes in four species.

Shaded colors indicate discordant patterns: dark blue, discordance between *M. miltonrushii* and the other species; red, discordance between *T. washingtonensis* + *O. novo-ulmi* and *M. miltonrushii* + *U. maydis*; gold, discordance between *T. washingtonensis* and the other species; light blue, discordance between *M. miltonrushii* + *T. washingtonensis* and *O. novo-ulmi* + *U. maydis*; green, discordance between *U. maydis* and the other species; yellow, discordance between *M. miltonrushii* + *O. novo-ulmi* and *T. washingtonensis* + *U. maydis*; gray, discordance between *O. novo-ulmi* and the other species

¹ + sign means upregulated in a former group and downregulated in a latter group, - sign means in an opposite way. Patterns (upregulated/downregulated) are based on the expression level in filamentous growth compared to yeast growth.

<i>U. maydis</i> gene id	Pattern ¹	KOG class	Potential function
UMAG_11698	-	C	ATP synthase alpha/beta family, beta-barrel domain
UMAG_04716	-	C	V-ATPase subunit C
UMAG_03761	-	C	Aldehyde dehydrogenase family
UMAG_10682	+	C	FMN-dependent dehydrogenase
UMAG_03775	+	C, H	Oxidoreductase FAD-binding domain
UMAG_03911	-	C	mitochondrial carrier protein RIM2
UMAG_11517	+	C	ETC complex I subunit conserved region
UMAG_11583	+	C	Zinc-finger domain
UMAG_10804	+	C	2-oxoacid dehydrogenases acyltransferase (catalytic domain)
UMAG_00940	+	C	Ubiquinol-cytochrome C reductase hinge protein
UMAG_01478	+	C	ubiquinol-cytochrome C reductase complex core protein 2
UMAG_02477	+	C	Cytochrome c oxidase subunit Va
UMAG_05625	+	C	Complex 1 protein (LYR family)
UMAG_06324	+	C	ATP synthase delta (OSCP) subunit
UMAG_06051	+	C	NADH dehydrogenase ubiquinone iron-sulfur protein
UMAG_10820	+	C	Mitochondrial ribosomal protein L51 / S25 / CI-B8 domain
UMAG_00975	+	C	Mitochondrial ATP synthase g subunit
UMAG_05090	+	C	Mitochondrial membrane ATP synthase
UMAG_05465	+	C	Cytochrome c oxidase subunit IV
UMAG_02360	+	C	ATP synthase
UMAG_10397	+	C	Produces ATP from ADP in the presence of a proton gradient across the membrane
UMAG_10548	+	C	Mitochondrial ATP synthase B chain precursor (ATP-synt_B)
UMAG_03956	+	C	NADH-ubiquinone oxidoreductase ASHI subunit (CI-ASHI or NDUFB8)
UMAG_01686	-	C	PB1 domain
UMAG_05754	+	C	The electron transfer flavoprotein
UMAG_11740	+	C	Aldo/keto reductase family
UMAG_01782	+	C	Mitochondrial carrier protein
UMAG_10934	+	C	protein scd2 ral3
UMAG_05061	+	C	FAD dependent oxidoreductase
UMAG_11276	+	C	FAD linked oxidases, C-terminal domain
UMAG_02683	-	C	Aldo/keto reductase family

Table 3.7 continued

UMAG_04612	-	E	Methylenetetrahydrofolate reductase
UMAG_03850	+	E	glutamate synthase
UMAG_02792	+	E	Cysteine synthase
UMAG_05776	-	E	Aminotransferase class-V
UMAG_01048	-	E	Ornithine decarboxylase
UMAG_04152	-	E, J	Elongation factor
UMAG_10792	-	E	Adenosylmethionine decarboxylase
UMAG_05531	+	E	Aminotransferase class-V
UMAG_10708	+	E	Small subunit of acetolactate synthase
UMAG_05032	+	E	Carbon-nitrogen hydrolase
UMAG_04873	+	E	Isocitrate/isopropylmalate dehydrogenase
UMAG_00872	+	E	Aspartokinase
UMAG_11231	+	E	Histidine biosynthesis protein
UMAG_04705	-	E	N-acetylglutamate synthase involved in arginine biosynthesis (By similarity)
UMAG_02685	-	E	Aminotransferase class I and II
UMAG_01329	+	E	Isocitrate/isopropylmalate dehydrogenase
UMAG_01328	+	E	Isocitrate dehydrogenase
UMAG_04497	+	E	Argininosuccinate lyase
UMAG_04253	-	E, J	mRNA export factor elf1
UMAG_00950	+	E	Trifunctional enzyme bearing the Gln amidotransferase (GATase) domain of anthranilate synthase, indole-glycerolphosphate synthase, and phosphoribosylanthranilate isomerase activities
UMAG_03449	-	D, U, Z	K16945 cell division control protein 11 (described Sep3 in <i>U. maydis</i>)
UMAG_03599	-	D, U, Z	putative CDC12-septin
UMAG_11479	+	Z	ARP2/3 complex 34 kDa subunit
UMAG_11265	+	Z	Putative actin-related protein (ARP) 3
UMAG_10173	+	Z	ARP2/3 complex 20 kDa subunit (ARPC4)
UMAG_04417	+	Z	Domain of unknown function (DUF1899)
UMAG_10246	+	Z	ARP2/3 complex 21 kDa subunit
UMAG_02388	+	Z	Functions as component of the Arp2/3 complex which is involved in regulation of actin polymerization
UMAG_00582	+	Z	I/LWEQ domain
UMAG_11114	+	Z	Type-I myosin implicated in the organization of the actin cytoskeleton
UMAG_04218	-	Z	KISc
UMAG_11985	-	Z	KISc
UMAG_05761	-	Z	EB1-like C-terminal motif
UMAG_10783	+	Z	CLASP N terminal
UMAG_05405	+	Z	Actin binding protein
UMAG_04603	+	Z	ACTIN
UMAG_00950	-	Z	Spc97 / Spc98 family

Table 3.8 Gene expression patterns of known dimorphism genes from *U. maydis* literature and respective orthologs.

Color codes in the table are the following: red, significantly downregulated; green, significantly upregulated (adjusted p-value < 0.05) and black, no ortholog is found. A decimal point after a gene name indicates a possible paralog discovered from OrthoFinder.

Genes	Meimi	Ophnu	Tilwa	Ustma	Genes	Meimi	Ophnu	Tilwa	Ustma
Receptors, transmembrane proteins					Transcriptional regulators				
<i>Ump1</i>	93504	1982531	299646	11661	<i>Hap2</i>	63435	1980515	291628	8469
<i>Ump2</i>	154569	1981622	332386	13067	<i>Rbf1</i>	115089	1983016	64125	10444
<i>Msb2</i>	153618		328964	7294	<i>Rbf1.2</i>		1985597	299149	10438
<i>Sho1</i>	110010	1982322	329392	10427	<i>Rop1</i>	172680	1981843	341532	13209
<i>Pra1</i>	123976	1986126	327221	9597	<i>Rop1.2</i>				8330
<i>Pra1.2</i>	161223				<i>Prf1</i>	93068		349873	9949
cAMP/PKA pathway					<i>Cib1</i>	94769	1983493	361399	10796
<i>Gpa3</i>	135672	1979563	44190	12001	<i>Hos2</i>	145967		328652	7483
<i>Bpp1</i>	7852	1986096	301502	7530	<i>Tup1</i>	168580	1978797	330804	10556
<i>Uac1</i>	159581	1983371	327954	9116	<i>Gcn5</i>	109940	1981996	330623	9050
<i>Ubc1</i>	54131	1980275		7338	<i>Gcn5.2</i>	109940	1986361	330623	9050
<i>Adr1</i>	164464	1986295	330674	11983	<i>Gcn5.3</i>	156372		288290	13064
<i>Uka1</i>	121836	1985296	300158	7983	<i>Ros1</i>	116026	1985623	326807	13028
<i>Umpde1</i>	92967	1985371	294947	9751	<i>Pac2</i>	160005	1985623	291463	9920
<i>Umpde2</i>	160837	1979652	87503	12716	<i>Med1</i>	111975	1985348	290986	10879
<i>Ucn1</i>	125436	1978938	331497	7783	Other effectors				
MAPK pathway					<i>Hgl1</i>	158647		332249	7461
<i>Ubc2</i>	150079	1986103	313073	12787	<i>Rak1</i>	162121	1983575	330968	9624
<i>Ubc2.2</i>			285466		<i>Myo5</i>	167563	1984299	332564	11693
<i>Kpp4</i>	171607	1981571	295377	11572	<i>Kin1</i>	161038	1979957	329004	11527
<i>Kpp2</i>	159158	1986977	329263	10580	<i>Kin3</i>	161639	1982169	331589	13437
<i>Kpp6</i>	151809		299388	9542	<i>Kin3.2</i>		1986700		
<i>Fuz7</i>	162086	1979960	315954	8392	<i>Rrm4</i>	160584	1985205	354933	10780
<i>Crk1</i>	159064	1980766	133071	9733	<i>Clb1</i>	114513	1981400	331995	11051
<i>Rok1</i>	80127	1979340	35755	10995	<i>Clb1.2</i>	152529	1983212	294025	9811
GTPase-mediated signaling					<i>Clp1</i>	173993		359281	9656
<i>Ras2</i>	129751	1979529	300558	8517	<i>Chs5</i>	105722	1984583	329830	9792
<i>Sql2</i>	110111	1984546	212730	8394	<i>Chs7</i>	62820		294408	12625
<i>Sql2.2</i>	125181	1980682	338692	10079	<i>Mcs1</i>	127190	1979105	329339	10473
<i>Pdc1</i>	120982	1981635	331796	8235	<i>Mcs1.2</i>	189370	1979106	362445	10310
<i>Pdc1.2</i>		1984354			<i>Yup1</i>	137139	1979647	109250	12940
<i>Rho1</i>	140715	1983803	336018	12322	<i>Khd4</i>	160354	1981069	342519	11129
<i>Rho1.2</i>	148640	1984978	333050	9714	<i>Sep3</i>	161324	1982310	328207	10731
<i>Rho1.3</i>	70836		343249	11063	<i>Sep3.2</i>	161603		331586	
<i>Rac1</i>	59096	1981722	335337	7605	<i>Tea4</i>	190143	1986114	345022	7865
<i>Cla4</i>	161680		305688	9622					

3.5 Discussion

In this study, we performed comparative transcriptomics to discover candidate genes involved in yeast-to-hyphal transition across multiple dimorphic species. Our strategy aims to determine if findings from the corn smut fungus *U. maydis*, a renowned model organism for fungal dimorphism (67,121), are similar to other non-model species. These include *T. washingtonensis*, a phylloplane yeast-like fungus that causes the ‘white haze’ syndrome on postharvest apples (105,106), *M. miltonrushii*, a recently described species from a magnolia leaf phylloplane (209), and *O. novo-ulmi*, a causal agent of the serious Dutch elm disease (216). The two former species belong to the same subphylum with *U. maydis* (Ustilaginomycotina), while the latter belongs to a different phylum (Ascomycota). Lipid or hydrophobicity was used as a trigger for yeast-to-hyphal transition of the three Ustilaginomycotina species (196), while nutrient richness was used for *O. novo-ulmi* (198). All four species have genomic resources available in public database (41,116,217), and that facilitated our comparative analyses.

Our hypothesis is that these species share similar mechanisms during dimorphic transition, and the level of conservation is correlated with phylogenetic relatedness. According to the sampled taxa, we originally expected that the patterns of transcriptional alteration would be highly conserved between *M. miltonrushii* and *T. washingtonensis*, as both of them belong to the same taxonomic class Exobasidiomycetes (41). Moreover, the transcriptomic profile during yeast-to-hyphal transition of *O. novo-ulmi* was expected to be more different than the other three species. Based on the results, however, most discordant patterns of differentially expressed genes are found between *T. washingtonensis* and the other three species (Figure 3.5E and F). Exemplars of these include genes in the mitochondrial electron transport system, as well as several genes in the MAPK signaling pathway (Tables 3.7 and 3.8). Moreover, there are many other genes of *T. washingtonensis* that behave similar to those of *O. novo-ulmi*, especially several cytoskeletal genes (Figure 3.5F and Table 3.7). This conflict is unlikely due to experimental regimes as the discordant patterns are also prominent when we compared the transcriptomic profiles of *T. washingtonensis* to *M. miltonrushii*, a closely related species that was treated under a similar condition (Figure 3.5A and D, see Materials and Methods). Although it remains enigmatic to explain how the divergence of transcriptomic alteration occurs in *T. washingtonensis*, our study raises a concern that findings

from one species may not be inferable to a similar biological phenomenon in another species, even a closely related one.

Many genes in amino acid transport and metabolism (the KOG class E) are downregulated in filamentous growth compared to yeast growth (Table 3.5). Previous studies have concurrently shown that genes in amino acid metabolism are either specific or induced during yeast phase of some dimorphic fungi such as *Candida albicans*, *Histoplasma capsulatum* and *Paracoccidioides brasiliensis* (199). Amino acid transport and metabolism can be involved in fungal dimorphism in a couple of ways. The first explanation is about the dynamics of resource allocation. *Ustilago maydis* perceives lipids or hydrophobicity as a signal that it has landed on a host surface (89,121,196). As nutrient condition on a host surface is very poor, the pathogen needs to expedite morphogenesis for infection and colonization prior to production of new fungal masses, and some metabolic processes are less prioritized. Whereas, the yeast-to-hyphal transition of *O. novo-ulmi* is triggered after transferring the cultures from the minimal medium to the complete medium (198). Due to nutrient-rich condition, the activation of amino acid transport and metabolism may be unnecessary. The second explanation is about intracellular signaling affected by metabolic alteration. Exogenous nitrogen sources play a critical role in determining growth forms in many dimorphic fungi (67). Many studies focused on how nutrient conditions affect morphological switching, but knowledge on how cellular metabolism interacts with a developmental program is poorly understood. In our study, *M. miltonrushii* and *T. washingtonensis* were cultured under the same nitrogen condition for both yeast and filamentous growth. In contrast to downregulation of many genes for amino acid transport and metabolism (Supplementary Material 13), these two species have upregulation of the ammonium transporter *Ump2*, so does *U. maydis* (Table 3.8). The increased *Ump2* expression has been shown to induce filamentous growth of *U. maydis* under a nitrogen-deprived condition by interacting with Rho1 GTPase (90). Thus, it is possible that the manipulation of intracellular amino acids may yield a similar consequence to the starvation of exogenous nitrogen sources. An example is shown in *Histoplasma capsulatum* that there is an alteration of intracellular cysteine levels during hyphal-to-yeast transition (79).

Cytoskeletons have been widely known for determining cell shape and growth. Our transcriptomic study found at least two cytoskeletal components which are upregulated during filamentous growth

in all studied dimorphic species. Kinesin 3 and beta-Tubulin serve as machineries that transport secretory vesicles, containing components to build new hyphal mass, towards a hyphal tip (24,233). Another upregulated gene in all species is a homolog of a dynamin-like GTPase called *SEY1* in *Saccharomyces cerevisiae* (228). *SEY1* is involved in maintenance of tubular endoplasmic reticulum. As this tubular network can contribute to long-distance transport in several filamentous fungi (25), we speculate it may affect the transport of vesicles and other machineries for hyphal growth.

In addition to cytoskeletal genes, a few signal transduction genes related to cytoskeletal arrangement are commonly upregulated during filamentous growth (Table 3.6). One is the gene encoding the cell end marker *Tea4*, named as *TeaC* in *Aspergillus nidulans* and *Bud14* in *S. cerevisiae*. One function of this gene is to regulate actin cable architecture through interaction with formins (11,170,234). Actin cables are important for accumulation of secretory vesicles at the Spitzenkörper, and for exocytosis of vesicles at the hyphal tip (6). The function of *Tea4* on polarized hyphal growth has also been demonstrated in *A. nidulans* and *U. maydis* (11,170). Orthologs of the phosphatidylinositol-4-kinase complex *Stt4* and *Efr3* are the other two genes upregulated during filamentous growth (231,232,235). This protein complex regulates the level of phosphatidylinositol-4-phosphate, which affects actin organization in a cell (231,235).

On the other hand, we found a couple of conflicting expression patterns that reveal differences in hyphal microarchitectures. First is the downregulation of two septin genes in *M. miltonrushii*, *Sep3* and *CDC12*; these genes are upregulated in the other three species (Table 3.7). *Sep3* is required for filamentous growth in *U. maydis* (36), while *CDC12* is critical for maintaining polarized growth in *C. albicans* (33). The downregulation of these two genes may not indicate aberrant hyphal formation, but instead how frequently septation (i.e. cross-wall formation between cells) is formed along a hypha. The second case is significant upregulation of several components of the ARP2/3 complex in *T. washingtonensis* and *O. novo-ulmi* (Table 3.7). This actin-related protein complex assembles actin patches beneath the plasma membrane at a sub-apical region. The actin patches are involved in an endocytic process to recycle excess membranes resulting from continuous exocytosis at a hyphal tip (14,17). A previous study in *C. albicans* showed that although endocytosis is not impaired in an *arp2/3* mutant, it has a severe defect in hyphal

development (236). As all studied species display a similar phenotype (yeast to hyphal transition), it is interesting to study how the alteration of *ARP2/3* expression level affects the internal arrangement of the actin cytoskeleton, as well as morpho-physical properties of newly generated hyphae.

Current research in dimorphic fungi has emphasized the characterization of genes involved in signal transduction and transcriptional regulation (37,88,121). The cAMP/PKA pathway and the MAPK pathway are conserved signaling pathways that regulate morphogenesis in many dimorphic fungi (37,64,67). Despite being highly conserved, a mechanism for how each molecular player transduces a signal can be diversified. According to our study, many genes in these two pathways are transcriptionally altered during filamentous growth, but none of these have concordant expression patterns across all four species (Table 3.8). Another striking finding is that filamentous growth of *T. washingtonensis* has the downregulation of genes in the downstream MAPK cascade such as *Crk1*, *Kpp2/Ubc3* and *Kpp6*. Paradoxically, these genes are experimentally shown to be involved in filamentous growth of *U. maydis* (68,139,140,174). Furthermore, most genes in the GTPase-mediated signaling are also downregulated during filamentous growth of *T. washingtonensis* but are upregulated in the other three species (Table 3.8).

Despite many dissimilarities in signal transductions among the studied species, we found commonly upregulated genes that are potentially involved in signaling through membrane-localized phosphoinositides, which is widely known in a mammalian system like the PTEN/PI3K/mTOR pathway (237). Some upregulated genes include those in the abovementioned phosphatidylinositol-4-kinase complex *Stt4* and *Efr3*. Phosphatidylinositol-4-phosphate on the plasma membrane is demonstrated as a signaling molecule to control morphologies of vacuole and Golgi body, vesicular secretion, actin organization and lipid storage (231,235). A recent study also demonstrated that phosphatidylinositol-4-phosphate is important for dimorphic transition in *C. albicans* (238). Another commonly upregulated gene is an ortholog of the phosphatidyl inositol-3,4,5-triphosphate (PI3K) phosphatase *PTEN*. Although the deletion of *PTEN* in *U. maydis* does not show a direct effect on filamentous growth, the mutant has reduction of mating efficiency, virulence and teliospore formation (229). The other gene is the membrane-localized ubiquitin E3 ligase *Pib1*. Since the encoded protein has the FYVE finger domain which specifically binds to

PI3K, it potentially acts as a downstream target of the PI3K-mediated signaling (230). In addition, we found four genes that are concordantly upregulated during filamentous growth of all Ustilaginomycotina species—the high-affinity ammonium transporter gene *Ump2* (129), the bZIP transcription factor *Cib1* (156), the paralog of protein kinase A *Uka1* (134) and a paralog of the gene encoding guanyl nucleotide exchange factor *Sql2* (146). These are interesting candidates for future investigation to test whether they play a common role in dimorphic transition.

Even though this study allows us to gain insight about fungal dimorphism, there are a couple of limitations that need to be considered. First, our study examines the transcriptional profiles between yeast and filamentous growth forms at a single timepoint. This means we could not determine master “switching” genes that trigger the transition from yeast to filamentous growth. In addition, a developmental program in a fungal cell changes through time, and each species may have a different “peak” time for dimorphic transition. Therefore, time-course transcriptomic profiles are necessary to determine which genes have the transcript levels that are correlated with different stages of dimorphic transition. For example, Nigg and Bernier (198) utilized this strategy to discover that the upregulation of the MAPK cascade is involved during yeast-to-hyphal transition in *O. novo-ulmi*. The second limitation is based on the fundamentals of gene expression. Like most transcriptomic studies, we used the transcript level as a proxy to determine gene function. However, the gene function is also regulated at the translational and post-translational levels—obvious exemplars are kinase proteins that have phosphorylation to activate/inactivate their functions. Future combinations of transcriptomic, proteomic and phosphoproteomic data would improve the robustness of the analyses. Finally, our study consists of only dimorphic fungi that are either plant-associated or plant pathogenic. Yeast-to-hyphal transition is a common morphological switch when dimorphic plant pathogens encounter hosts (67). This is similar to the opportunistic pathogen *C. albicans* when it enters into a human body (37). Meanwhile, many dimorphic human pathogens such as *H. capsulatum* and *Blastomyces dermatidis* have a switch from hyphal to yeast growth in the human body (43). It will be intriguing to find out if the transcriptomic alterations between the yeast-to-hyphal stage in dimorphic plant pathogens and the hyphal-to-yeast stage in dimorphic human pathogens are mirrored with each other.

In conclusion, we performed multispecies transcriptomic analyses to understand how yeast and filamentous growth forms behave differently. During filamentous growth, functional classes in amino acid transport and metabolism, cytoskeleton and energy production and conversion are significantly enriched among differentially expressed genes in all studied species. Based on concordant expression patterns, we discovered several core candidates for yeast-to-hyphal dimorphic transition. However, many discordant expression patterns suggest several divergent biological responses, especially in *T. washingtonensis*. We also noticed that there are very few dimorphism genes that have similar expression patterns in all studied species. This raises a concern that knowledge derived from a model species like *U. maydis* may not be completely translational to other dimorphic fungi despite their phylogenetic relatedness.

CHAPTER 4. INVESTIGATING AN ASSOCIATION BETWEEN GENOMIC PROFILES AND GROWTH FORMS OF FUNGI IN DIKARYA

4.1 Introduction

With at least 5.1 million estimated species, the kingdom Fungi represents one of the most diverse eukaryotic groups in terms of modes of living, survival and reproduction (1,239). Most fungi produce a multicellular filament called a hypha as the basic component for complex structures like mushrooms, fruiting bodies, dormancy tissues, or even infection apparatuses. However, many other species survive and reproduce as a unicellular organism collectively termed 'yeast'. Yeast growth appears to be interspersed in the fungal kingdom. Dikarya, the subkingdom comprising the two major phyla Ascomycota and Basidiomycota, is widely known to harbor yeast-like fungi (3,38,42,62). In Ascomycota, two major clades containing yeasts are Saccharomycotina (budding yeasts) and Taphrinomycotina (fission yeasts). In Basidiomycota, yeast-like fungi are predominantly found in Ustilaginomycotina (smut fungi), Pucciniomycotina (relatives of rust fungi) and Tremellomycetes (jelly fungi, an early-diverging group of mushroom-forming fungi). Yeast growth can be found in certain stages of some species from Pezizomycotina and Mucoromycotina (43,98), although both lineages primarily comprise filamentous fungi. In some cases, fungi that can grow both as yeasts and as hyphae are termed as dimorphic fungi.

Understanding how yeasts are different from filamentous fungi remains a fundamental question in fungal cell biology, even in a post-genomic era. In terms of evolutionary aspects, it is also intriguing to understand how yeast-like fungi emerge in several lineages. Previous genomic studies have shown that the genomes of ascomycetes yeast-like fungi are relatively small and compact compared to filamentous fungi (240,241). A recent study of Nagy et al. (44) suggested that the filamentous growth form appeared as an ancestral state of Dikarya, and yeast-like fungi have independently evolved multiple times. They also found the parallel diversification of the Zn-cluster transcription factor as a potential regulatory toolkit for a yeast-like strategy. More recently, Nguyen et al. (190) discovered a set of complex multicellularity-associated genes that are mostly lost in yeast-like fungi in Saccharomycotina and Taphrinomycotina. However, these two studies provided limited sampling of yeast-like fungi in Basidiomycota, thus whether their findings are truly applicable for all yeast-like fungi throughout the fungal kingdom remains elusive.

Thanks to an advent of high-throughput sequencing and recent advances in bioinformatic analyses, numerous fungal genomes have been generated in the past few years (189). A huge number of currently available fungal genomes can help us revisit an idea of how genomes of yeast-like fungi are different from those of filamentous fungi, which can lead to explanation of potential mechanisms for their growth strategies. In this study we attempt to utilize multivariate approaches, commonly used in Community Ecology, to determine which genome properties, as well as which genes, are associated with types of growth form. We primarily focus on yeast-like and filamentous fungi in Dikarya since it is complicated to identify growth forms in many early-diverging fungi.

4.2 Hypotheses

- Genome statistics can be used to determine types of growth form of fungi in Dikarya. Being a simpler life form than filamentous fungi, yeasts have a simpler genome architecture like smaller genome size and fewer genes.
- As yeast-like fungi have independently emerged in several lineages, gene gain for becoming yeast-like fungi is lineage-specific. However, they may have a general trend of gene loss that makes them unable to grow as a prolonged multicellular stage.
- Genes involved in types of growth form would have functions in one of these categories: cell wall and membrane structures, cytoskeletons, vesicular trafficking, cell division, gene regulation and signal transduction pathway. Rationales behind this can be found in the literature review (Chapter 1).

4.3 Materials and Methods

4.3.1 Data collection

The 190 fungal genomes, comprising 123 ascomycete species and 67 basidiomycetes species, were included in this study (41,116,190,217,242–366). A list of studied genomes is provided in Table S1. The DNA assembly and protein models of each genome were downloaded from the DOE-JGI MycoCosm fungal genome portal (189). We classified the 190 species into three categories based on types of growth form: hyphal/filamentous fungi (H), dimorphic fungi (D) and yeasts (Y). In some cases, we considered both dimorphic and yeast species as yeast-like fungi. We partitioned the studied genomes into three datasets—Dikarya dataset, Ascomycota dataset and Basidiomycota

dataset. The Ascomycota and Basidiomycota datasets were split into halves as cross-validation (CV) datasets. The CV datasets were used to verify the consistency of the analyses. The numbers of studied species are summarized in Table 4.1.

Table 4.1 Numbers of genomes included in this study.

Lineages	Types of growth form			Sum
	Hyphal	Dimorphic	Yeast	
Agaricomycotina				
- Agaricomycetes	29	0	0	29
- Dacrymycetes	2	0	0	2
- Tremellomycetes	0	4	0	4
- Wallemiomycetes	1	0	0	1
Pucciniomycotina	4	4	7	15
Ustilaginomycotina	1	14	1	16
Summary: Basidiomycota	37	22	8	67
Pezizomycotina				
- Dothideomycetes	19	3	0	22
- Eurotiomycetes	16	9	0	25
- Leotiomycetes	10	0	0	10
- Orbiliomycetes	1	0	0	1
- Pezizomycetes	1	0	0	1
- Xylonomycetes	1	0	0	1
Saccharomycotina	1	15	17	33
Taphrinomycotina	1	1	5	7
Summary: Ascomycota	67	34	22	123
Summary: Dikarya	104	56	30	190

Six genome statistics were obtained as follows: genome size (in megabases) by counting the total number of bases in a genome assembly, gene number by recording the number of genes reported in a published genome, gene density by dividing the total number of genes by the genome size, GC content by calculating the percentage of C and G bases divided by the total number of four DNA bases (A, T, C, G), the percentage of repetitive elements by dividing the number of repeat-masked bases by the total base number of the genome assembly, and median number of exons per gene by finding the median of exons across all protein-coding genes. The genome statistics of the 190 genomes are tabulated in Supplementary Material 14.

Since the published 190 genomes were annotated under different platforms, we utilized eggNOG version 4.5 (219) as a standardized approach for functional annotation. Eukaryotic cluster of

orthogroup for the kingdom Fungi (fuNOG) was an annotation property selected for subsequent analyses. Then, we created a fuNOG gene distribution table. Each row represents each fungal genome/species and each column represents each fuNOG ID. In total, there are 37,732 fuNOG IDs among the 190 genomes. The gene distribution table can be found in Supplementary Material 15.

4.3.2 Analytical platform

All analyses were performed in RStudio version 1.1.463 equipped with R version 3.5.0. The following R packages were used: *vegan* version 2.5-3 (367), *car* version 3.0.2 (368), *DescTools* version 0.99.26 (369), *indicspecies* version 1.7.6 (370), *phytools* version 0.6.60 (371) and *ggplot2* version 3.1.0 (206).

4.3.3 Multivariate analyses of genome statistics

The six genome statistics of 190 genomes were included in multivariate analyses. Because the variables were measured in different scales, we standardized them by subtracting with a mean and dividing by a standard deviation. After that, we performed a multidimensional scaling (MDS) plot by using the Euclidean dissimilarity matrix as an input. Permutational analysis of variance (PERMANOVA) was performed, using the ‘adonis’ function from the *vegan* package, to test the difference between types of growth form.

After that, we used logistic regression to determine which genome statistics could serve as predictors for types of growth form. A yeast-like property was set as a binary value (0 as hyphal/filamentous and 1 as yeast-like). Receiver operating characteristic (ROC) curves were used to assess the prediction efficiency from the logistic regression analyses. The area under the ROC curve larger than 0.80 indicates a good variable for the prediction.

4.3.4 Multivariate analyses of gene composition

Because there are numerous identified fuNOG IDs, a heuristic way was designed to subset the data for our multivariate analyses. We selected fuNOG IDs having functional classes that are likely to be involved in fungal growth and development: classes M (cell wall, membrane and envelope biogenesis), U (intracellular trafficking, secretion, and vesicular transport), Z (cytoskeleton), D (cell cycle control, cell division and chromosome partitioning), K (transcription) and T (signal

transduction mechanisms). For each functional class, we performed NMDS to see how data points are ordinated and PERMANOVA to test the difference among types of growth form.

To determine which genes are associated with types of growth form, we utilized the function ‘multipatt’ from the *indicspecies* package (370). In Community Ecology, the function calculates sensitivity and specificity values and combines them as the indicator value index for each species on each site group, like a habitat type or a treatment (372). A site group that has the highest indicator value index infers that a given species serves as an indicator for the site group. Finally, the significance of the indicator species is tested through permutation. We used the following analogies to adopt this analysis to our study: each sampled site in Ecology is analogous to each sampled genome, each species present in a site is analogous to each gene harbored in a genome, and each site group is analogous to a desired trait (types of growth form in this case). We selected only significant genes having the indicator value index > 0.7 for the Dikarya dataset or > 0.75 for the Ascomycota and Basidiomycota datasets (arbitrary cutoffs). After analyzing the gene distribution in six functional classes (M, U, Z, D, K and T), genes that passed the cutoff criteria were combined and re-analyzed one more time as the combined datasets.

In addition to genes in the six functional classes, we adopted a list of 1050 complex multicellularity-associated genes from the previous study of Nguyen et al. (190) as an input for the analysis. These 1050 genes were annotated through eggNOG to get the fuNOG IDs, which were then used to subset the data and analyzed in a similar way as mentioned above. All analyses were performed under different scenarios (Dikarya, Ascomycota, Basidiomycota and cross-validation datasets). Genes associated with types of growth form are summarized as Venn diagrams and gene presence-absence matrices.

4.4 Results

First, we questioned if basic genome statistics can be used to explain fungal growth forms. Pairwise scatterplots of six variables reveal that there is a linear relationship between genome size and annotated gene number (Figure S1). There is also a correlation between genome size and gene density, but the trend is unlikely to be in a linear fashion. According to the NMDS plots, there is a clear separation between yeasts and filamentous fungi of Ascomycota (Figure 4.1). Dimorphic

ascomycetes fungi are found in both clusters, depending on which lineages they belong to. In Basidiomycota, yeast-like fungi (both dimorphic and yeast species) have distinct ordination from filamentous fungi. Results from PERMANOVA indicate that genome statistics are different among types of growth form, with R^2 values around 0.18 – 0.30 (Table S2). The homogeneity of group dispersion is assumed in all cases.

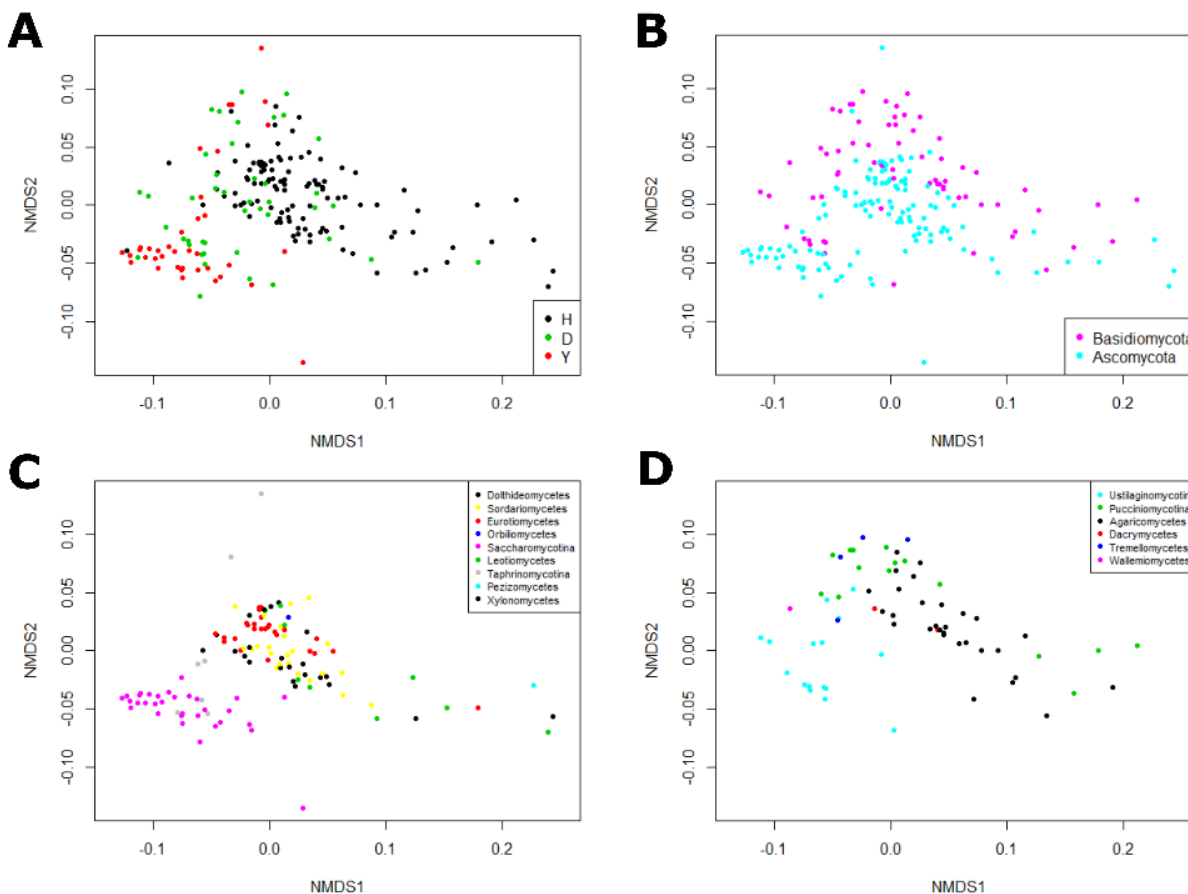


Figure 4.1 NMDS plots of genome statistics of 190 fungal genomes. Six variables of genome statistics were included in the analyses: genome size, gene number, gene density, percentage of transposable elements, GC content and median of exon numbers per gene. Data points are labelled based on (A) types of growth form (H, hyphal; D, dimorphic and Y, yeast), (B) phyla (Ascomycota and Basidiomycota), (C) lineages of Ascomycota and (D) lineages of Basidiomycota.

After that, we performed logistic regression analyses to find out which genome statistics are good predictors for types of growth form. Based on the areas under the ROC curves more than a standard cutoff (> 0.8), only genome size and gene number pass the criteria (Figure 4.2, S2). Boxplots show that yeast-like fungi have smaller genome sizes and lower gene numbers compared to filamentous fungi (Figure 4.2A, D). The critical values for yeast-like property ($p = 0.5$) are 27.28 Mb for genome size and 9119 for gene number, respectively (Figure 4.2B, E). The results are quite similar when analyzing across different datasets (Ascomycota, Basidiomycota and cross-validation datasets), except with slightly shifted critical values (Figure S3, Supplementary Material 16).

Next, we analyzed gene composition for the six functional classes potentially involved in fungal growth and development (classes M, U, Z, D, K and T). The NMDS plots are similar for all analyzed functional classes (Figure S4 – S9). In particular, the data ordinations of Ascomycota and Basidiomycota do not overlap with each other. Data points of Ascomycota are split into at least two clusters—one is composed of many yeast-like fungi of Saccharomycotina and the other comprises filamentous and dimorphic fungi in Pezizomycotina. An ordination pattern of Taphrinomycotina varies for each functional class. For Basidiomycota, there is a separation between the data clusters of yeast-like fungi and filamentous fungi. However, the distance between the two clusters is much less than the one between Saccharomycotina and Pezizomycotina (Figure S5 – S9). The exception is in the class M; data points of yeast-like fungi in Ustilaginomycotina are clustered together with filamentous fungi in Agaricomycotina (Figure S4). Details on which genes are associated with types of growth form in each dataset can be found in Supplementary Material 17, and numbers of indicator genes for each functional class are tabulated in Table S3.

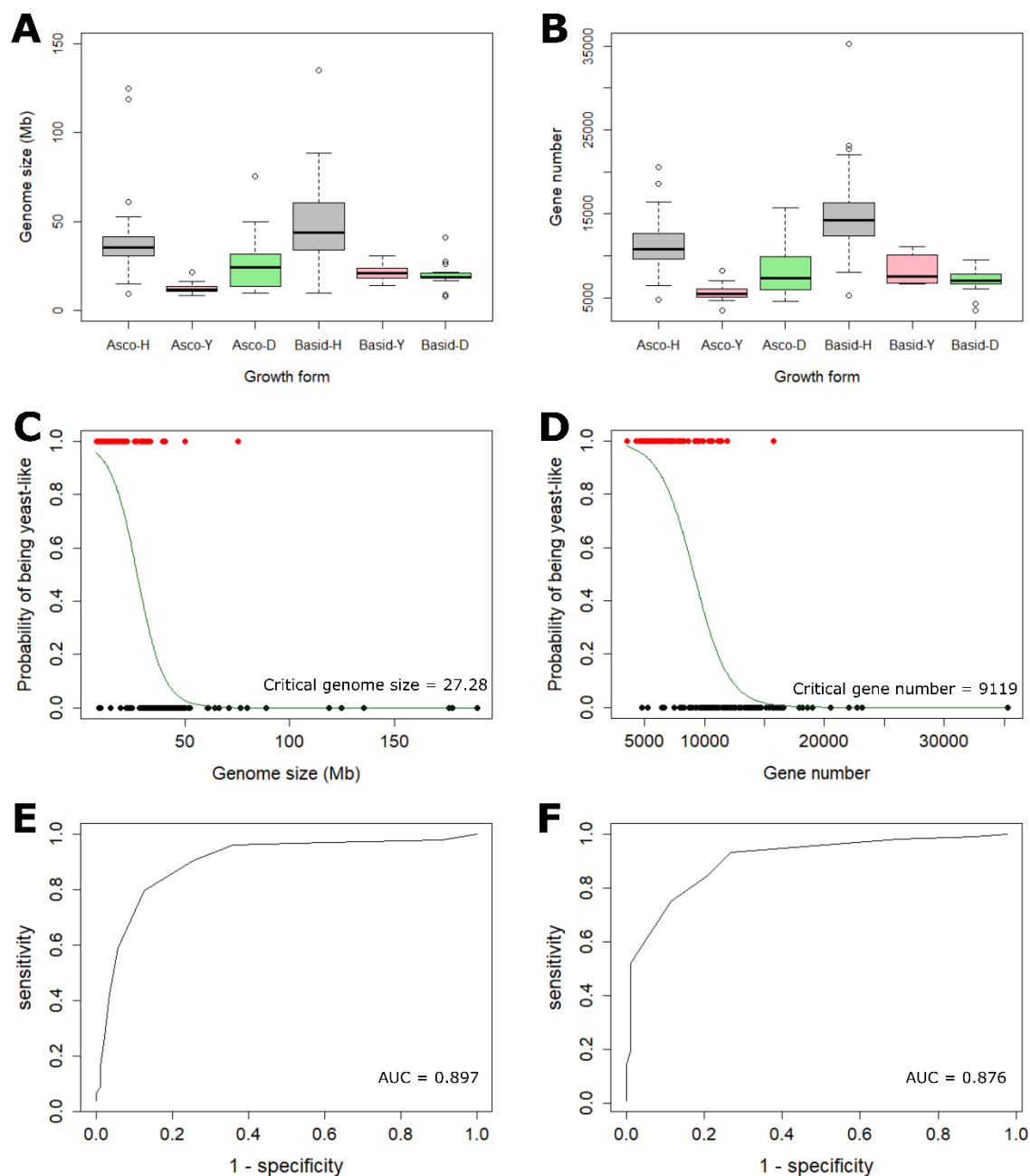


Figure 4.2 Logistic regression analyses of predictive variables for types of growth form. From six genome statistics, we found that genome size and gene number are good predictors for yeast-like fungi. (A) and (B) Boxplots showing the distributions of (A) genome size and (B) gene number grouped by types of growth form and phyla. (C) and (D) Logistic regression curves of (C) genome size and (D) gene number to predict yeast-like fungi. Critical values indicate the values having a probability of being yeast-like equal to 0.5. (E) and (F) Receiver operating characteristic (ROC) curves to assess prediction quality of (E) genome size and (F) gene number.

As fuNOG distribution patterns are unique for both phyla, we analyzed indicator genes separately for Ascomycota and Basidiomycota (Figure 4.3). Data ordination of the combined dataset in Ascomycota (the number of indicator genes = 192) confirms the findings from individual functional classes—yeast-like fungi (both dimorphic and yeast species) in Saccharomycotina and Taphrinomycotina have distinct gene compositions, but yeast-like fungi in Pezizomycotina have very similar gene distributions to their filamentous fungi relatives (Figure 4.3A and C). There are 152 out of 192 indicator genes present in all cross-validation datasets. Most of them are found in hyphal and dimorphic species of Pezizomycotina, while others are mostly found in Saccharomycotina (Figure 4.3E and S10). For the combined dataset in Basidiomycota (the number of indicator genes = 213), the data points are ordinated based on fungal lineages (Figure 4.3B and D). One major cluster comprises filamentous fungi in Agaricomycotina. This excepts Tremellomycetes, which consists of dimorphic species forming a distinct cluster. The other clusters are Pucciniomycotina and Ustilaginomycotina—these groups primarily contain yeast-like species with few exceptions of hyphal species. There are 133 out of 213 indicator genes present in all cross-validation datasets. Most of these are associated with hyphal growth form. However, gene presence/absence profiles do not show a distinct pattern between yeast-like fungi and filamentous fungi when compared to Ascomycota (Figure S11). Finally, there are only 16 indicator genes—four of which are present in all cross-validation datasets—found in both Ascomycota and Basidiomycota (Figure 4.3E and Table 4.2). Exemplars are NADPH oxidase regulator (fuNOG ID OPGC0), ubiquitin ligase (OPGFA), kinesin light chain (OPJ03) and components in the gamma-tubulin complex (OPK2S, OPKU6 and OPFIT). The presence/absence matrix of the 16 indicator genes is shown in Figure 4.5A.

Table 4.2 Indicator genes, identified by fuNOG IDs, that are associated with types of growth form in both Ascomycota and Basidiomycota. Input genes selected for the analyses are from six functional classes: M (cell wall, membrane and envelope biogenesis), U (intracellular trafficking, secretion, and vesicular transport), Z (cytoskeleton), D (cell cycle control, cell division and chromosome partitioning), K (transcription) and T (signal transduction mechanism). Terms shaded in gray are indicator genes that are present in all cross-validation datasets.

fuNOG ids	Class	Function
0PGFA	D	ubiquitin ligase subunit CulD
0PIG7	K	homeobox transcription factor
0PHAZ	K	Transcription factor
0PHYK	LT	Cryptochrome DASH
0PHGT	M	Trehalose synthase
0PMDB	MW	conserved hypothetical protein
0PJ6K	T	Neutral alkaline nonlysosomal ceramidase
0PGC0	T	NADPH oxidase regulator NoxR
0PM0V	T	Triacylglycerol lipase
0PJW1	U	Dynamin family
0PJ5A	U	Cell surface receptor MFS transporter
0PK2S	Z	gamma-tubulin complex component GCP6
0PJ03	Z	Kinesin family
0PKU6	Z	Spc97 Spc98 family protein
0PFIT	Z	gamma-tubulin complex component GCP5
0PK98	Z	conserved hypothetical protein

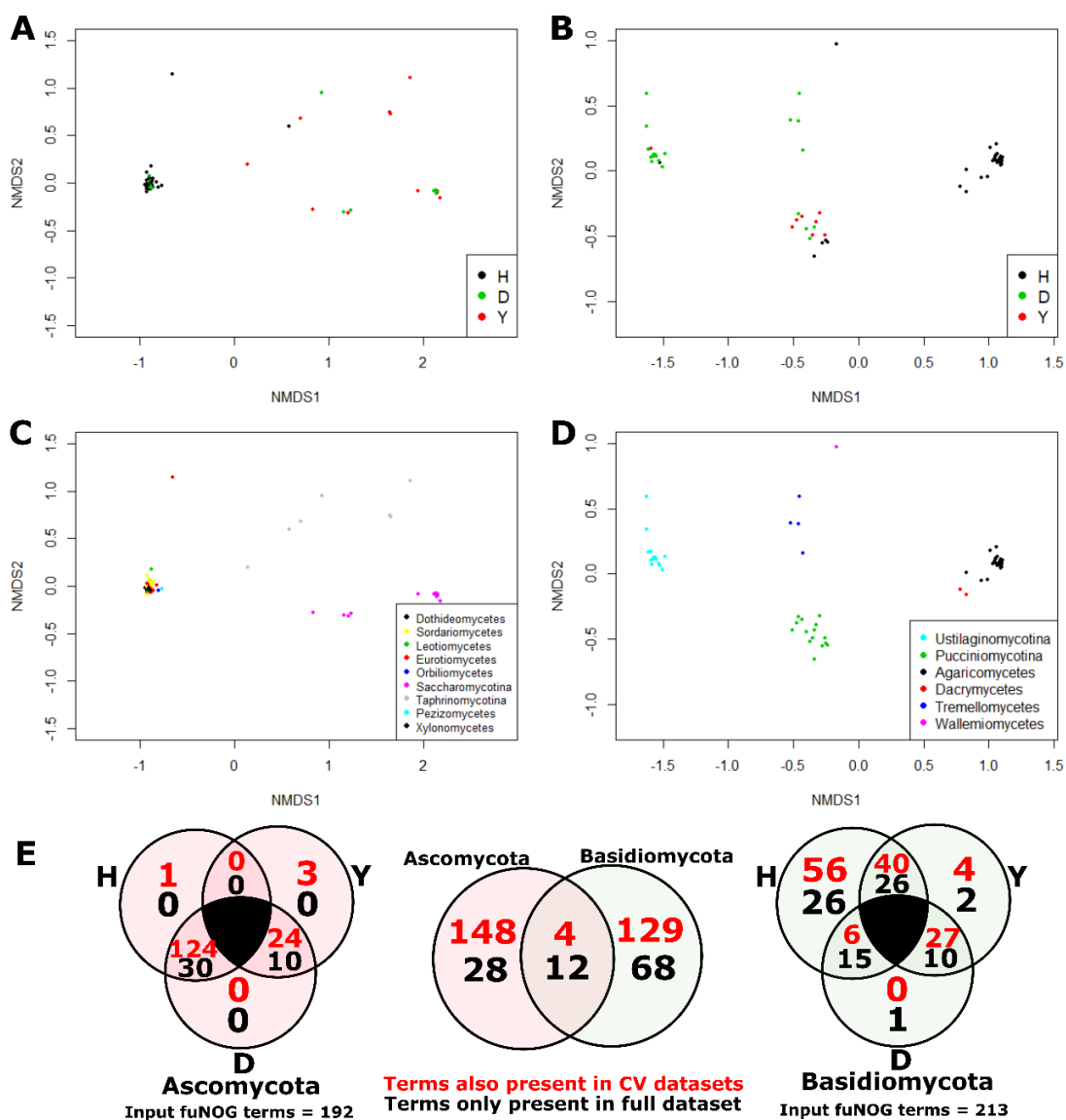


Figure 4.3 Analyses of indicator genes derived from six functional classes.

Input genes are from six functional classes: M (cell wall, membrane and envelope biogenesis), U (intracellular trafficking, secretion, and vesicular transport), Z (cytoskeleton), D (cell cycle control, cell division and chromosome partitioning), K (transcription) and T (signal transduction mechanism). Significant indicator genes from each class that passed cutoff criteria were combined and analyzed. As there is a remarkable difference in gene composition between Ascomycota and Basidiomycota, we performed separate analyses for each phylum. (A) and (C) NMDS plots of the distribution of 192 indicator genes across 123 Ascomycota species. Data points are labelled based on (A) types of growth form and (C) lineages of Ascomycota. (B) and (D) NMDS plots of the distribution of 213 indicator genes across 67 Basidiomycota species. Data points are labelled based on (B) types of growth form and (D) lineages of Basidiomycota. (E) Venn diagrams depicting numbers of indicator genes for each type of growth form (H, hyphal; D, dimorphic; and Y, yeast) for Ascomycota and Basidiomycota. The middle diagram depicts gene numbers that are either shared or unique in both phyla. Numbers of genes found in cross-validation datasets are labelled in red texts.

Finally, we adopted the 1050 complex multicellularity-associated genes from the study of Nguyen et al. (190) to find out if they can be used to explain types of growth form in Dikarya. After annotation through eggNOG, 1016 fuNOG IDs were identified and further used for multivariate analyses. The NMDS plots follow the same pattern to the ones from each individual fuNOG functional class: there is a clear separation between data points of Saccharomycotina and Pezizomycotina, while the degree of separation between yeast-like and filamentous fungi in Basidiomycota is much less than in Ascomycota (Figure 4.4A–D). The indicator species analyses discover 256 genes (210 of these in all cross-validation datasets) that are associated with types of growth form in Ascomycota. Almost all of them are not found in yeast growth (Figure 4.4E and S12). In contrast, only 65 genes (42 of these in all cross-validation datasets) pass the cutoff in the Basidiomycota datasets. There are indicator genes that are also found in yeast growth forms, while some others are not found in hyphal growth form (Figure 4.4E and S13). Considering both phyla, there are only 25 shared indicator genes, only 10 of which are found in all cross-validation datasets. The presence/absence matrix indicates that the majority of indicator genes are lost in Saccharomycotina and Ustilaginomycotina. Exemplars include NADPH oxidase (fuNOG ID 0PFUK), NADPH oxidase regulator (0PGC0) and Cytochrome p450 (0PGK3). Some others, like components in the gamma-tubulin complex (0PK2S, 0PKU6), are predominantly lost in Saccharomycotina and Pucciniomycotina yeasts. Conversely, there is a set of genes that is lost in Saccharomycotina but also Agaricomycotina (Figure 4.5B), suggesting that an association between gene presence/absence and types of growth form can be lineage-specific. These are such as GMC superfamily oxidoreductase (0PH8X), acyl-CoA dehydrogenase (0PFI9), branched-chain amino acid aminotransferase (0PI4C) and conserved hypothetical proteins (0PH3C and 0PHP9). The gene presence/absence matrix of the 25 indicators genes is shown in Figure 4.5B.

Table 4.3 Indicator genes, identified by fuNOG IDs, that are associated with types of growth form in both Ascomycota and Basidiomycota.

Input genes selected for the analyses are derived from the 1,050 complex multicellularity-associated genes from the previous study (190). Terms shaded in gray are indicator genes that are present in all cross-validation datasets.

Family	Class	Function
0PFAS	E	Alcohol oxidase
0PH8X	E	GMC superfamily oxidoreductase
0PI4C	E	Branched-chain amino acid aminotransferase
0PM5M	E	Developmental protein fluG
0QDQG	EI	NAD dependent epimerase dehydratase family protein
0PG84	G	Beta-glucosidases
0PK1M	G	Tetracycline transporter
0PFI9	I	acyl-CoA dehydrogenase
0PH37	O	HSP70 family
0PFUK	PQ	NADPH Oxidase
0PGK3	Q	Cytochrome p450
0PH41	S	decarboxylase
0PH3C	S	conserved hypothetical protein
0PHP9	S	conserved hypothetical protein
0PIG2	S	conserved hypothetical protein
X0PJIS	S	conserved hypothetical protein
0PJX5	S	conserved hypothetical protein
0PM6F	S	conserved hypothetical protein
0PNSC	S	Cystathionine beta-synthase
0PGC0	T	NADPH oxidase regulator NoxR
0PM0V	T	Triacylglycerol lipase
0PJ5A	U	Cell surface receptor MFS transporter
0PK2S	Z	gamma-tubulin complex component GCP6
0PK98	Z	conserved hypothetical protein
0PKU6	Z	Spc97 Spc98 family protein

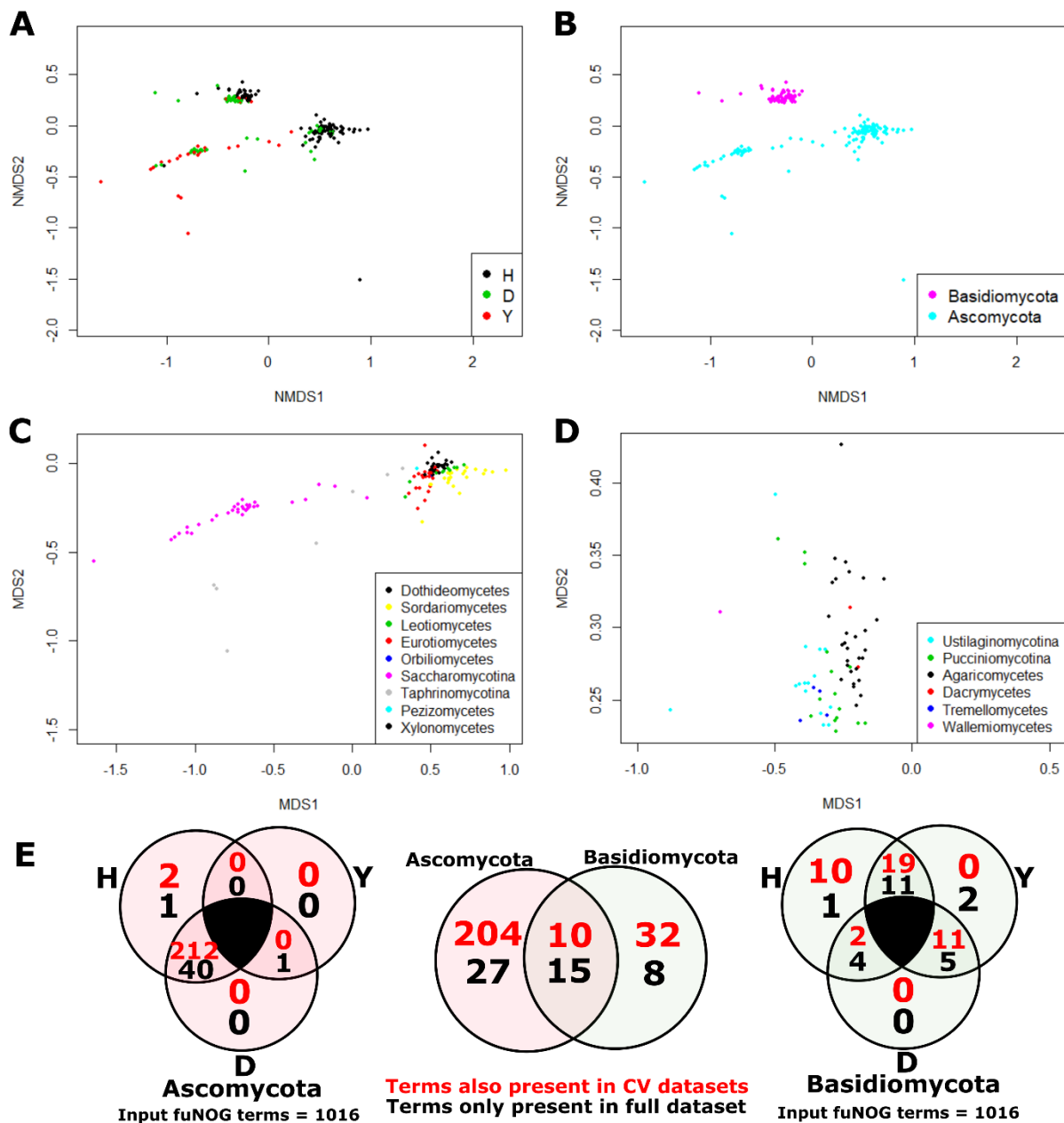


Figure 4.4 Analyses of indicator genes derived from multicellularity-associated genes recently published in a previous study.

(A) – (D) NMDS plots of the distribution of 1016 fuNOG IDs across 190 fungal genomes. Data points are labelled based on (A) types of growth form (H, hyphal; D, dimorphic; and Y, yeast), (B) phyla (Ascomycota and Basidiomycota), (C) lineages of Ascomycota and (D) lineages of Basidiomycota. (E) Venn diagrams depicting numbers of indicator genes for each type of growth form (H, hyphal; D, dimorphic and Y, yeast) for Ascomycota and Basidiomycota. The middle diagram indicates gene numbers that are either shared or unique in both phyla. Numbers of genes found in cross-validation datasets are labelled in red texts.

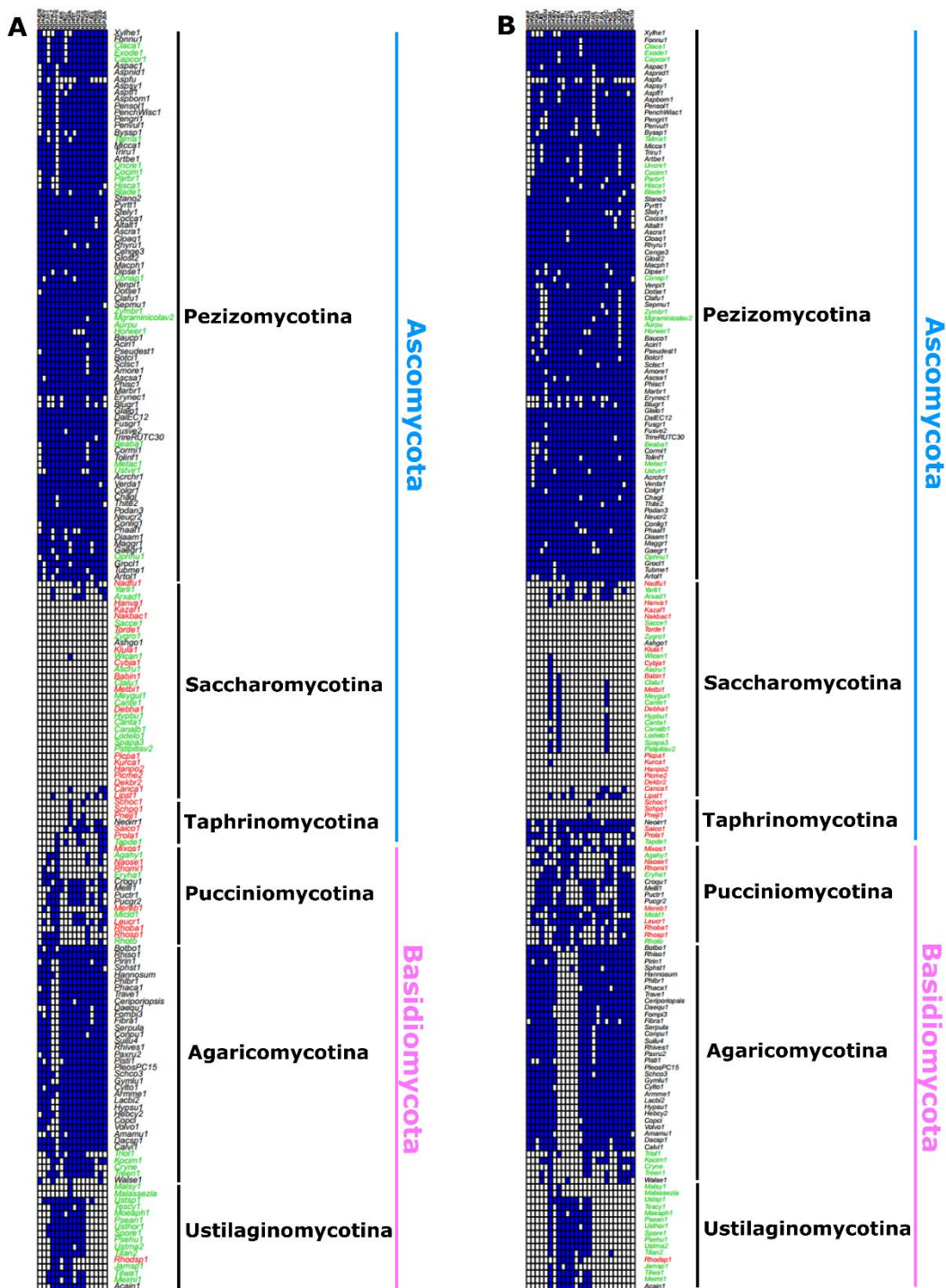


Figure 4.5 Presence-absence matrices of indicator genes shared in both Ascomycota and Basidiomycota datasets.

(A) 16 indicator genes derived from six functional classes. (B) 25 indicator genes derived from the complex multicellularity-associated genes published in Nguyen et al. (190). Growth forms are labelled by text colors: black, hyphal; green, dimorphic; and red, yeast. Gene presence and absence are indicated by blue and white fillings, respectively.

4.5 Discussion

In this study, we investigated if there is an association between genomic profiles and types of growth form in Dikarya fungi. Our analyses of genome statistics show that genome size serves as a proxy for yeast-like fungi—the smaller genome size is, the more likely a fungus has yeast growth (Figure 4.2, S3). Gene density, however, is not a good predictor for yeast-like growth. A small, but not always compact, genome is an indicator for yeasts especially in Basidiomycota (Figure 4.2, S2). Considering yeasts as a simpler life form than filamentous fungi, our findings support a traditional view that haploid genome size is positively correlated with organismal complexity (373). However, this is not always true in many eukaryotes since non-coding DNA can be a major constituent for large genome size (373). In addition, exceptions exist in a few species. For example, *Wallemia mellicola*, *Eremothecium gossypii* and *Neolecta irregularis* are among the smallest genomes sampled from this study (9.82, 9.10 and 14.59 Mb, respectively), but they are all filamentous fungi. In particular, *N. irregularis* can produce several cell types to produce visible fruiting bodies similar to many filamentous ascomycetes, which have an average genome size of 41.21 Mb (190).

Gene composition in each fungal genome is highly dependent on its phylogenetic placement in the fungal tree of life, so is the occurrence of yeast-like fungi (Figure 4.3, S4–S11). Better bioinformatic algorithms are necessary to account for phylogenetic signals to examine only the effect of types of growth form. However, to date the method has poorly been developed in this field. One thing that can be inferred from our study is the divergent level across different yeast-like lineages. Saccharomycotina has a unique gene composition from other fungal groups, suggesting a long evolutionary history for this clade to become yeast-like fungi. However, some Pezizomycotina species having a yeast stage harbor similar gene composition to their filamentous fungi relatives. This suggests alternative mechanisms, such as epigenetics or functional divergence, for their yeast-like strategy. Meanwhile, a degree of difference in gene composition between yeast-like fungi and filamentous fungi in Basidiomycota is much less when compared to the one in Ascomycota (Figure S4–S9). In addition, very low number of candidate genes (16 out of 389 genes) can explain types of growth form for both Ascomycota and Basidiomycota, most of which are lost in many yeast-like fungi (Figure 4.3E, 5A). Thus, our study supports the evolutionary hypothesis from Nagy et al. (44) that yeast-like fungi have independently evolved from

filamentous fungi ancestors. Loss of some genes may converge to the yeast strategy, but many other genes contribute to types of growth form in a lineage-specific fashion.

A similar trend is found when analyzing the set of genes from Nguyen et al. (190)—there is a clear separation of data points between Saccharomycotina and Pezizomycotina (Figure 4.4). Based on their assignment as complex multicellularity-associated genes, our initial expectation was that they would be uniquely found in filamentous fungi, but not yeast-like fungi. All indicator genes derived from our analyses are mostly absent in yeast species, including most Saccharomycotina species and some Taphrinomycotina species (Figure 4.4E, S12). It is notable that *Eremothecium gossypii*, the only filamentous fungus in Saccharomycotina, harbors none of these genes. Surprisingly, when we analyzed the Basidiomycota dataset, some of the ‘complex multicellularity-associated genes’ are also associated with yeast growth form, and they are absent in most mushroom-forming fungi in Agaricomycotina (Figure 4.4B, S13). In addition, some of the indicator genes are mostly present in filamentous ascomycetes, but predominantly absent in filamentous basidiomycetes (Figure 4.5B). As Nguyen et al. sampled fewer than 20 taxa for their study (190), this illustrates a case when limited taxon sampling can lead to a finding that may not be generalized in a broader context.

Although yeast-like fungi are products of convergent evolution, we noticed several candidate genes that are repeatedly lost in multiple yeast-like lineages (Figure 4.5). Some of these have been experimentally characterized as involved in fungal growth and development. For example, the trehalose synthase (OPHGT) was shown to control sporulation under a circadian rhythm in *Neurospora crassa* (374). The *Aspergillus nidulans* glutamine synthetase gene named *fluG* (OPM5M) functions in producing an extracellular signal that triggers asexual spore formation (375,376). The NADPH oxidase complex is another component extensively shown to regulate hyphal growth, sporulation and multicellular development of several ascomycetes species (377). Our analyses reveal that two components of the complex, NADPH oxidase 1 (OPFUK) and NADPH oxidase regulator (OPGC0), are lost in Saccharomycotina and Ustilaginomycotina. This confirms similar results from previous studies (190,378). In addition, some candidate genes are likely involved in hyphal growth. For instance, the kinesin family gene (OPJ03) is absent in most yeast-like lineages. Kinesin proteins serve as motor proteins that transport a vesicle and/or organelle through microtubules. Some kinesins are crucial for hyphal tip growth (24). Three genes

encoding components of the gamma-tubulin complex (OPFIT, OPK2S and OPKU6) are prevalently absent in Saccharomycotina, Taphrinomycotina and Pucciniomycotina (Figure 4.5). The gamma-tubulin complex controls where a microtubule spindle is formed, and it may guide a direction for polarized growth and septation (6). These listed genes, together with many other conserved hypothetical proteins (such as OPK98, OPMDB and OPJX5), would be interesting targets for future molecular genetic studies to understand how they contribute to fungal growth and development.

Overall, we conducted a pioneer study that utilizes publicly available genomic resources to determine how genomes of yeast-like fungi are different from those of filamentous fungi. Despite being independently evolved multiple times in the fungal tree of life, small genome size and loss of some homeotic genes are common traits for yeast-like fungi. Still, there are many more lineage-specific genes that need to be investigated. Also, the numerical approach we used in this study indicates association but not causation. Further empirical studies would shed a light on how yeast growth emerges from ancestors with hyphal growth. Finally, we anticipate that our study may spur computational biologists to develop an algorithm which incorporates phylogenetic signals into a large-scale comparative genomics in the future.

CHAPTER 5. CONCLUSION AND FUTURE DIRECTIONS

In this dissertation, I conducted multidisciplinary studies to understand the basis of fungal growth forms, especially in dimorphic fungi. Because the corn smut fungus *Ustilago maydis* serves as a model organism for fungal dimorphism and its role in pathogenesis (67,121), I selected Ustilaginomycotina, the subphylum to which *U. maydis* belongs, as the study framework to find out whether the dimorphic mechanism from the model organism is conserved throughout the lineage.

Findings from comparative physiological studies reveal that lipids can be potential common cues for morphological switching of several dimorphic species. Lipids are abundantly found on waxy plant surfaces (125), thus it is possible that these fungi perceive the lipids as sensation of their arrival on host surfaces. Lipids from plant surfaces have also demonstrated morphogenesis of other plant pathogens such as *Magnaporthe oryzae* and *Blumeria graminis* (211,212). According to this, modification of plant surface properties may play a preventive role against pathogen infection and colonization. Intriguingly, few other signals can induce yeast-to-hyphal transition in some studied species. Pectin, as a component of the plant cell wall, is shown to induce filamentous growth in dimorphic fungi for the very first time. This suggests that host recognition may still occur after plant pathogens penetrate plant tissues. In addition, high temperature can promote filamentous growth of a few Ustilaginomycotina species. In particular, *Moesziomyces aphidis* is shown to have extensive hyphal growth under human body temperature (37°C). This species, recently found as an opportunistic pathogen in immunocompromised patients (56,213), illustrates a case where a fungus belonging to a plant pathogenic group is able to facilitate a host jump by utilizing a cue from a new host for morphological transition. More researches are needed to determine whether these emerging pathogens can become a potential threat for human populations in the near future.

Comparative transcriptomics is another powerful tool to discover candidate genes for a similar biological phenomenon across multiple species. Surprisingly, although genes known for filamentous growth are highly conserved, I found very few genes are upregulated in all studied species. This indicates dissimilarity in their molecular mechanisms during yeast-to-hyphal dimorphic transition. Despite having low numbers, discovered ‘core’ genes such as the cell end

marker *Tea4* (170), the kinesin 3 *Kin3* (165) and the high-affinity ammonium transport *Ump2* (90) would be interesting targets for the design of chemicals or inhibitors to block morphological transition across different dimorphic fungi. Because dimorphic transition is often associated with pathogenicity (60), interfering with the transition would result in inhibition of disease development. My findings also discover other core candidate genes for which the roles in dimorphic transition are poorly understood. Examples are genes involved in the phosphatidylinositol-mediated signaling like genes in the Stt4 complex and *PTEN* (229,231,232,235). A recent study has shown that phosphoinositides affect dimorphic transition of *Candida albicans* (238). Therefore, I hope this study would initiate an interest in how lipids on the plasma membrane play a role in fungal growth and development. Future comparison with dimorphic animal pathogens would be useful to find out if there are any differences in their molecular mechanisms compared to dimorphic plant pathogens.

To consider a bigger picture, I performed large-scale comparative genomics to examine the association between genomic properties and types of fungal growth form (yeast, filamentous fungi and dimorphic fungi). Clearly, a lot of genomic properties are more dependent on phylogenetic lineages than types of growth form *per se*. Basidiomycetes dimorphic fungi have similar genomic properties to basidiomycetes yeasts. Meanwhile, dimorphic fungi in Ascomycota can be divided into two major groups: one having similarity with yeasts in Saccharomycotina and the other having similarity with filamentous fungi in Pezizomycotina. This finding supports a previous study that yeast-like fungi, considering both yeasts and dimorphic fungi, have been independently evolved multiple times in the fungal tree of life (44). One thing that yeast-like fungi, excluding those found in Pezizomycotina, share in common are smaller genome size and fewer gene numbers than filamentous fungi. In addition, many yeast-like lineages do not harbor several genes which are typically found in filamentous fungi. Some of these have roles in fungal growth and development, while some others need further experiments to verify their functions. However, it remains challenging at this point to find out what emerging machineries are critical for a yeast-like strategy. Indeed, only orthology assessment is not an adequate tool to study convergent evolution, and better bioinformatic algorithms are required to take phylogenetic relatedness into account when performing this association study.

Finally, I anticipate that my dissertation would stress an importance of studying non-model species. It is true that most molecular and genetic knowledge in biology has been derived from studies of model organisms. However, some systems do not appear to be comparable across other biological systems. Comparative research with inclusion of multiple species could be used to determine if the findings from the model organisms can be generalized in a broader context. Some interesting topics that can be studied under this framework are such as the evolution of plant pathogenicity, the emergence of obligate parasites and the diversification of secondary metabolism.

APPENDIX A. SUPPLEMENTARY FIGURES AND TABLES

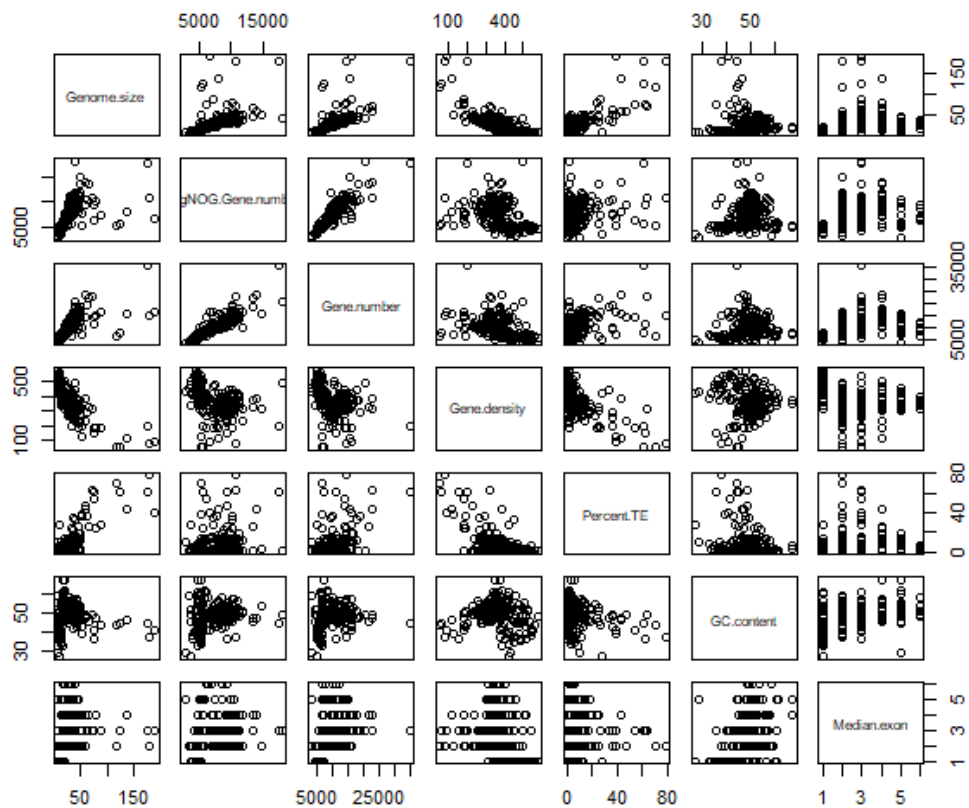


Figure S1 Pairwise scatterplots of genome statistics. Six variables from 190 fungal genomes were used for the plots: genome size, gene number, gene density, percentage of transposable elements, percentage of GC content and median of exon numbers per gene.

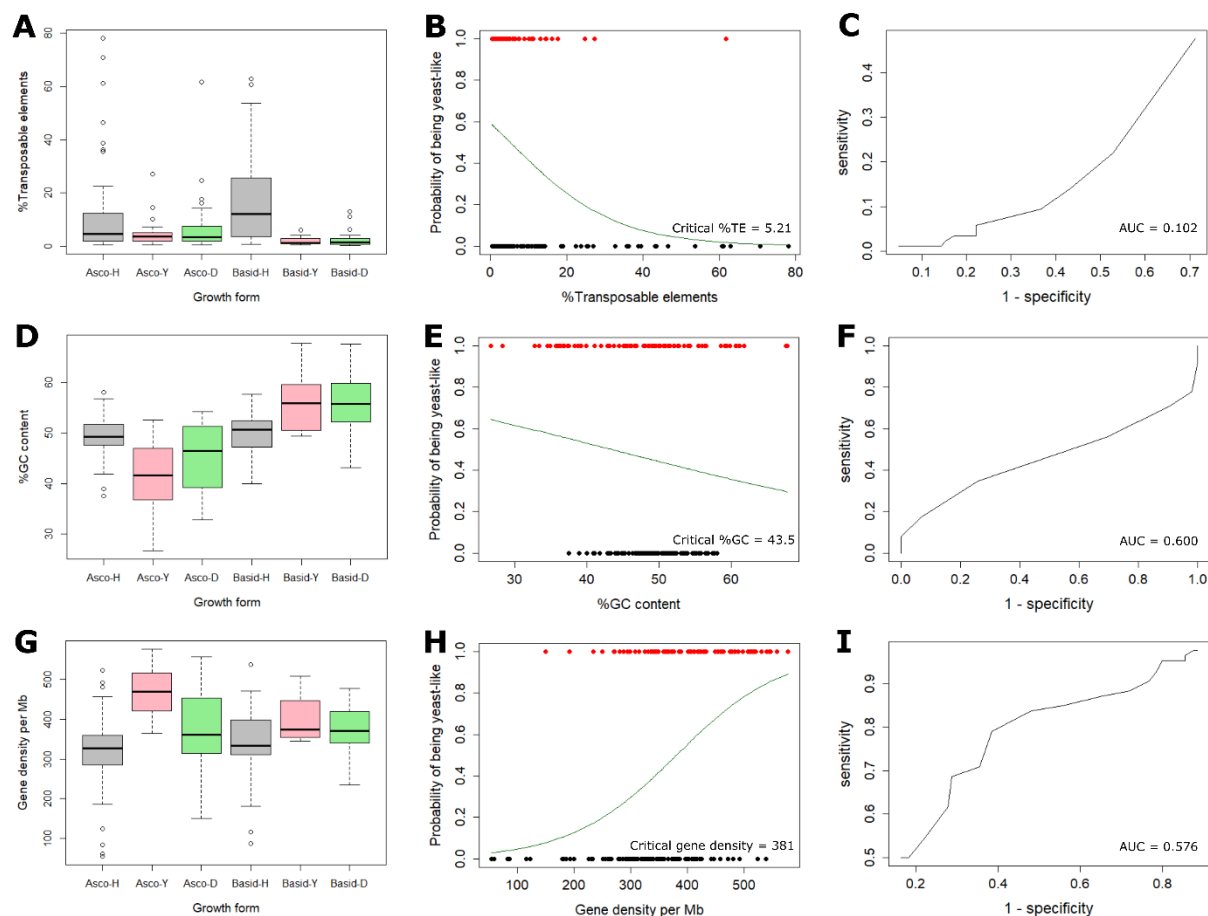


Figure S2 Logistic regression analyses of three genome statistics for predicting types of growth form. (A), (D) and (G) Boxplots showing the distribution of (A) percentage of transposable elements, (D) percentage of GC content and (G) gene density. (B), (E) and (H) Logistic regression curves of (B) percentage of transposable elements, (E) percentage of GC content and (G) gene density to predict yeast-like fungi. Critical values mean the values having a probability of being yeast-like equal to 0.5. (C), (F) and (I) Receiver operating characteristic (ROC) curves to assess prediction quality of (C) percentage of transposable elements, (F) percentage of GC content and (I) gene density.

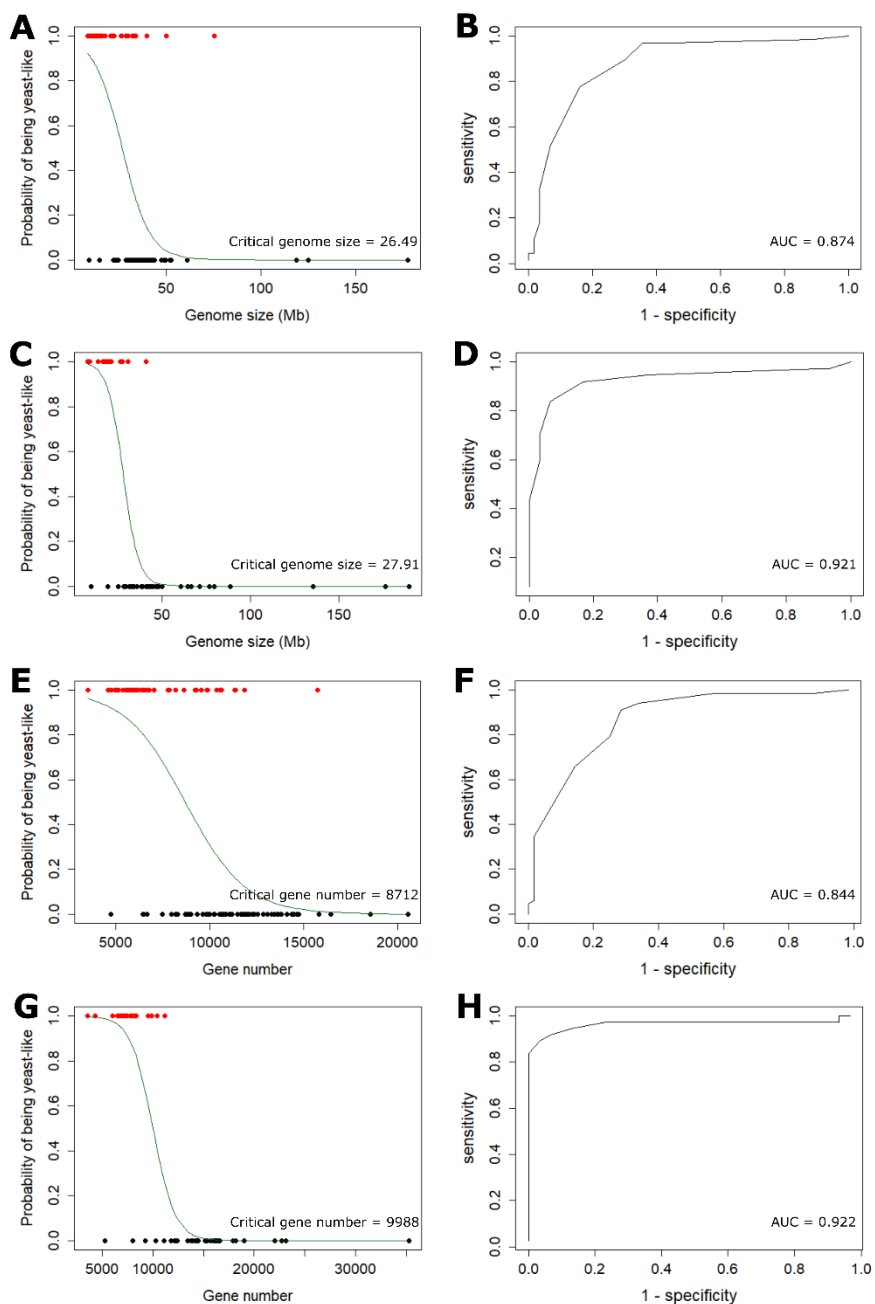


Figure S3 Logistic regression analyses of (A) – (D) genome size and (E) – (H) gene number for predicting types of growth form. The analyses were performed separately for (A, B, E, F) Ascomycota and (C, D, G, H) Basidiomycota. (A, C, E, G) Logistic regression curves of (A, E) genome size and (C, G) gene number to predict yeast-like fungi. Critical values mean the values having a probability of being yeast-like equal to 0.5. (B, D, F, H) Receiver operating characteristic (ROC) curves to assess prediction quality of (B, F) genome size and (D, H) gene number.

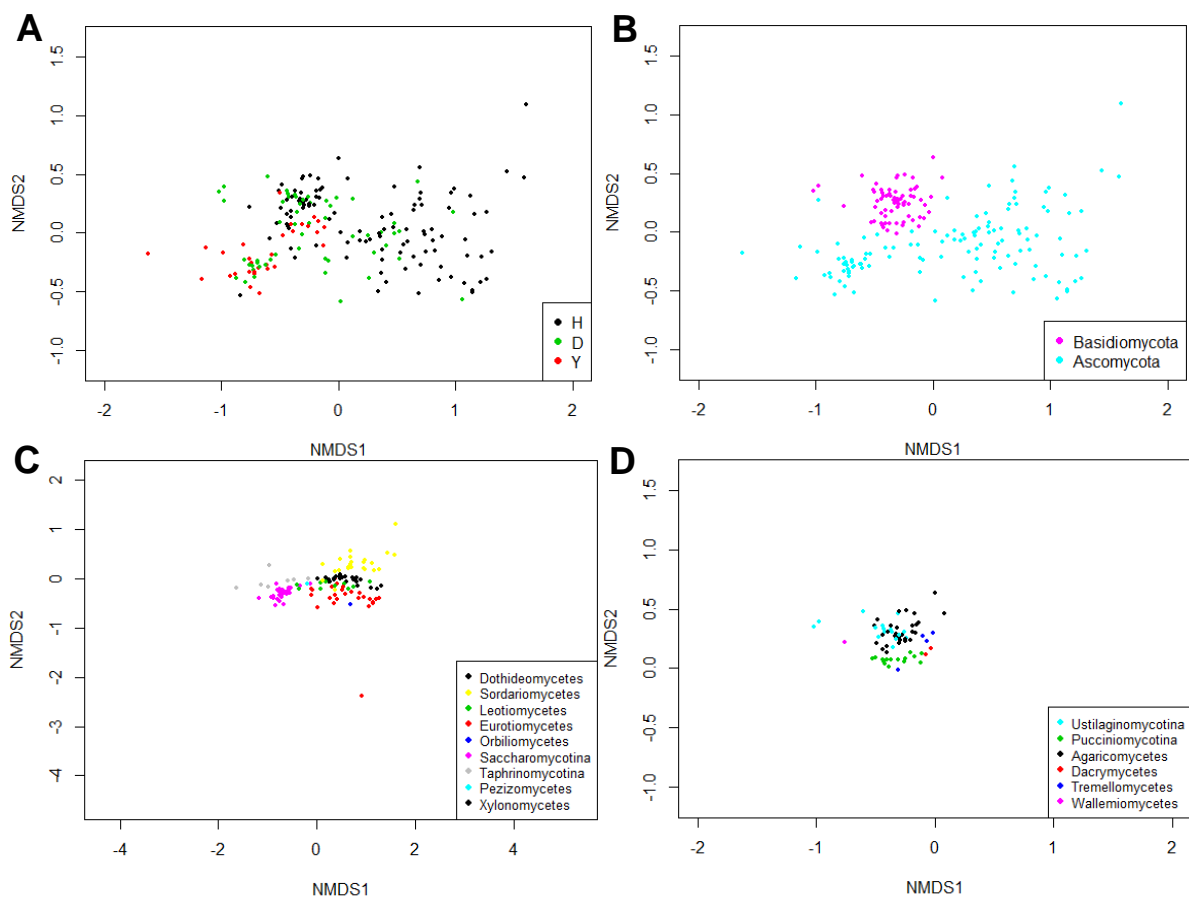


Figure S4 NMDS plots of genes involved in cell wall, membrane and envelope biogenesis (class M). The 356 fuNOG IDs classified in class M were included in the gene distribution table of 190 fungal genomes. Data points are labelled based on (A) types of growth form (H, hyphal; D, dimorphic; and Y, yeast), (B) phyla (Ascomycota and Basidiomycota), (C) lineages in Ascomycota and (D) lineages in Basidiomycota.

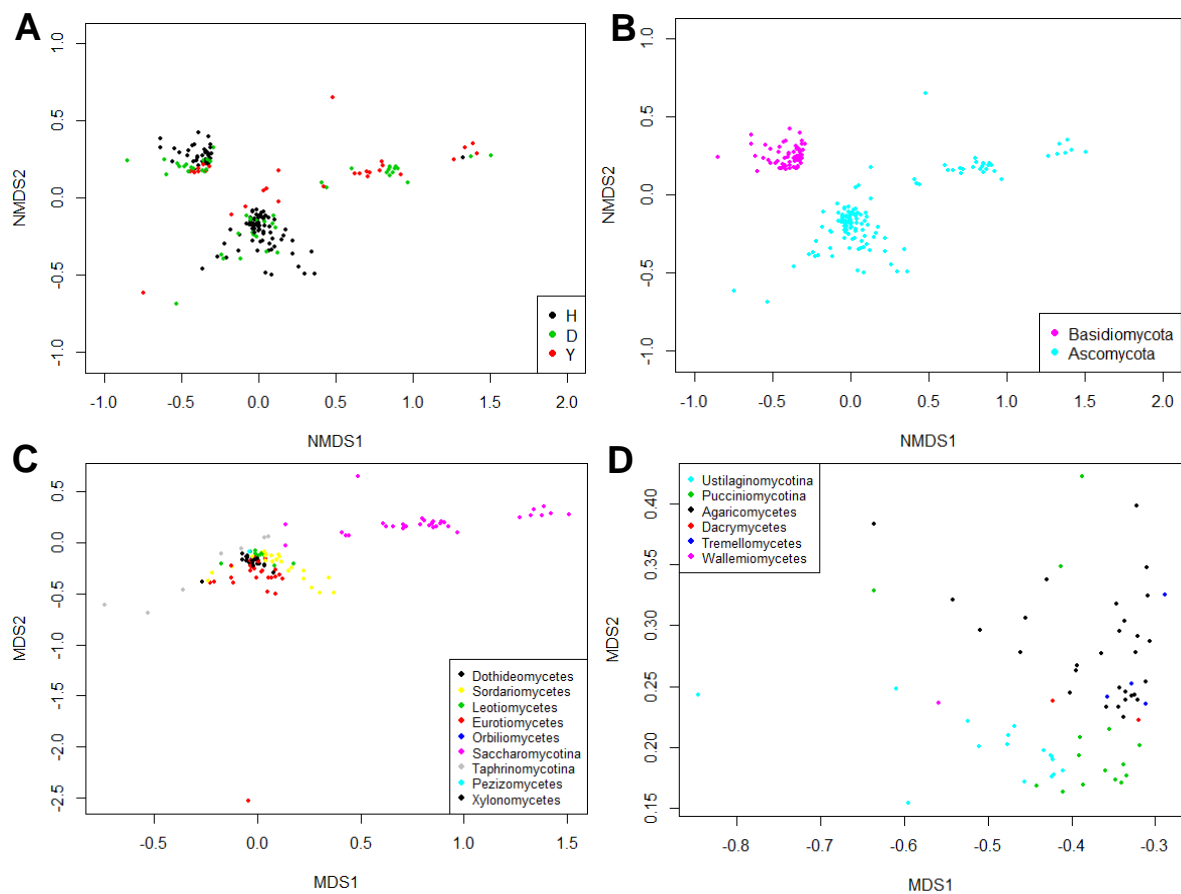


Figure S5 NMDS plots of genes involved in intracellular trafficking, secretion, and vesicular transport (class U). The 1045 fuNOG IDs classified in class U were included in the gene distribution table of 190 fungal genomes. Data points are labelled based on (A) types of growth form (H, hyphal; D, dimorphic; and Y, yeast), (B) phyla (Ascomycota and Basidiomycota), (C) lineages in Ascomycota and (D) lineages in Basidiomycota.

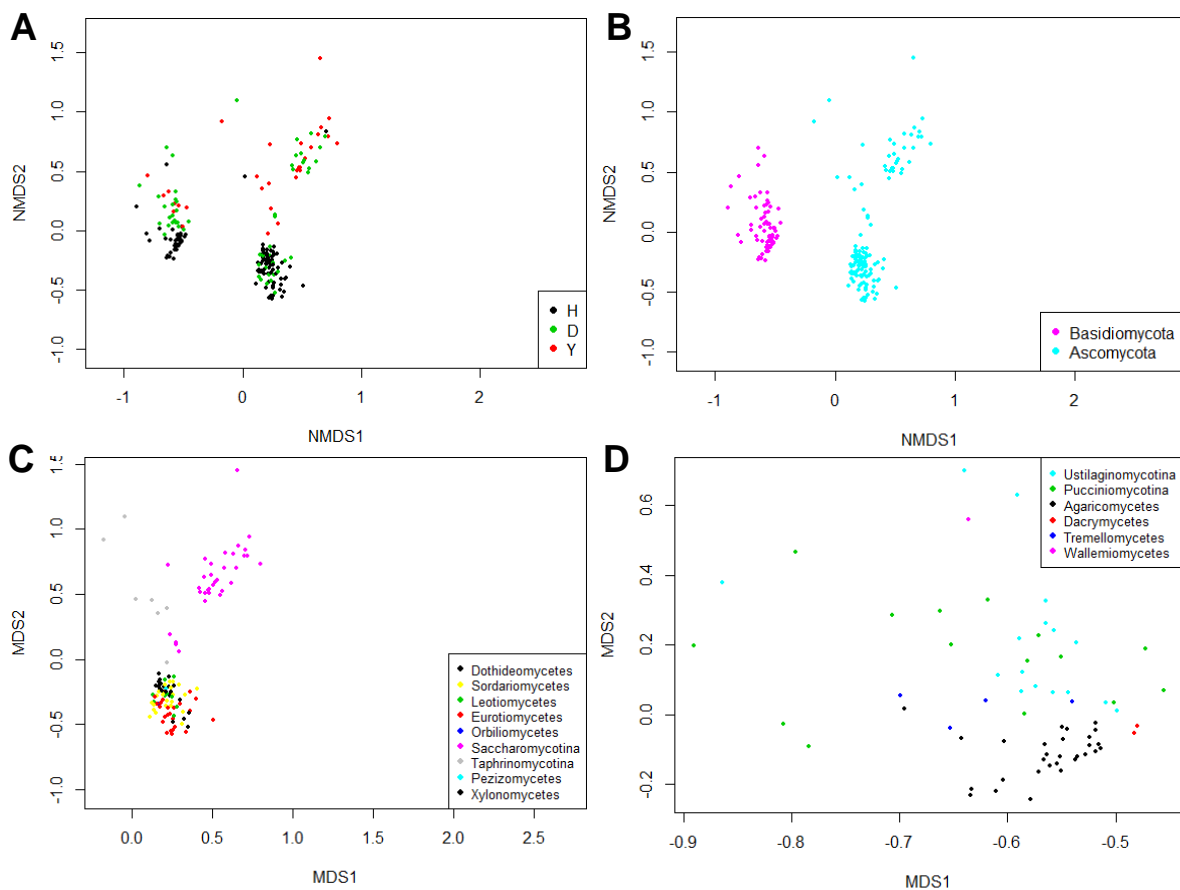


Figure S6 NMDS plots of genes involved in cytoskeletons (class Z). The 281 fuNOG IDs classified in class Z were included in the gene distribution table of 190 fungal genomes. As the NMDS plots could not be generated under 281 dimensions (genes), we trimmed the dimensions down by selecting only fuNOG IDs present in 5 – 95% of studied genomes. The 139 fuNOG IDs were ultimately used for constructing the plots. Data points are labelled based on (A) types of growth form (H, hyphal; D, dimorphic; and Y, yeast), (B) phyla (Ascomycota and Basidiomycota), (C) lineages in Ascomycota and (D) lineages in Basidiomycota.

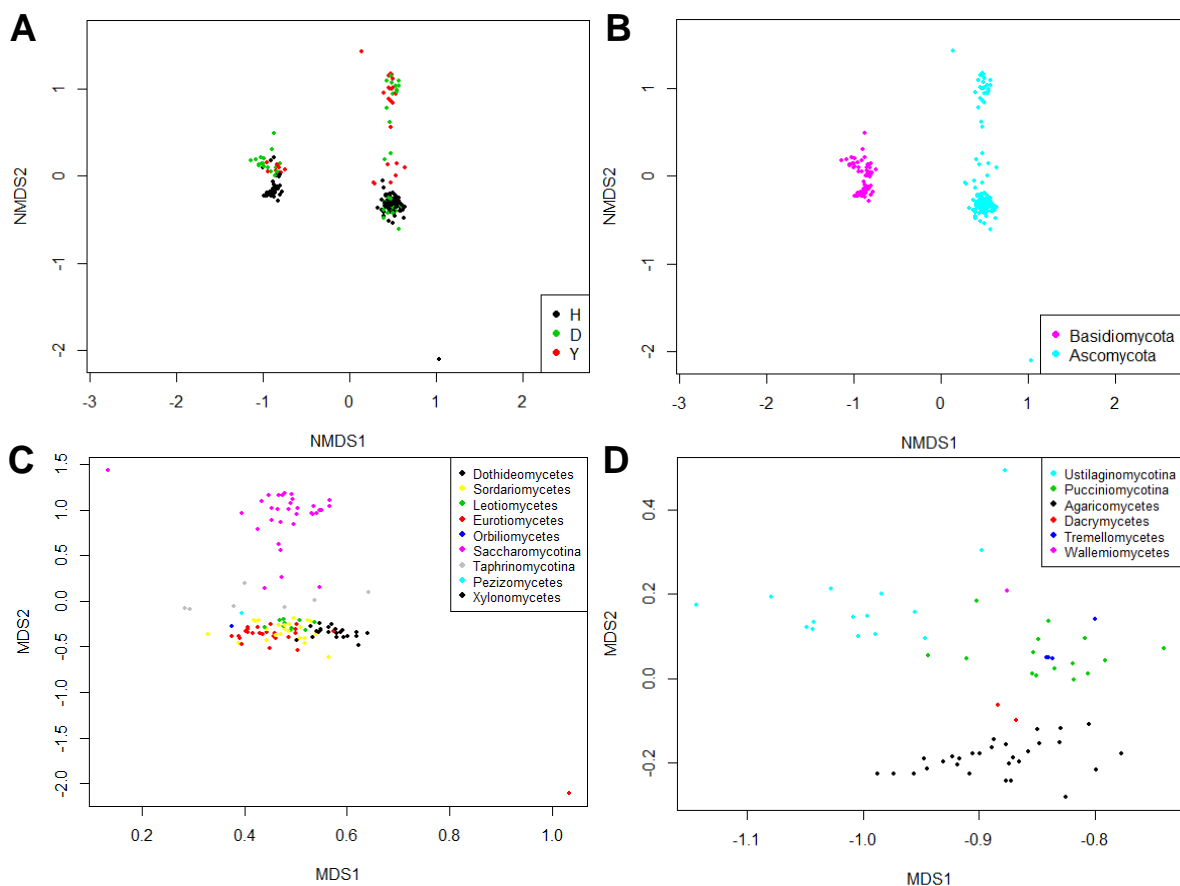


Figure S7 NMDS plots of genes involved in cell cycle control, cell division and chromosome partitioning (class D). The 344 fuNOG IDs classified in class D were included in the gene distribution table of 190 fungal genomes. As the NMDS plots could not be generated under 344 dimensions (genes), we trimmed the dimensions down by selecting only fuNOG IDs present in 5 – 95% of studied genomes. The 134 fuNOG IDs were ultimately used for constructing the plots. Data points are labelled based on (A) types of growth form (H, hyphal; D, dimorphic; and Y, yeast), (B) phyla (Ascomycota and Basidiomycota), (C) lineages in Ascomycota and (D) lineages in Basidiomycota.

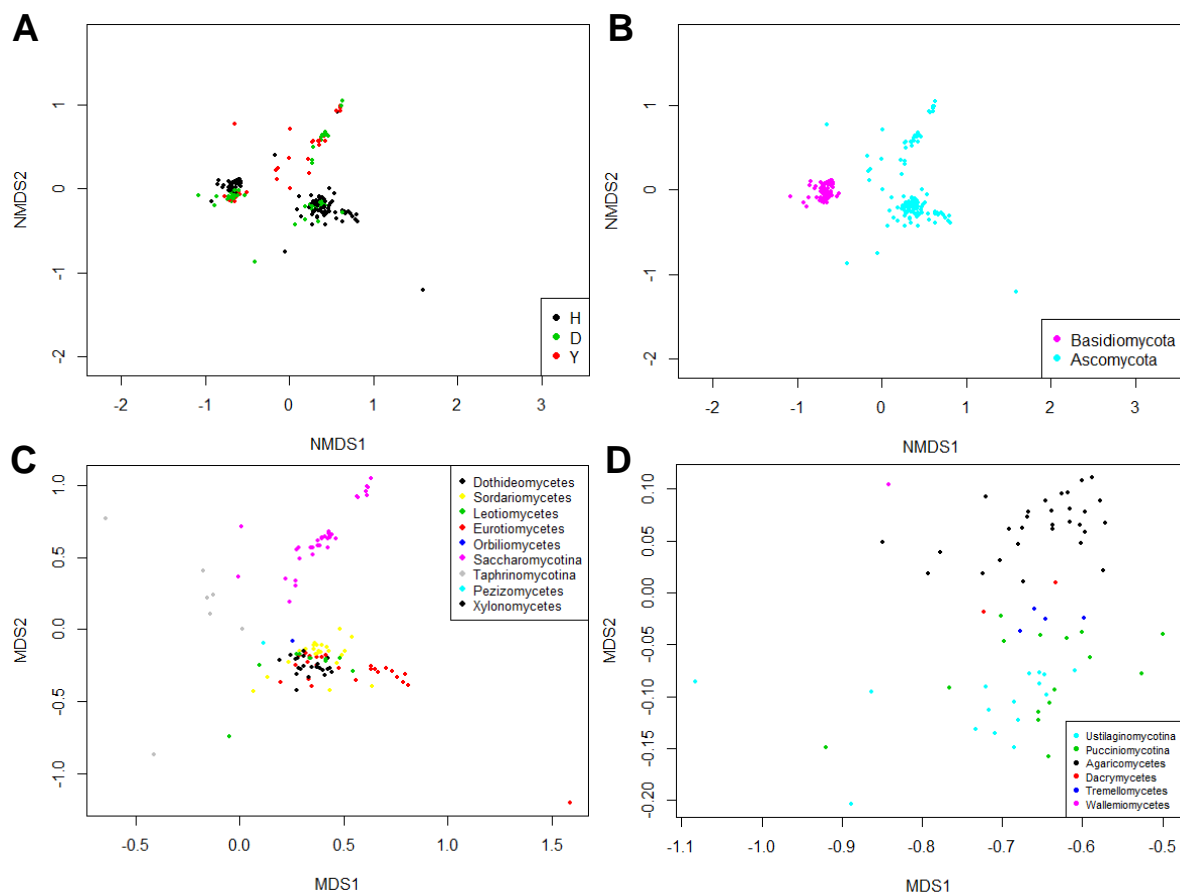


Figure S8 NMDS plots of genes involved in transcription (class K). The 1177 fuNOG IDs classified in class K were included in the gene distribution table of 190 fungal genomes. Data points are labelled based on (A) types of growth form (H, hyphal; D, dimorphic; and Y, yeast), (B) phyla (Ascomycota and Basidiomycota), (C) lineages in Ascomycota and (D) lineages in Basidiomycota.

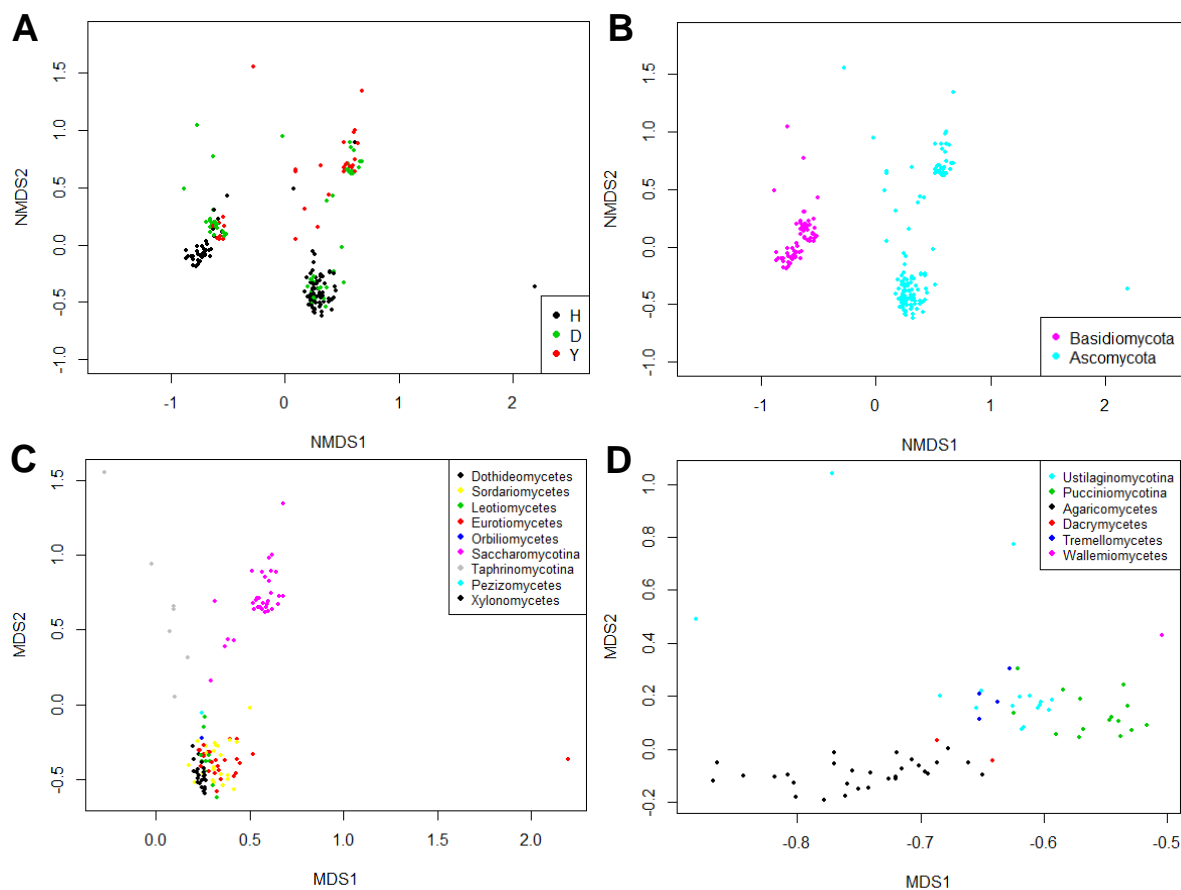


Figure S9 NMDS plots of genes involved in signal transduction mechanisms (class T). The 1103 fuNOG IDs classified in class T were included in the gene distribution table of 190 fungal genomes. As the NMDS plots could not be generated under 1103 dimensions (genes), we trimmed the dimensions down by selecting only fuNOG IDs present in 5 – 95% of studied genomes. The 582 fuNOG IDs were ultimately used for constructing the plots. Data points are labelled based on (A) types of growth form (H, hyphal; D, dimorphic; and Y, yeast), (B) phyla (Ascomycota and Basidiomycota), (C) lineages in Ascomycota and (D) lineages in Basidiomycota.

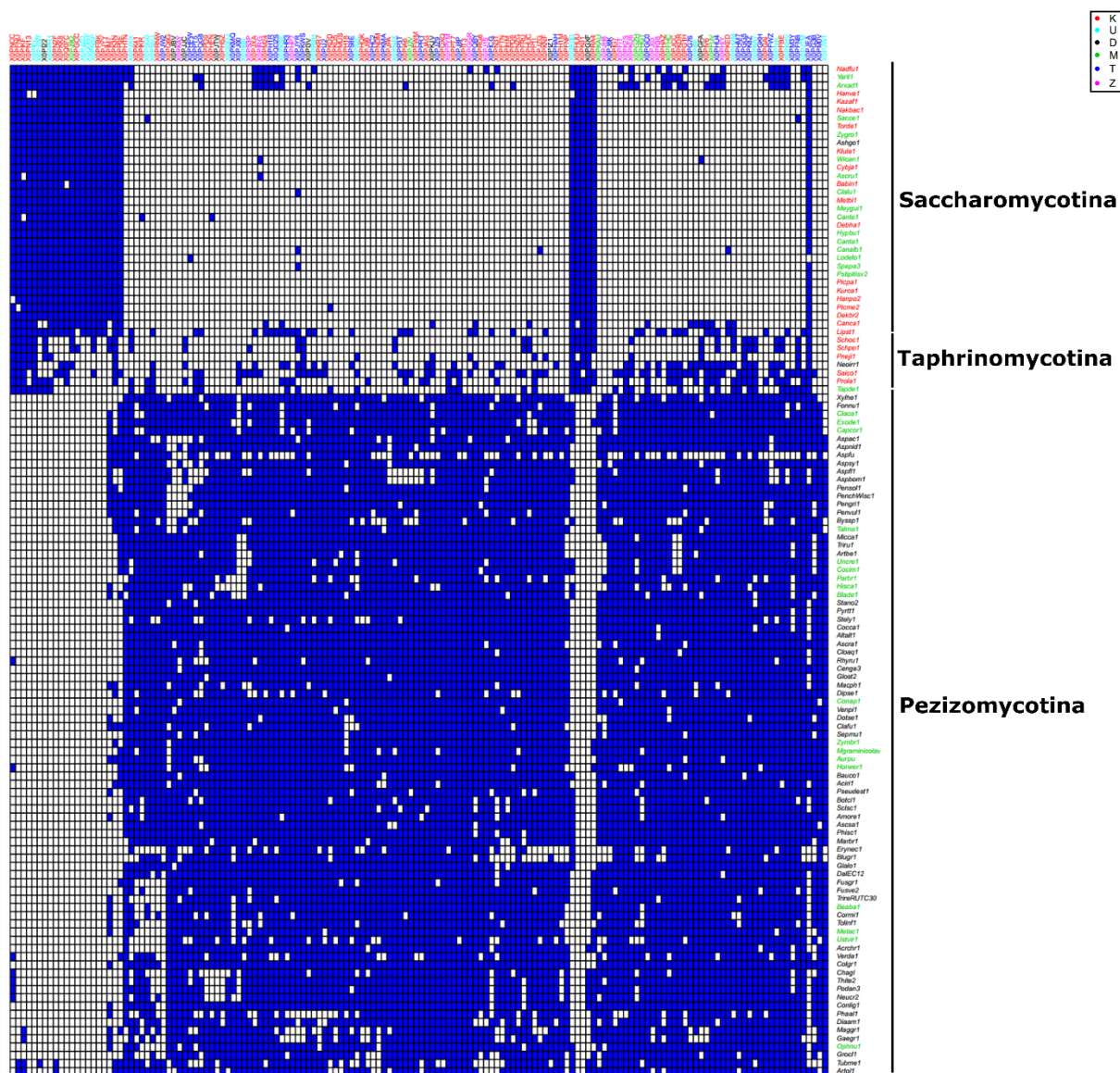


Figure S10 Presence-absence matrix of 152 indicator genes for types of growth form in Ascomycota. These indicator genes were derived from six functional classes (M, U, Z, D, K and T) that passed cutoff from the analyses in both full and cross-validation datasets. Growth forms are labelled by text colors: black, hyphal; green, dimorphic; and red, yeast. Gene presence and absence are indicated by blue and white fillings, respectively.

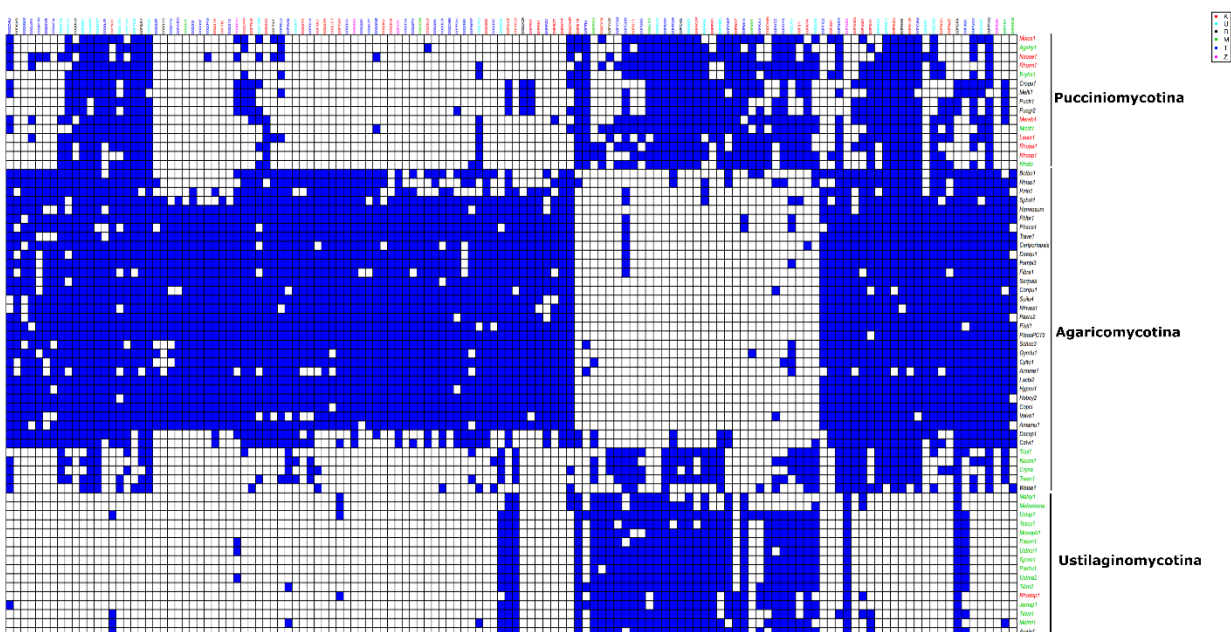


Figure S11 Presence-absence matrix of 133 indicator genes for types of growth form in Basidiomycota. These indicator genes were derived from the six functional classes (M, U, Z, D, K and T) that passed cutoff from the analyses in both full and cross-validation datasets. Growth forms are labelled by text colors: black, hyphal; green, dimorphic; and red, yeast. Gene presence and absence are indicated by blue and white fillings, respectively.

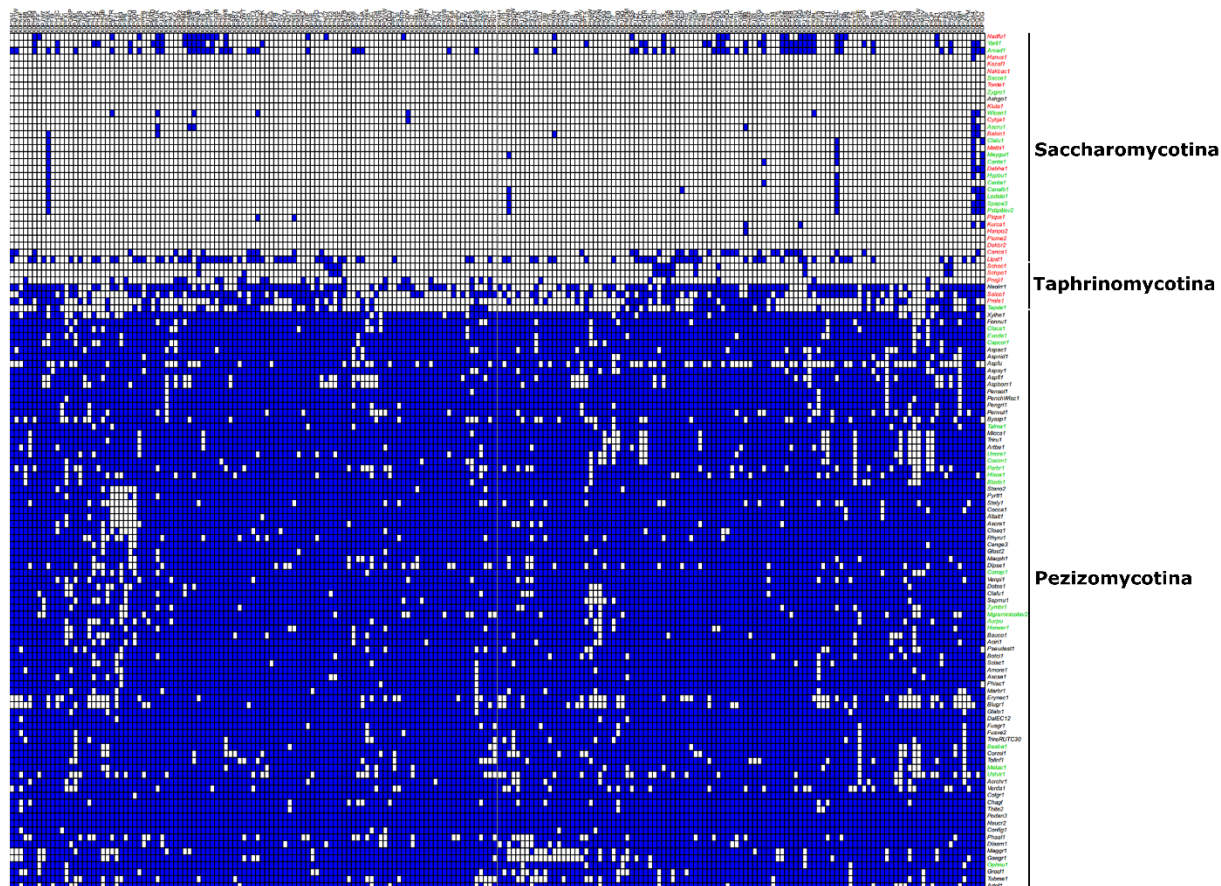


Figure S12 Presence-absence matrix of 210 indicator genes for types of growth form in Ascomycota. These indicator genes were derived from the complex multicellularity-associated genes published in Nguyen et al. (190) that passed cutoff from the analyses in both full and cross-validation datasets. Growth forms are labelled by text colors: black, hyphal; green, dimorphic; and red, yeast. Gene presence and absence are indicated by blue and white fillings, respectively.

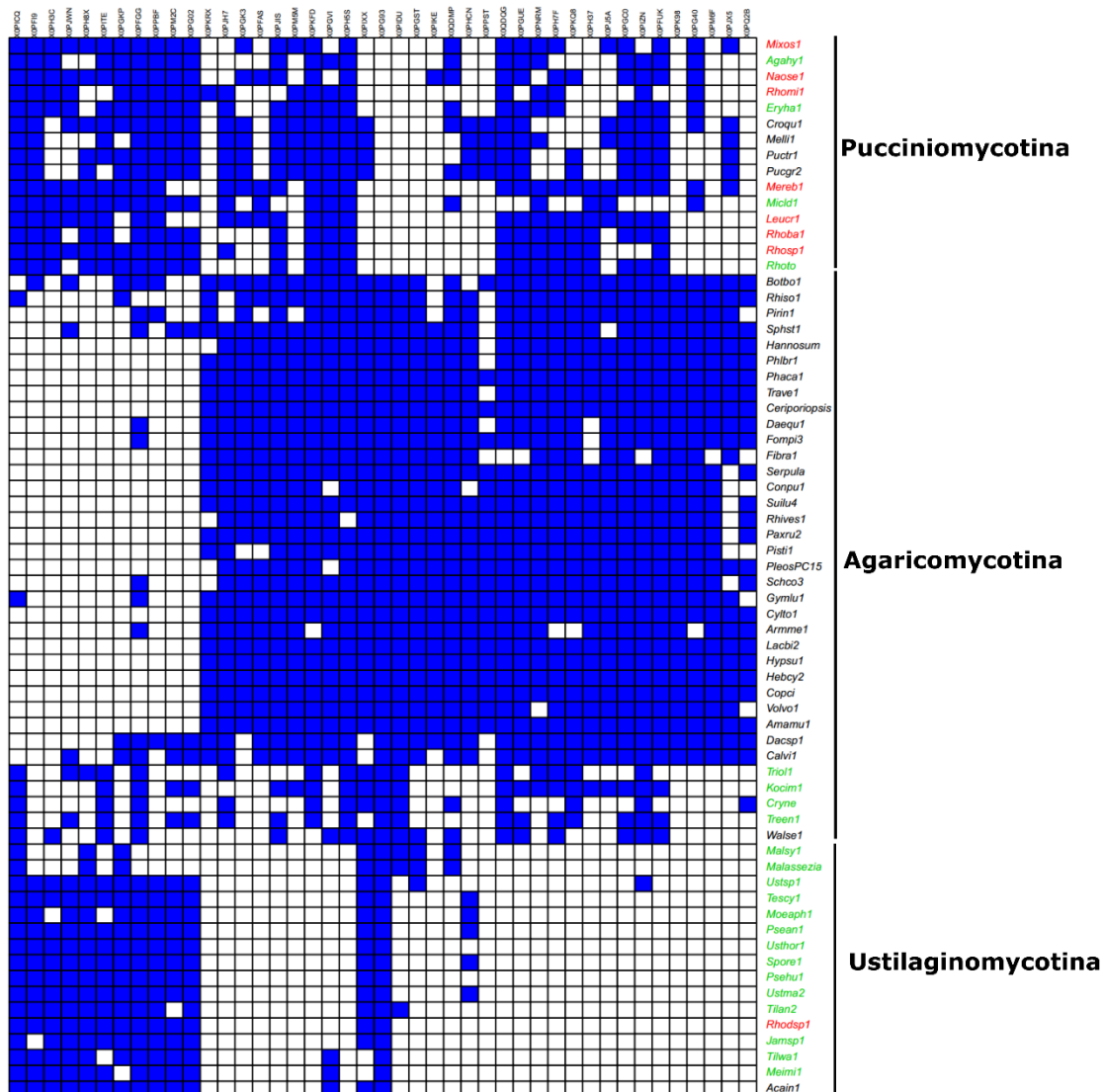


Figure S13 Presence-absence matrix of 42 indicator genes for types of growth form in Basidiomycota. These indicator genes were derived from the complex multicellularity-associated genes published in Nguyen et al. (190) that passed cutoff from the analyses in both full and cross-validation datasets. Growth forms are labelled by text colors: black, hyphal; green, dimorphic; and red, yeast. Gene presence and absence are indicated by blue and white fillings, respectively.

Table S1 A list of fungal genomes included in this study

Species	Abbreviation	Lineage.subphylum	Lineage.coarse	Growth.form	References
<i>Acaromyces ingoldii</i> MCA4198	Acain1	Ustilaginomycotina	Basidiomycota	H	Kijpomyongpan et al. 2018 MBE
<i>Acidomyces richmondensis</i> BFW	Aciri1	Dothideomycetes	Ascomycota	H	Mosier et al. 2016 Front Microbiol.
<i>Acremonium chrysogenum</i> ATCC 11550	Acrchr1	Sordariomycetes	Ascomycota	H	Terfehr et al. 2014 Genome Announc
<i>Agaricostilbum hyphaenes</i> ATCC MYA-4628 v1.0	Agahy1	Pucciniomycotina	Basidiomycota	D	Aime unpublished
<i>Alternaria alternata</i> SRC11rK2f v1.0	Altalt1	Dothideomycetes	Ascomycota	H	Zeiner et al. 2016 PLoS One
<i>Amanita muscaria</i> Koide v1.0	Amamu1	Agaricomycetes	Basidiomycota	H	Kohler et al. 2015 Nat Genetics
<i>Amorphotheca resinae</i> v1.0	Amore1	Leotiomycetes	Ascomycota	H	Martino et al. 2018 New Phytologist
<i>Armillaria mellea</i>	Armme1	Agaricomycetes	Basidiomycota	H	Collins et al 2013 J Proteome Res
<i>Arthroderma benhamiae</i> CBS 112371	Artbe1	Eurotiomycetes	Ascomycota	H	Burmester et al. 2011 Genome Biology 2011
<i>Arthrobotrys oligospora</i> ATCC 24927	Artol1	Orbiliomycetes	Ascomycota	H	Yang et al. 2011 PLoS Pathogen
<i>Blastobotrys (Arxula) adeninivorans</i>	Arxad1	Saccharomycotina	Ascomycota	D	Kunze et al. 2014 Biotechnol Biofuels
<i>Ascochyta rabiei</i> ArDII	Ascra1	Dothideomycetes	Ascomycota	H	Verma et al. 2016 Sci Rep
<i>Ascoidea rubescens</i> NRRL Y17699 v1.0	Ascru1	Saccharomycotina	Ascomycota	D	Riley et al. 2016 PNAS
<i>Ascocoryne sarcoides</i> NRRL50072	Ascsa1	Leotiomycetes	Ascomycota	H	Gianoulis TA et al., 2012 PLoS Genetics
<i>Eremothecium gossypii</i> ATCC 10895	Ashgo1	Saccharomycotina	Ascomycota	H	Dietrich et al. 2004 Science
<i>Aspergillus aculeatus</i> ATCC16872	Aspac1	Eurotiomycetes	Ascomycota	H	de Vries et al. 2017 Genome Biology
<i>Aspergillus bombycis</i> NRRL 26010	Aspbom1	Eurotiomycetes	Ascomycota	H	Moore et al. 2016 Genome Biol Evolution
<i>Aspergillus flavus</i> NRRL3357	Aspfl1	Eurotiomycetes	Ascomycota	H	Arnaud et al. 2012 Nucleic AcIDs Res.
<i>Aspergillus fumigatus</i> A1163	Aspfu	Eurotiomycetes	Ascomycota	H	Fedorova ND et al., 2008 PLoS Genetics
<i>Aspergillus nidulans</i>	Aspnid1	Eurotiomycetes	Ascomycota	H	Arnaud et al. 2012 Nucleic AcIDs Res.
<i>Aspergillus sydowii</i> CBS 593.65 v1.0	Aspsyl	Eurotiomycetes	Ascomycota	H	de Vries et al. 2017 Genome Biology
<i>Aureobasidium pullulans</i> var. <i>pullulans</i> EXF-150	Aurpu	Dothideomycetes	Ascomycota	D	Gostincar et al. 2014 BMC Genomics
<i>Babjeviella inositovora</i> NRRL Y-12698 v1.0	Babin1	Saccharomycotina	Ascomycota	Y	Riley et al. 2016 PNAS
<i>Baudoinia compniacensis</i> UAMH 10762	Bauco1	Dothideomycetes	Ascomycota	H	Ohm et al. 2012 PLoS Patho
<i>Beauveria bassiana</i> ARSEF 2860	Beaba1	Sordariomycetes	Ascomycota	D	Xiao et al. 2012 Sci Rep
<i>Blastomyces dermatitidis</i> SLH14081	Blade1	Eurotiomycetes	Ascomycota	D	Munoz et al. 2015 PLoS Genetics
<i>Blumeria graminis</i> f.sp. <i>hordei</i> DH14	Blugr1	Leotiomycetes	Ascomycota	H	Spanu et al. 2010 Science
<i>Botryobasidium botryosum</i> v1.0	Botbo1	Agaricomycetes	Basidiomycota	H	Riley et al. 2014 PNAS
<i>Botrytis cinerea</i> v1.0	Botci1	Leotiomycetes	Ascomycota	H	Staats and Kan 2012 Eukaryotic Cell

Table S1 continued

<i>Byssochlamys spectabilis</i>	Byssp1	Eurotiomycetes	Ascomycota	H	Oka et al. Genome Announc 2014
<i>Calocera viscosa</i>	Calvi1	Dacrymycetes	Basidiomycota	H	Nagy et al. 2016 MBE
<i>Candida albicans</i> SC5314	Canalb1	Saccharomycotina	Ascomycota	D	Jones et al. 2004 PNAS
<i>Tortispora caseinolytica</i> Y-17796	Canca1	Saccharomycotina	Ascomycota	Y	Riley et al. 2016 PNAS
<i>Candida tanzawaensis</i> NRRL Y-17324	Canta1	Saccharomycotina	Ascomycota	D	Riley et al. 2016 PNAS
<i>Candida tenuis</i> NRRL Y-1498	Cante1	Saccharomycotina	Ascomycota	D	Wohlbach et al. 2011 PNAS
<i>Capronia coronata</i> CBS 617.96	Capcor1	Eurotiomycetes	Ascomycota	D	Teixeira et al. 2017 Studies in Mycology
<i>Cenococcium geophilum</i> 1.58	Cenge3	Dothideomycetes	Ascomycota	H	Peter et al. 2016 Nat Comm
<i>Ceriporiopsis (Gelatorporia) subvermispora</i> B	Ceriporiopsis	Agaricomycetes	Basidiomycota	H	Fernandez-Fueyo et al. 2012 PNAS
<i>Chaetomium globosum</i>	Chagl1	Sordariomycetes	Ascomycota	H	Cuomo et al. 2015 Genome Announc
<i>Cladophialophora carrionii</i> CBS 160.54	Claca1	Eurotiomycetes	Ascomycota	D	Teixeira et al. 2017 Studies in Mycology
<i>Cladosporium fulvum</i>	Clafu1	Dothideomycetes	Ascomycota	H	de Wit et al. 2012 PLoS Genet
<i>Clavisporea lusitaniae</i> ATCC 42720	Clalu1	Saccharomycotina	Ascomycota	D	Butler et al. 2009 Nature
<i>Clohesyomyces aquaticus</i>	Cloaq1	Dothideomycetes	Ascomycota	H	Mondo et al. 2017 Nat Genetics
<i>Cochliobolus carbonum</i> 26-R-13	Cocca1	Dothideomycetes	Ascomycota	H	Condon et al. 2013 PLoS Genet.
<i>Coccidioides immitis</i> RS	Cocim1	Eurotiomycetes	Ascomycota	D	Sharpton et al. 2009 Genome Res
<i>Colletotrichum graminicola</i> M1.001	Colgr1	Sordariomycetes	Ascomycota	H	O'Connell et al. 2012 Nat. Genet
<i>Coniosporium apollinis</i> CBS 100218	Conap1	Eurotiomycetes	Ascomycota	D	Teixeira et al. 2017 Studies in Mycology
<i>Coniochaeta ligniaria</i> NRRL 30616	Conlig1	Sordariomycetes	Ascomycota	H	Jimenez et al. 2017 Genome Announc
<i>Coniophora puteana</i>	Conpu1	Agaricomycetes	Basidiomycota	H	Floudas et al. 2012 Science
<i>Coprinopsis cinerea</i> AmutBmut pab1-1	Copci	Agaricomycetes	Basidiomycota	H	Muraguchi et al. 2015 PLoS One
<i>Cordyceps militaris</i> CM01	Cormi1	Sordariomycetes	Ascomycota	H	Zheng et al. 2011 Genome Biol.
<i>Cronartium quercuum</i> f. sp. fusiforme	Croqu1	Pucciniomycotina	Basidiomycota	H	Pendleton et al. 2014 Front Plant Sci
<i>Cryptococcus neoformans</i> var <i>neoformans</i> JEC21	Cryne	Tremellomycetes	Basidiomycota	D	Loftus et al. 2005 Science
<i>Cyberlindnera jadinii</i> NRRL Y-1542	Cybj1	Saccharomycotina	Ascomycota	Y	Riley et al. 2016 PNAS
<i>Cylindrobasidium torrendii</i> FPI5055	Cylto1	Agaricomycetes	Basidiomycota	H	Floudas et al. 2012 Science
<i>Dacryopinax primogenitus</i> DJM 731 SSP1	Dacsp1	Dacrymycetes	Basidiomycota	H	Floudas et al. 2012 Science
<i>Daedalea quercina</i>	Daequ1	Agaricomycetes	Basidiomycota	H	Nagy et al. 2016 MBE
<i>Daldinia eschscholzii</i> EC12	DalEC12	Sordariomycetes	Ascomycota	H	Wu et al. 2017 App Microbiol Biotechnol
<i>Debaryomyces hansenii</i>	Debha1	Saccharomycotina	Ascomycota	Y	Sacerdot et al. 2008 FEMS Yeast Res
<i>Dekkera bruxellensis</i>	Dekbr2	Saccharomycotina	Ascomycota	Y	Piskur et al. 2012 Int J Food Microbiol

Table S1 continued

<i>Diaporthe ampelina</i> UCDDA912	Diaam1	Sordariomycetes	Ascomycota	H	Morales-Cruz A et al., 2015 BMC Genomics
<i>Diplodia seriata</i> DS831	Dipse1	Dothideomycetes	Ascomycota	H	Morales-Cruz A et al., 2015 BMC Genomics
<i>Dothistroma septosporum</i> NZE10	Dotse1	Dothideomycetes	Ascomycota	H	de Wit et al. 2012 PLoS Genet
<i>Erythrobasidium hasegawianum</i>	Eryha1	Pucciniomycotina	Basidiomycota	D	Toome et al. unpublished
<i>Erysiphe necator</i> c	Eryne1	Leotiomycetes	Ascomycota	H	Jones et al. 2014 BMC Genomics
<i>Exophiala dermatitidis</i> UT8656	Exode1	Eurotiomycetes	Ascomycota	D	Teixeira et al. 2017 Studies in Mycology
<i>Fibroporia radiculosa</i> TFFH 294	Fibra1	Agaricomycetes	Basidiomycota	H	Tang et al. 2012 Appl Environ Microbiol
<i>Fomitopsis pinicola</i> FP-58527 SS1	Fompi3	Agaricomycetes	Basidiomycota	H	Floudas et al. 2012 Science
<i>Fonsecaea nubica</i> CBS 269.64	Fonnu1	Eurotiomycetes	Ascomycota	H	Costa et al. 2016 Genome Announc
<i>Fusarium graminearum</i>	Fusgr1	Sordariomycetes	Ascomycota	H	Cuomo CA et al., 2007 Science
<i>Fusarium verticillioides</i> 7600	Fusve2	Sordariomycetes	Ascomycota	H	Ma et al. 2010 Nature
<i>Gaeumannomyces graminis</i> var. <i>tritici</i> R3-111a-1	Gaegr1	Sordariomycetes	Ascomycota	H	Okagaki et al. 2015 G3
<i>Glaea lozoyensis</i> ATCC 20868	Glalo1	Leotiomycetes	Ascomycota	H	Chen et al. 2013 BMC Genomics
<i>Glonium stellatum</i> CBS 207.34	Glost2	Dothideomycetes	Ascomycota	H	Peter et al. 2016 Nat Comm
<i>Grosmannia clavigera</i> kw1407	Grocl1	Sordariomycetes	Ascomycota	H	DiGuistini et al. 2011 PNAS
<i>Gymnopus luxurians</i>	Gymlu1	Agaricomycetes	Basidiomycota	H	Kohler et al. 2015 Nat Genetics
<i>Heterobasidium annosum</i>	Hannosum	Agaricomycetes	Basidiomycota	H	Olson et al. 2012 New Phytol
<i>Ogataea polymorpha</i> NCYC 495	Hanpo2	Saccharomycotina	Ascomycota	Y	Riley et al. 2016 PNAS
<i>Hanseniaspora valbyensis</i> NRRL Y-1626	Hanva1	Saccharomycotina	Ascomycota	Y	Riley et al. 2016 PNAS
<i>Hebeloma cylindrosporum</i> h7	Hebcy2	Agaricomycetes	Basidiomycota	H	Kohler et al. 2015 Nat Genetics
<i>Histoplasma capsulatum</i> NAm1	Hisca1	Eurotiomycetes	Ascomycota	D	Sharpton et al. 2009 Genome Res
<i>Hortaea werneckii</i> EXF-2000 M0	Horwer1	Dothideomycetes	Ascomycota	D	Lenassi et al. 2013 PLoS One
<i>Hyphopichia burtonii</i> NRRL Y-1933	Hypbu1	Saccharomycotina	Ascomycota	D	Riley et al. 2016 PNAS
<i>Hypholoma sublateritium</i>	Hypsu1	Agaricomycetes	Basidiomycota	H	Kohler et al. 2015 Nat Genetics
<i>Jaminaea rosea</i> MCA5214	Jamsp1	Ustilaginomycotina	Basidiomycota	D	Kijpornyongpan et al. 2018 MBE
<i>Kazachstania africana</i>	Kazaf1	Saccharomycotina	Ascomycota	Y	Gordon et al. 2011 PNAS
<i>Kluyveromyces lactis</i>	Klula1	Saccharomycotina	Ascomycota	Y	Dujon et al. 2004 Nature
<i>Kockovaella imperatae</i> NRRL Y-17943	Kocim1	Tremellomycetes	Basidiomycota	D	Mondo et al. 2017 Nat Genetics
<i>Kuraishia capsulata</i> CBS 1993	Kurca1	Saccharomycotina	Ascomycota	Y	Morales et al. 2013 Genome Biol Evol
<i>Laccaria bicolor</i>	Lacbi2	Agaricomycetes	Basidiomycota	H	Martin et al. 2008 Nature
<i>Leucosporidiella creatinivora</i> 62-1032	Leucr1	Pucciniomycotina	Basidiomycota	Y	Mondo et al. 2017 Nat Genetics

Table S1 continued

<i>Lipomyces starkeyi</i> NRRL Y-11557	Lipst1	Saccharomycotina	Ascomycota	Y	Riley et al. 2016 PNAS
<i>Lodderomyces elongisporus</i> NRRL YB-4239	Lodelo1	Saccharomycotina	Ascomycota	D	Butler et al. 2009 Nature
<i>Macrophomina phaseolina</i> MS6	Macph1	Dothideomycetes	Ascomycota	H	Islam et al. 2012 BMC Genomics
<i>Magnaporthe grisea</i>	Maggr1	Sordariomycetes	Ascomycota	H	Dean et al. 2005 Nature
<i>Malassezia globosa</i>	Malassezia	Ustilaginomycotina	Basidiomycota	D	Xu et al. 2007 PNAS
<i>Malassezia sympodialis</i>	Malsy1	Ustilaginomycotina	Basidiomycota	D	Gioti et al. 2013 Mbio
<i>Marssonina brunnea</i> f. sp. <i>multigermtubi</i>	Marbr1	Leotiomycetes	Ascomycota	H	Zhu et al. 2012 BMC Genomics
<i>Meira miltonrushii</i> MCA 3882	Meimi1	Ustilaginomycotina	Basidiomycota	D	Kijpomyongpan et al. 2018 MBE
<i>Melampsora lini</i> CH5	Melli1	Pucciniomycotina	Basidiomycota	H	Nemri et al. 2014 Front Plant Sci
<i>Meredithblackwellia eburnea</i>	Mereb1	Pucciniomycotina	Basidiomycota	Y	Toome et al. unpublished
<i>Metarhizium acridum</i> CQMa	Metac1	Sordariomycetes	Ascomycota	D	Gao et al. 2011 PLoS Genet
<i>Metschnikowia bicuspidata</i> NRRL YB-4993	Metbi1	Saccharomycotina	Ascomycota	Y	Riley et al. 2016 PNAS
<i>Meyerozyma guilliermondii</i> ATCC 6260	Meygui1	Saccharomycotina	Ascomycota	D	Butler et al. 2009 Nature
<i>Mycosphaerella graminicola</i>	Mgraminicolav2	Dothideomycetes	Ascomycota	D	Goodwin et al. 2011 PLoS Genet
<i>Microsporium canis</i> CBS 113480	Micca1	Eurotiomycetes	Ascomycota	H	Martinez DA et al., 2012 Mbio
<i>Microbotryum lychnidis-dioicae</i> p1A1 Lamole	Micld1	Pucciniomycotina	Basidiomycota	D	Perlin et al. 2015 BMC Genomics
<i>Mixia osmundae</i> IAM 14324	Mixos1	Pucciniomycotina	Basidiomycota	Y	Toome et al. 2014 New Phytol
<i>Moesziomyces aphidis</i> DSM 70725	Moeaph1	Ustilaginomycotina	Basidiomycota	D	Lorenz et al. 2014 Genome Announc
<i>Nadsonia fulvescens</i> var. <i>elongata</i> DSM 6958	Nadfu1	Saccharomycotina	Ascomycota	Y	Riley et al. 2016 PNAS
<i>Nakaseomyces bacillisporus</i> CBS 7720	Nakbac1	Saccharomycotina	Ascomycota	Y	Gabalton et al. 2013 BMC Genomics
<i>Naohidea sebacea</i> CBS 8477	Naose1	Pucciniomycotina	Basidiomycota	Y	Toome et al. unpublished
<i>Neolecta irregularis</i> DAH-1	Neoirr1	Taphrinomycotina	Ascomycota	H	Nguyen et al. 2017 Nat Commun
<i>Neurospora crassa</i> OR74A	Neucr2	Sordariomycetes	Ascomycota	H	Galagan et al. 2003 Nature
<i>Ophiostoma novo-ulmi</i> subsp. <i>novo-ulmi</i> H327	Ophnu1	Sordariomycetes	Ascomycota	D	Forgetta V et al. 2013 J Biomol Tech
<i>Paracoccidioides brasiliensis</i> Pb03	Parbr1	Eurotiomycetes	Ascomycota	D	Desjardins et al. 2011 PLoS Genet
<i>Paxillus adelphus</i> Ve08.2h10	Paxru2	Agaricomycetes	Basidiomycota	H	Kohler et al. 2015 Nat Genetics
<i>Penicillium chrysogenum</i> Wisconsin 54-1255	PenchWisc1	Eurotiomycetes	Ascomycota	H	van den Berg et al. 2008 Nature Biotech
<i>Penicillium griseofulvum</i> PG3	Pengri1	Eurotiomycetes	Ascomycota	H	Banani et al. 2016 BMC Genomics
<i>Penicillium solitum</i>	Pensol1	Eurotiomycetes	Ascomycota	H	Nielsen et al. 2017 Nature Microbiology
<i>Penicillium vulpinum</i> IBT 29486	Penvul1	Eurotiomycetes	Ascomycota	H	Nielsen et al. 2017 Nature Microbiology
<i>Phaeoacremonium aleophilum</i> UCRPA7	Phaal1	Sordariomycetes	Ascomycota	H	Blanco-Ulate et al. 2013 Genome Announc

Table S1 continued

<i>Phanerochaete carnos</i> HHB-10118-Sp	Phaca1	Agaricomycetes	Basidiomycota	H	Suzuki et al. 2012 BMC Genomics
<i>Phialocephala scopiformis</i> 5WS22E1	Phisc1	Leotiomycetes	Ascomycota	H	Walker et al. 2016 Genome Announc
<i>Phlebia brevispora</i> HHB-7030 SS6	Phlbr1	Agaricomycetes	Basidiomycota	H	Binder et al. 2013 Mycologia
<i>Pichia membranifaciens</i>	Picme2	Saccharomycotina	Ascomycota	Y	Riley et al. 2016 PNAS
<i>Pichia pastoris</i>	Picpa1	Saccharomycotina	Ascomycota	Y	De Schutter et al. 2009 Nature Biotech
<i>Piriformospora indica</i> DSM 11827	Pirin1	Agaricomycetes	Basidiomycota	H	Zuccaro et al. 2011 PLoS Pathog
<i>Pisolithus tinctorius</i> Marx 270	Pisti1	Agaricomycetes	Basidiomycota	H	Kohler et al. 2015 Nat Genetics
<i>Pleurotus ostreatus</i> PC9	PleosPC15	Agaricomycetes	Basidiomycota	H	Riley et al. 2014 PNAS
<i>Pneumocystis jirovecii</i>	Pnej1	Taphrinomycotina	Ascomycota	Y	Cisse et al. 2012 Mbio
<i>Podospora anserina</i> S mat+	Podan3	Sordariomycetes	Ascomycota	H	Espagne et al. 2008 Genome Biol
<i>Protomyces lactucaedebilis</i> 12-1054	Prola1	Taphrinomycotina	Ascomycota	Y	Mondo et al. 2017 Nat Genetics
<i>Pseudozyma antarctica</i> T-34	Psean1	Ustilaginomycotina	Basidiomycota	D	Morita et al. 2013 Genome Announc
<i>Pseudozyma hubeiensis</i> SY62	Psehu1	Ustilaginomycotina	Basidiomycota	D	Konishi et al. 2013 Genome Announc
<i>Pseudogymnoascus destructans</i> 20631-21	Pseudest1	Leotiomycetes	Ascomycota	H	Drees et al. 2016 Genome Announc
<i>Scheffersomyces stipitis</i> NRRL Y-11545	Pstipitv2	Saccharomycotina	Ascomycota	D	Jeffries et al. 2007 Nature Biotech
<i>Puccinia graminis</i> f. sp. <i>tritici</i>	Pucgr2	Pucciniomycotina	Basidiomycota	H	Duplessis et al. 2011 PNAS
<i>Puccinia triticina</i> 1-1 BBBB	Puctr1	Pucciniomycotina	Basidiomycota	H	Cuomo et al. 2017 G3
<i>Pyrenophora teres</i> f. sp. <i>teres</i>	Pyrtt1	Dothideomycetes	Ascomycota	H	Ellwood et al. 2010 Genome Biol
<i>Rhizoctonia solani</i> AG-1 IB	Rhiso1	Agaricomycetes	Basidiomycota	H	Wibberg et al. 2013 J Biotechnol
<i>Rhizopogon vesiculosus</i> Smith	Rhives1	Agaricomycetes	Basidiomycota	H	Mujic et al. 2017 G3
<i>Rhodotorula graminis</i> strain WP1 v1.1	Rhoba1	Pucciniomycotina	Basidiomycota	Y	Firincieli et al. Front Microbiol 2015
<i>Pseudomicrostroma glucosiphilum</i> MCA4718	Rhodsp1	Ustilaginomycotina	Basidiomycota	Y	Kijpomyongpan et al. 2018 MBE
<i>Rhodotorula minuta</i> MCA 4210	Rhomi1	Pucciniomycotina	Basidiomycota	Y	Toome et al. unpublished
<i>Rhodotorula</i> sp. JG-1b	Rhosp1	Pucciniomycotina	Basidiomycota	Y	Goordial et al. 2016 Genome Announc
<i>Rhodosporidium toruloides</i> IFO0559_1	Rhoto	Pucciniomycotina	Basidiomycota	D	Zhu et al. 2012 Nat Comm
<i>Rhizidhysterium rufulum</i>	Rhyru1	Dothideomycetes	Ascomycota	H	Ohm et al. 2012 PLoS Patho
<i>Saccharomyces cerevisiae</i> S288C	Sacce1	Saccharomycotina	Ascomycota	D	Goffeau et al. 1996 Science
<i>Saitoella complicata</i> NRRL Y-17804	Saico1	Taphrinomycotina	Ascomycota	Y	Riley et al. 2016 PNAS
<i>Schizophyllum commune</i> H4-8	Schco3	Agaricomycetes	Basidiomycota	H	Ohm et al. 2010 Nat Biotechnol
<i>Schizosaccharomyces octosporus</i> yFS286	Schoe1	Taphrinomycotina	Ascomycota	Y	Rhind et al. 2011 Science
<i>Schizosaccharomyces pombe</i>	Schpo1	Taphrinomycotina	Ascomycota	Y	Wood et al. 2002 Nature

Table S1 continued

<i>Sclerotinia sclerotiorum</i>	Scpsc1	Leotiomycetes	Ascomycota	H	Amselem et al. 2011 PLoS Genet
<i>Septoria musiva</i> SO2202	Sepmu1	Dothideomycetes	Ascomycota	H	Ohm et al. 2012 PLoS Patho
<i>Serpula lacrymans</i> S7.3	Serpula	Agaricomycetes	Basidiomycota	H	Eastwood et al. 2011 Science
<i>Spathaspora passalidarum</i> NRRL Y-27907	Spapa3	Saccharomycotina	Ascomycota	D	Wohlbach et al. 2011 PNAS
<i>Sphaerobolus stellatus</i>	Sphst1	Agaricomycetes	Basidiomycota	H	Kohler et al. 2015 Nat Genetics
<i>Sporisorium reilianum</i> SRZ2	Spore1	Ustilaginomycotina	Basidiomycota	D	Schirawski et al. 2010 Science
<i>Stagonospora nodorum</i> SN15	Stano2	Dothideomycetes	Ascomycota	H	Hane et al. 2007 Plant Cell
<i>Stemphylium lycopersici</i> CIDEFI-216	Stely1	Dothideomycetes	Ascomycota	H	Franco et al. 2015 Genome Announc
<i>Suillus luteus</i> UH-Slu-Lm8-n1	Suilu4	Agaricomycetes	Basidiomycota	H	Kohler et al. 2015 Nat Genetics
<i>Talaromyces marneffeii</i> ATCC 18224	Talma1	Eurotiomycetes	Ascomycota	D	Nierman et al. 2015 Genome Announc
<i>Taphrina deformans</i>	Tapde1	Taphrinomycotina	Ascomycota	D	Cisse et al. 2013 Mbio
<i>Testicularia cyperi</i> MCA 3645	Tescy1	Ustilaginomycotina	Basidiomycota	D	Kijpomyongpan et al. 2018 MBE
<i>Thielavia terrestris</i>	Thite2	Sordariomycetes	Ascomycota	H	Berka et al. 2011 Nat Biotechnol
<i>Tilletiaria anomala</i> UBC 951	Tilan2	Ustilaginomycotina	Basidiomycota	D	Toome et al. 2014 Genome Announc
<i>Tilletiopsis washingtonensis</i> MCA 4186	Tilwa1	Ustilaginomycotina	Basidiomycota	D	Kijpomyongpan et al. 2018 MBE
<i>Tolypocladium inflatum</i> NRRL 8044	Tolinfl1	Sordariomycetes	Ascomycota	H	Bushley et al. 2013 PLoS Genet
<i>Torulasporea delbrueckii</i> CBS 1146	Torde1	Saccharomycotina	Ascomycota	Y	Gordon et al. 2011 PNAS
<i>Trametes versicolor</i>	Trave1	Agaricomycetes	Basidiomycota	H	Floudas et al. 2012 Science
<i>Tremella encephala</i> 68-887.2	Treen1	Tremellomycetes	Basidiomycota	D	Mondo et al. 2017 Nat Genetics
<i>Trichosporon oleaginosus</i> IBC0246	Triol1	Tremellomycetes	Basidiomycota	D	Kourist et al. 2015 Mbio
<i>Trichoderma reesei</i> RUT C-30	TrireRUTC30	Sordariomycetes	Ascomycota	H	Jourdier et al. 2017 Biotechnol Biofuels
<i>Trichophyton rubrum</i> CBS 118892	Triru1	Eurotiomycetes	Ascomycota	H	Martinez et al. 2012 Mbio
<i>Tuber melanosporum</i> Mel28	Tubme1	Pezizomycetes	Ascomycota	H	Martin et al. 2010 Nature
<i>Uncinocarpus reesii</i> 1704	Uncre1	Eurotiomycetes	Ascomycota	D	Sharpton et al. 2009 Genome Res
<i>Ustilago hordei</i> Uh4857_4	Usthor1	Ustilaginomycotina	Basidiomycota	D	Laurie et al. 2012 Plant Cell
<i>Ustilago maydis</i> 521	Ustma2	Ustilaginomycotina	Basidiomycota	D	Kamper et al. 2006 Nature
<i>Violaceomyces palustris</i> SA807	Ustsp1	Ustilaginomycotina	Basidiomycota	D	Kijpomyongpan et al. 2018 MBE
<i>Ustilaginoidea virens</i>	Ustvir1	Sordariomycetes	Ascomycota	D	Kumagai et al. 2016 Genome Announc
<i>Venturia pirina</i>	Venpi1	Dothideomycetes	Ascomycota	H	Deng et al. 2017 BMC Genomics
<i>Verticillium dahliae</i>	Verda1	Sordariomycetes	Ascomycota	H	Klosterman et al. PLoS Pathog 2011
<i>Volvariella volvacea</i>	Volvo1	Agaricomycetes	Basidiomycota	H	Bao et al. 2013 PLoS One

Table S1 continued

<i>Wallemia mellicola</i>	Walse1	Wallemiomycetes	Basidiomycota	H	Padamsee et al. 2012 Fungal Geneti Biol
<i>Wickerhamomyces anomalus</i> NRRL Y-366-8	Wican1	Saccharomycotina	Ascomycota	D	Riley et al. 2016 PNAS
<i>Xylona heveae</i> TC161	Xylhe1	Xylonomycetes	Ascomycota	H	Gazis et al. 2016 Fungal Biol
<i>Yarrowia lipolytica</i>	Yarli1	Saccharomycotina	Ascomycota	D	Dujon et al. 2004 Nature
<i>Zygosaccharomyces rouxii</i> CBS732	Zygro1	Saccharomycotina	Ascomycota	D	Souciet et al. 2009 Genome Res
<i>Zymoseptoria brevis</i> Zb18110	Zymbr1	Dothideomycetes	Ascomycota	D	Grandaubert et al. 2015 G3

Table S2 Results from Adonis tests of multivariate genome statistics

Dataset	Adonis			Beta dispersion TukeyHSD p-value		
	pseudo-F	pseudo R ² ?	p-value	Y-H	D-H	D-Y
Overall	21.070	0.184	<0.001	0.982	0.988	0.998
Ascomycota	19.863	0.249	<0.001	0.620	0.571	0.243
Asco.cv1	9.571	0.245	<0.001	0.567	0.960	0.777
Asco.cv2	10.467	0.265	<0.001	0.663	0.147	0.112
Basidiomycota	13.452	0.296	<0.001	0.450	0.437	0.938
Basid.cv1	6.423	0.293	0.002	0.439	0.843	0.641
Basid.cv2	7.267	0.326	<0.001	0.661	0.371	0.970

Table S3 Numbers of genes associated with types of growth form (statistically significant and passed the Indicator value cutoff) across datasets. The letter 'n' indicates a number of input genes.

Dataset	Class M (n=356)	Class U (n=1045)	Class Z (n=281)	Class D (n=344)	Class K (n=1177)	Class T (n=1103)	Nguyen2017 (n=1016)
Dikarya	4	3	6	2	12	5	42
Ascomycota	12	31	16	11	78	44	255
cv.Ascomycota	13	34	16	13	88	47	224
cv2.Ascomycota	21	72	24	32	120	81	319
Shared in all Asco datasets	7	23	14	9	63	36	214
Basidiomycota	8	40	15	22	63	65	65
cv.Basidiomycota	14	39	7	22	60	56	68
cv2.Basidiomycota	9	47	16	25	70	67	73
Shared in all Basid datasets	7	24	5	11	39	47	43

APPENDIX B. LIST OF SUPPLEMENTARY MATERIALS

- Supplementary Material 1** Gene ID and probe ID conversion of *Ustilago maydis*
- Supplementary Material 2** Scripts for processing Illumina data of *Meira miltonrushii* and *Tilletiopsis washingtonensis*
- Supplementary Material 3** Scripts for processing Illumina data of *Ophiostoma novo-ulmi*
- Supplementary Material 4** Raw gene read count of *M. miltonrushii*
- Supplementary Material 5** Raw gene read count of *T. washingtonensis*
- Supplementary Material 6** Raw gene read count of *O. novo-ulmi*
- Supplementary Material 7** Normalized microarray gene expression data of *U. maydis*
- Supplementary Material 8** R scripts for DESeq2 analyses
- Supplementary Material 9** R scripts for Microarray data analyses
- Supplementary Material 10** R scripts for comparative transcriptomic analyses
- Supplementary Material 11** R scripts for Functional analyses
- Supplementary Material 12** Single-copy orthogroups among the four studied species
- Supplementary Material 13** Summary tables for comparative transcriptomic analyses
- Supplementary Material 14** Table showing genome statistics of 190 fungal genomes
- Supplementary Material 15** Table showing fuNOG gene distribution of 190 fungal genomes
- Supplementary Material 16** Summary tables of analyses on genome statistics
- Supplementary Material 17** Summary tables of analyses on fuNOG gene distribution

REFERENCES

1. Blackwell M. The fungi: 1, 2, 3 ... 5.1 million species? *Am J Bot.* 2011;98(3):426–38.
2. Dai Y-C, Cui B-K. *Fomitiporia ellipsoidea* has the largest fruiting body among the fungi. *Fungal Biol* [Internet]. 2011;115(9):813–4. Available from: <http://www.sciencedirect.com/science/article/pii/S1878614611001139>
3. Aime MC, Toome M, McLaughlin DJ. Pucciniomycotina. In: McLaughlin DJ, Spatafora JW, editors. *Mycota VII Systematics and Evolution Part A*. 2nd ed. New York: Springer-Verlag Berlin Heidelberg; 2014. p. 271–94.
4. Smith ML, Bruhn JN, Anderson JB. The fungus *Armillaria bulbosa* is among the largest and oldest living organisms. *Nature* [Internet]. 1992;356(6368):428–31. Available from: <https://doi.org/10.1038/356428a0>
5. Vávra J, Lukeš J. Chapter Four - Microsporidia and ‘The Art of Living Together.’ In: Rollinson DBT-A in P, editor. Academic Press; 2013. p. 253–319. Available from: <http://www.sciencedirect.com/science/article/pii/B9780124077065000046>
6. Riquelme M, Aguirre J, Bartnicki-García S, Braus GH, Feldbrügge M, Fleig U, et al. Fungal Morphogenesis, from the Polarized Growth of Hyphae to Complex Reproduction and Infection Structures. *Microbiol Mol Biol Rev.* 2018;82(2):1–47.
7. Brunswik H. Untersuchungen über die Geschlechts- und Kernverhältnisse bei der Hymenomyzetengattung *Coprinus*. *Bot Abhandlung.* 1924;5:1–152.
8. López-Franco R, Bracker CE. Diversity and dynamics of the Spitzenkörper in growing hyphal tips of higher fungi. *Protoplasma.* 1996;195(1–4):90–111.
9. Wedlich-Söldner R, Bölker M, Kahmann R, Steinberg G. A putative endosomal t-SNARE links exo- and endocytosis in the phytopathogenic fungus *Ustilago maydis*. *EMBO J.* 2000;19(9):1974–86.
10. Riquelme M, Roberson RW, Sanchez-Alonso P. Hyphal Tip Growth in Filamentous Fungi. In: *the Mycota I Growth, Differentiation and Sexuality*. Springer-Verlag Berlin Heidelberg; 2016. p. 47–66.
11. Higashitsuji Y, Herrero S, Takeshita N, Fischer R. The cell end marker protein TeaC is involved in growth directionality and septation in *Aspergillus nidulans*. *Eukaryot Cell.* 2009;8(7):957–67.

12. Liu W, Santiago-Tirado FH, Bretscher A. Yeast formin Bni1p has multiple localization regions that function in polarized growth and spindle orientation. *Mol Biol Cell*. 2012;23(3):412–22.
13. Chen H, Kuo C-C, Kang H, Howell AS, Zyla TR, Jin M, et al. Cdc42p regulation of the yeast formin Bni1p mediated by the effector Gic2p. *Mol Biol Cell*. 2012;23(19):3814–26.
14. Berepiki A, Lichius A, Read ND. Actin organization and dynamics in filamentous fungi. *Nat Rev Microbiol* [Internet]. 2011;9(12):876–87. Available from: <http://dx.doi.org/10.1038/nrmicro2666>
15. Echaui-Espinosa RO, Callejas-Negrete OA, Roberson RW, Bartnicki-García S, Mouriño-Pérez RR. Coronin is a component of the endocytic collar of hyphae of *Neurospora crassa* and is necessary for normal growth and morphogenesis. *PLoS One*. 2012;7(5):e38237.
16. Egile C, Rouiller I, Xu X-P, Volkmann N, Li R, Hanein D. Mechanism of Filament Nucleation and Branch Stability Revealed by the Structure of the Arp2/3 Complex at Actin Branch Junctions. *PLOS Biol* [Internet]. 2005 Nov 8;3(11):e383. Available from: <https://doi.org/10.1371/journal.pbio.0030383>
17. Shaw BD, Chung DW, Wang CL, Quintanilla LA, Upadhyay S. A role for endocytic recycling in hyphal growth. *Fungal Biol* [Internet]. 2011;115(6):541–6. Available from: <http://dx.doi.org/10.1016/j.funbio.2011.02.010>
18. Becht P, König J, Feldbrügge M. The RNA-binding protein Rrm4 is essential for polarity in *Ustilago maydis* and shuttles along microtubules. *J Cell Sci* [Internet]. 2006 Dec 1;119(23):4964 LP – 4973. Available from: <http://jcs.biologists.org/content/119/23/4964.abstract>
19. Salogiannis J, Egan MJ, Reck-Peterson SL. Peroxisomes move by hitchhiking on early endosomes using the novel linker protein PxdA. *J Cell Biol* [Internet]. 2016 Feb 1;212(3):289 LP – 296. Available from: <http://jcb.rupress.org/content/212/3/289.abstract>
20. Takeshita N, Mania D, Herrero S, Ishitsuka Y, Nienhaus GU, Podolski M, et al. The cell-end marker TeaA and the microtubule polymerase AlpA contribute to microtubule guidance at the hyphal tip cortex of *Aspergillus nidulans* to provide polarity maintenance. *J Cell Sci* [Internet]. 2013 Dec 1;126(23):5400 LP – 5411. Available from: <http://jcs.biologists.org/content/126/23/5400.abstract>

21. Mata J, Nurse P. teal and the Microtubular Cytoskeleton Are Important for Generating Global Spatial Order within the Fission Yeast Cell. *Cell* [Internet]. 1997;89(6):939–49. Available from: <http://www.sciencedirect.com/science/article/pii/S0092867400802792>
22. Konzack S, Rischitor PE, Enke C, Fischer R. The role of the kinesin motor KipA in microtubule organization and polarized growth of *Aspergillus nidulans*. *Mol Biol Cell*. 2005;16(2):497–506.
23. Mouriño-Pérez RR, Roberson RW, Bartnicki-García S. Microtubule dynamics and organization during hyphal growth and branching in *Neurospora crassa*. *Fungal Genet Biol* [Internet]. 2006;43(6):389–400. Available from: <http://www.sciencedirect.com/science/article/pii/S1087184506000119>
24. Steinberg G. MINIREVIEW Hyphal Growth: a Tale of Motors , Lipids , and the Spitzenkörper. *Eukaryot Cell*. 2007;6(3):351–60.
25. Veses V, Richards A, Gow NAR. Vacuoles and fungal biology. *Curr Opin Microbiol*. 2008;11:503–10.
26. Steinberg G, Schliwa M, Lehmler C, Bolker M, Kahmann R, McIntosh JR. Kinesin from the plant pathogenic fungus *Ustilago maydis* is involved in vacuole formation and cytoplasmic migration. *J Cell Sci*. 1998;111(15):2235–46.
27. Riquelme M, Bartnicki-García S, González-Prieto JM, Sánchez-León E, Verdín-Ramos JA, Beltrán-Aguilar A, et al. Spitzenkörper localization and intracellular traffic of green fluorescent protein-labeled CHS-3 and CHS-6 chitin synthases in living hyphae of *Neurospora crassa*. *Eukaryot Cell*. 2007;6(10):1853–64.
28. Levina NN, Lew RR. The role of tip-localized mitochondria in hyphal growth. *Fungal Genet Biol*. 2006;43(2):65–74.
29. Janmey PA. Phosphoinositides and calcium as regulators of cellular actin assembly and disassembly. *Annu Rev Physiol*. 1994;56(1):169–91.
30. Schneggenburger R, Neher E. Presynaptic calcium and control of vesicle fusion. *Curr Opin Neurobiol*. 2005;15(3):266–74.
31. Khan A, McQuilken M, Gladfelter AS. Septins and Generation of Asymmetries in Fungal Cells. *Annu Rev Microbiol*. 2015;69(1):487–503.

32. Hernández-Rodríguez Y, Hastings S, Momany M. The Septin AspB in *Aspergillus nidulans* Forms Bars and Filaments and Plays Roles in Growth Emergence and Conidiation. *Eukaryot Cell* [Internet]. 2012 Mar 1;11(3):311 LP – 323. Available from: <http://ec.asm.org/content/11/3/311.abstract>
33. Li L, Zhang C, Konopka JB. A *Candida albicans* Temperature-Sensitive cdc12-6 Mutant Identifies Roles for Septins in Selection of Sites of Germ Tube Formation and Hyphal Morphogenesis. *Eukaryot Cell* [Internet]. 2012 Oct 1;11(10):1210 LP – 1218. Available from: <http://ec.asm.org/content/11/10/1210.abstract>
34. Shioya T, Nakamura H, Ishii N, Takahashi N, Sakamoto Y, Ozaki N, et al. The *Coprinopsis cinerea* septin Cc. Cdc3 is involved in stipe cell elongation. *Fungal Genet Biol*. 2013;58:80–90.
35. Berepiki A, Read ND. Septins are important for cell polarity, septation and asexual spore formation in *Neurospora crassa* and show different patterns of localisation at germ tube tips. *PLoS One*. 2013;8(5):e63843.
36. Boyce KJ, Chang H, D'&Souza C a., Kronstad JW. An *Ustilago maydis* septin is required for filamentous growth in culture and for full symptom development on maize. *Eukaryot Cell*. 2005;4(12):2044–56.
37. Sudbery PE. Growth of *Candida albicans* hyphae. *Nat Publ Gr* [Internet]. 2011;9(10):737–48. Available from: <http://dx.doi.org/10.1038/nrmicro2636>
38. Kurtzman CP, Sugiyama J. Saccharomycotina and Taphrinomycotina: The Yeasts and Yeastlike Fungi of the Ascomycota. In: McLaughlin DJ, Spatafora JW, editors. *The Mycota VII Systematics and Evolution Part B*. 2nd ed. New York: Springer-Verlag Berlin Heidelberg; 2015. p. 3–34.
39. Berman J. Morphogenesis and cell cycle progression in *Candida albicans*. *Curr Opin Microbiol*. 2006;9(6):595–601.
40. Cullen PJ, Sprague GF. The regulation of filamentous growth in yeast. *Genetics*. 2012;190(1):23–49.
41. Kijpornyongpan T, Mondo SJ, Barry K, Sandor L, Lee J, Lipzen A, et al. Broad Genomic Sampling Reveals a Smut Pathogenic Ancestry of the Fungal Clade Ustilaginomycotina. *Mol Biol Evol* [Internet]. 2018;35(8):1840–54. Available from: <https://academic.oup.com/mbe/article/35/8/1840/4976507>

42. Weiss M, Bauer R, Sampaio JP, Oberwinkler F. Tremellomycetes and Related Groups. In: McLaughlin DJ, Spatafora JW, editors. *Mycota VII Systematics and Evolution Part A*. 2nd ed. New York: Springer-Verlag Berlin Heidelberg; 2014. p. 331–55.
43. Sil A, Andrianopoulos A. Thermally dimorphic human fungal pathogens—Polyphyletic pathogens with a convergent pathogenicity trait. *Cold Spring Harb Perspect Med*. 2015;5(8):1–17.
44. Nagy LG, Ohm R a, Kovács GM, Floudas D, Riley R, Gácsér A, et al. Latent homology and convergent regulatory evolution underlies the repeated emergence of yeasts. *Nat Commun* [Internet]. 2014;5:4471. Available from: <http://www.ncbi.nlm.nih.gov/pubmed/25034666>
45. Naranjo-Ortiz MA, Gabaldón T. Fungal evolution: major ecological adaptations and evolutionary transitions. *Biol Rev*. 2019;
46. Oshero N, Yarden O. The Cell Wall of Filamentous Fungi. In: Borkovich KA, Ebbole DJ, editors. *Cellular and Molecular Biology of Filamentous Fungular Biology of Filamentous Fungi*. American Society for Microbiology (ASM); 2010. p. 224–37.
47. Wu CF, Lew DJ. Beyond symmetry-breaking: Competition and negative feedback in GTPase regulation. *Trends Cell Biol* [Internet]. 2013;23(10):476–83. Available from: <http://dx.doi.org/10.1016/j.tcb.2013.05.003>
48. Wloka C, Bi E. Mechanisms of cytokinesis in budding yeast. *Cytoskeleton*. 2012;69(10):710–26.
49. Sipiczki M. Splitting of the fission yeast septum. *FEMS Yeast Res* [Internet]. 2007 Sep 1;7(6):761–70. Available from: <https://doi.org/10.1111/j.1567-1364.2007.00266.x>
50. Čáp M, Štěpánek L, Harant K, Váchová L, Palková Z. Cell Differentiation within a Yeast Colony: Metabolic and Regulatory Parallels with a Tumor-Affected Organism. *Mol Cell*. 2012;46(4):436–48.
51. Palková Z, Váchová L. Yeast cell differentiation: Lessons from pathogenic and non-pathogenic yeasts. *Semin Cell Dev Biol*. 2016;57:110–9.
52. Noble SM, Gianetti BA, Witchley JN. *Candida albicans* cell-type switching and functional plasticity in the mammalian host. *Nat Rev Microbiol* [Internet]. 2017;15(2):96–108. Available from: <http://dx.doi.org/10.1038/nrmicro.2016.157>

53. Ruiz-herrera J, Campos-Góngora E. An Introduction to Fungal Dimorphism. In: Ruiz-herrera J, editor. *Dimorphic Fungi: Their importance as models for differentiation and fungal pathogenesis*. Bentham Science; 2012. p. 3–15.
54. Henninger W, Windisch S. A New Yeast of *Sterigmatomyces*, *S. aphidis* sp. nov. *Arch Microbiol*. 1975;105:49–50.
55. Boekhout T. *Pseudozyma Bandoni* emend. for yeast-like anamorphs of Ustilaginales. *J Gen Appl Microbiol*. 1995;41:359–66.
56. Herb A, Sabou M, Delhorme J-B, Pessaux P, Mutter D, Candolfi E, et al. *Pseudozyma aphidis* fungemia after abdominal surgery: first adult case. *Med Mycol Case Rep*. 2015;8:37–9.
57. Günther M, Grumaz C, Lorenz S, Stevens P, Lindemann E, Hirth T, et al. The transcriptomic profile of *Pseudozyma aphidis* during production of mannosylerythritol lipids. *Appl Microbiol Biotechnol*. 2015;99:1375–88.
58. Doiphode N, Joshi C, Ghormade V, Deshpande M V. Biotechnological Applications of Dimorphic Yeasts. In: Satyanarayana T, Kunze G, editors. *Yeast Biotechnology: Diversity and Applications*. Springer; 2009. p. 635–50.
59. Ceccato-antonini SR, Sudbery PE. Filamentous Growth in *Saccharomyces cerevisiae*. *Brazilian J Microbiol*. 2004;35:173–81.
60. Gauthier GM. Dimorphism in Fungal Pathogens of Mammals, Plants, and Insects. *PLoS Pathog*. 2015;11(2):1–7.
61. Berkeley MJ. On a confervoid state of *Mucor clavatus*, Lk. *Mag Zool Bot*. 1838;2:340–3.
62. Begerow D, Schaffer AM, Kellner R, Youkov A, Kemler M, Oberwinkler F, et al. Ustilaginomycotina. In: McLaughlin DJ, Spatafora JW, editors. *Mycota VII Systematics and Evolution Part A*. 2nd ed. New York: Springer-Verlag Berlin Heidelberg; 2014. p. 295–329.
63. Oberwinkler F. Yeasts in Pucciniomycotina. *Mycol Prog*. 2017;16(9):831–56.
64. Boyce KJ, Andrianopoulos A. Fungal dimorphism: the switch from hyphae to yeast is a specialized morphogenetic adaptation allowing colonization of a host. *FEMS Microbiol Rev*. 2015;39(6):797–811.

65. Morrow CA, Fraser JA. Sexual reproduction and dimorphism in the pathogenic basidiomycetes. *FEMS Yeast Res* [Internet]. 2009 Mar [cited 2014 Mar 12];9(2):161–77. Available from: <http://www.ncbi.nlm.nih.gov/pubmed/19220864>
66. Boucias D, Liu S, Meagher R, Baniszewski J. Fungal dimorphism in the entomopathogenic fungus *Metarhizium rileyi*: Detection of an in vivo quorum-sensing system. *J Invertebr Pathol* [Internet]. 2016;136:100–8. Available from: <http://dx.doi.org/10.1016/j.jip.2016.03.013>
67. Nadal M, García-Pedrajas MD, Gold SE. Dimorphism in fungal plant pathogens. *FEMS Microbiol Lett* [Internet]. 2008 Jul [cited 2014 Dec 23];284(2):127–34. Available from: <http://www.ncbi.nlm.nih.gov/pubmed/18479435>
68. Garrido E, Pérez-Martín J. The Crk1 gene encodes an Ime2-related protein that is required for morphogenesis in the plant pathogen *Ustilago maydis*. *Mol Microbiol*. 2003;47(3):729–43.
69. Garrido E, Voß U, Müller P, Castillo-Lluva S, Kahmann R, Pérez-Martín J. The induction of sexual development and virulence in the smut fungus *Ustilago maydis* depends on Crk1, a novel MAPK protein. *Genes Dev*. 2004;18(24):3117–30.
70. Horst RJ, Zeh C, Saur A, Sonnewald S, Sonnewald U, Voll LM. The *Ustilago maydis* Nit2 Homolog Regulates Nitrogen Utilization and Is Required for Efficient Induction of Filamentous Growth. *Eukaryot Cell*. 2012;11(3):368–80.
71. Hartmann HA, Kahmann R, Bolker M. The pheromone response factor coordinates filamentous growth and pathogenicity in *Ustilago maydis*. *Embo J* [Internet]. 1996;15(7):1632–41. Available from: <http://www.ncbi.nlm.nih.gov/pubmed/8612587>
<http://www.ncbi.nlm.nih.gov/pmc/articles/PMC450074/pdf/emboj00007-0164.pdf>
72. Schade D, Walther A, Wendland J. The development of a transformation system for the dimorphic plant pathogen *Holleya sinecauda* based on *Ashbya gossypii* DNA elements. *Fungal Genet Biol* [Internet]. 2003;40(1):65–71. Available from: <http://www.sciencedirect.com/science/article/pii/S1087184503000641>
73. Ruiz-Herrera J, Sentandreu R. Different effectors of dimorphism in *Yarrowia lipolytica*. *Arch Microbiol*. 2002;178(6):477–83.

74. Kim J, Cheon SA, Park S, Song Y, Kim JY. Serum-induced hypha formation in the dimorphic yeast *Yarrowia lipolytica*. FEMS Microbiol Lett. 2000;190(1):9–12.
75. Szabo R. Dimorphism in *Yarrowia lipolytica*: Filament formation is suppressed by nitrogen starvation and inhibition of respiration. Folia Microbiol (Praha). 1999;44(1):19–24.
76. Rodrigues MG, Fonseca A. Molecular systematics of the dimorphic ascomycete genus *Taphrina*. Int J Syst Evol Microbiol. 2003;53(2):607–16.
77. Amoah-buahin E, Bone N, Armstrong J. Hyphal Growth in the Fission Yeast. Microbiology. 2005;4(7):1287–97.
78. Gilmore SA, Naseem S, Konopka JB, Sil A. N-acetylglucosamine (GlcNAc) Triggers a Rapid, Temperature-Responsive Morphogenetic Program in Thermally Dimorphic Fungi. PLoS Genet. 2013;9(9).
79. Maresca B, Lambowitz AM, Kumar VB, Grant GA, Kobayashi GS, Medoff G. Role of cysteine in regulating morphogenesis and mitochondrial activity in the dimorphic fungus *Histoplasma capsulatum*. Proc Natl Acad Sci U S A. 1981;78(7):4596–600.
80. Hornby JM, Jacobitz-Kizzier SM, McNeel DJ, Jensen EC, Treves DS, Nickerson KW. Inoculum size effect in dimorphic fungi: extracellular control of yeast-mycelium dimorphism in *Ceratocystis ulmi*. Appl Environ Microbiol. 2004;70(3):1356–9.
81. Kulkarni RK, Nickerson KW. Nutritional control of dimorphism in *Ceratocystis ulmi*. Exp Mycol. 1981;5(2):148–54.
82. Keen NT, Wang MC, Long M, Erwin DC. Dimorphism in *Verticillium albo-atrum* as affected by initial spore concentration and antispore chemicals. Phytopathology. 1971;61:1266–9.
83. Yemelin A, Brauchler A, Jacob S, Laufer J, Heck L, Foster AJ, et al. Identification of factors involved in dimorphism and pathogenicity of *Zymoseptoria tritici*. PLoS One. 2017;12(8):1–31.
84. Reeslev M, Jorgensen BB, Jorgensen OB. Influence of Zn²⁺ on yeast-mycelium dimorphism and exopolysaccharide production by the fungus *Aureobasidium pullulans* grown in a defined medium in continuous culture. J Gen Microbiol. 1993;139(12):3065–70.
85. Park D. Population density and yeast mycelial dimorphism in *Aureobasidium pullulans*. Trans - Br Mycol Soc [Internet]. 1984;82(1):39–44. Available from: [http://dx.doi.org/10.1016/S0007-1536\(84\)80209-0](http://dx.doi.org/10.1016/S0007-1536(84)80209-0)

86. Hardcastle R V., Szaniszló PJ. Characterization of dimorphism in *Cladosporium werneckii*. *J Bacteriol.* 1974;119(1):294–302.
87. Houston MR, Meyer KH, Thomas N, Wolf FT. Dimorphism in *Cladosporium werneckii*. *Sabouraudia J Med Vet Mycol* [Internet]. 1969 Jan 1;7(3):195–8. Available from: <https://www.tandfonline.com/doi/abs/10.1080/00362177085190351>
88. Brefort T, Doehlemann G, Mendoza-mendoza A, Reissmann S, Djamei A, Kahmann R. *Ustilago maydis* as a Pathogen. *Annu Rev phyto.* 2009;47:423–45.
89. Mendoza-Mendoza A, Berndt P, Djamei A, Weise C, Linne U, Marahiel M, et al. Physical-chemical plant-derived signals induce differentiation in *Ustilago maydis*. *Mol Microbiol.* 2009;71(4):895–911.
90. Paul JA, Barati MT, Cooper M, Perlin H. Physical and Genetic Interaction between Ammonium Transporters and the Signaling Protein Rho1 in the Plant Pathogen *Ustilago maydis*. *Eukaryot Cell.* 2014;13(10):1328–36.
91. Ruiz-Herrera J, Guevara-Olvera CGLL, Cdrabez-Trejo A. Yeast-mycelial dimorphism of haploid and diploid strains of *Ustilago maydis*. *Microbiology.* 1995;(141):695–703.
92. Youngchim S, Nosanchuk JD, Pornsuwan S, Kajiwarara S, Vanittanakom N. The role of L-DOPA on melanization and mycelial production in *Malassezia furfur*. *PLoS One.* 2013;8(6):e63764.
93. Faergemann J, Bernander S. Micro-aerophilic and anaerobic growth of *Pityrosporum* species. *Med Mycol* [Internet]. 1981 May 1;19(2):117–21. Available from: <https://doi.org/10.1080/00362178185380181>
94. Faergemann J. A new model for growth and filament production of *Pityrosporum ovale* (*orbiculare*) on human stratum corneum in vitro. *J Invest Dermatol* [Internet]. 1989;92(1):117–9. Available from: <http://dx.doi.org/10.1111/1523-1747.ep13071328>
95. Schäfer AM, Kemler M, Bauer R, Begerow D. The illustrated life cycle of *Microbotryum* on the host plant *Silene latifolia*. *Botany.* 2010;88(10):875–85.
96. Lin X. *Cryptococcus neoformans*: Morphogenesis, infection, and evolution. *Infect Genet Evol.* 2009;9:401–16.

97. Zhu L Bin, Wang Y, Zhang Z Bin, Yang HL, Yan RM, Zhu D. Influence of environmental and nutritional conditions on yeast – mycelial dimorphic transition in *Trichosporon cutaneum*. 2017;2818(May). Available from: <http://dx.doi.org/10.1080/13102818.2017.1292149>
98. Orłowski M. *Mucor* Dimorphism. *Microbiol Rev*. 1991;55(2):234–58.
99. Tulasne L-R, Tulasne C. Mémoire sur les Ustilaginées comparées aux Urédinées. *Ann Sci Nat Bot*. 1847;7:12-127 + Pls. 2-7.
100. Bauer R, Garnica S, Oberwinkler F, Riess K, Weiß M, Begerow D. Entorrhizomycota: A New Fungal Phylum Reveals New Perspectives on the Evolution of Fungi. *PLoS One* [Internet]. 2015;10(7):e0128183. Available from: <http://dx.plos.org/10.1371/journal.pone.0128183>
101. Tanaka E, Ashizawa T, Sonoda R, Tanaka C. *Villosiclava virens* gen. nov., com. nov., teleomorph of *Ustilaginoidea virens*, the causal agent of rice false smut. *Mycotaxon*. 2008;106(December):491–501.
102. Riess K, Schön ME, Lutz M, Butin H, Oberwinkler F, Garnica S. On the Evolutionary History of *Uleiella chilensis*, a Smut Fungus Parasite of *Araucaria araucana* in South America: Uleiellales ord. nov. in Ustilaginomycetes. *PLoS One* [Internet]. 2016;11(1):e0147107. Available from: <http://dx.plos.org/10.1371/journal.pone.0147107>
103. Lutz MC, Sanchez AD, Vera L, Scarso AG, Sosa MC. First report of *Pseudomicrostroma juglandis* (syn. *Microstroma juglandis*) causing downy leaf spot of walnut in Argentina. *J Plant Pathol*. 2018;100(2):349–349.
104. Brewer MT, Turner AN, Brannen PM, Cline WO, Richardson EA. *Exobasidium maculosum*, a new species causing leaf and fruit spots on blueberry in the southeastern USA and its relationship with other *Exobasidium* spp. parasitic to blueberry and cranberry. *Mycologia* [Internet]. 2014 May 1;106(3):415–23. Available from: <https://doi.org/10.3852/13-202>
105. Boekhout T, Gildemacher P, Theelen B, Müller WH, Heijne B, Lutz M. Extensive colonization of apples by smut anamorphs causes a new postharvest disorder. *FEMS Yeast Res*. 2006;6(1):63–76.
106. Baric S, Lindner L, Marschall K, Dalla Via J. Haplotype diversity of *Tilletiopsis* spp. causing white haze in apple orchards in Northern Italy. *Plant Pathol*. 2010;59(3):535–41.

107. Albu S. A survey of ballistosporic phylloplane yeasts in Baton Rouge, Louisiana. Louisiana State University; 2012.
108. Albu S, Toome M, Aime MC. *Violaceomyces palustris* gen. et sp. nov. and a new monotypic lineage, Violaceomycetales ord. nov. in Ustilaginomycetes. *Mycologia*. 2015;107(6):1193–204.
109. Guého E, Boekhout T, Ashbee HR, Guillot J, Van Belkum A, Faergemann J. The role of *Malassezia* species in the ecology of human skin and as pathogens. *Med Mycol*. 1998;36(Suppl 1):220–9.
110. Guého E, Batra R, Boekhout T. *Malassezia* Baillon (1889). In: Kurtzman CP, Fell JW, Boekhout T, editors. *The Yeasts: A Taxonomic Study Vol 3*. 5th ed. Amsterdam, Netherlands: Elsevier; 2011. p. 1807–32.
111. de Hoog GS, Smith MT, Rosa CA. *Moniliella* Stolk & Dakin (1966). In: Kurtzman CP, Fell JW, Boekhout T, editors. *The Yeasts: A Taxonomic Study Vol 3*. 5th ed. Elsevier; 2011. p. 1837–46.
112. Boekhout T, Theelen B, Houbraken J, Robert V, Scorzetti G, Gafni A, et al. Novel anamorphic mite-associated fungi belonging to the Ustilaginomycetes: *Meira geulakonigii* gen. nov., sp. nov., *Meira argovae* sp. nov. and *Acaromyces ingoldii* gen. nov., sp. nov. *Int J Syst Evol Microbiol*. 2003;53(5):1655–64.
113. Holliday R. A mechanism for gene conversion in fungi. *Genet Res (Camb)*. 1964;5(2):282–304.
114. Holliday R. Early studies on recombination and DNA repair in *Ustilago maydis*. *DNA Repair (Amst)*. 2004;3(6):671–82.
115. Basse CW, Steinberg G. *Ustilago maydis*, model system for analysis of the molecular basis of fungal pathogenicity. *Mol Plant Pathol*. 2004;5(2):83–92.
116. Kämper J, Kahmann R, Bölker M, Ma L-J, Brefort T, Saville BJ, et al. Insights from the genome of the biotrophic fungal plant pathogen *Ustilago maydis*. *Nature [Internet]*. 2006 Nov 2 [cited 2014 Feb 20];444(7115):97–101. Available from: <http://www.ncbi.nlm.nih.gov/pubmed/17080091>
117. Spellig T, Bölker M, Lottspeich F, Frank RW, Kahmann R. Pheromones trigger filamentous growth in *Ustilago maydis*. *EMBO J*. 1994;13(7):1620–7.

118. García-Muse T, Steinberg G, Pérez-Martín J. Pheromone-induced G2 arrest in the phytopathogenic fungus *Ustilago maydis*. *Eukaryot Cell*. 2003;2(3):494–500.
119. Lanver D, Mendoza-Mendoza A, Brachmann A, Kahmann R. Sho1 and Msb2-related proteins regulate appressorium development in the smut fungus *Ustilago maydis*. *Plant Cell*. 2010;22(6):2085–101.
120. Piepenbring M, Bauer R, Oberwinkler F. Teliospores of smut fungi general aspects of teliospore walls and sporogenesis. *Protoplasma*. 1998;204(3–4):155–69.
121. Vollmeister E, Schipper K, Baumann S, Haag C, Pohlmann T, Stock J, et al. Fungal development of the plant pathogen *Ustilago maydis*. *FEMS Microbiol Rev*. 2012;36(1):59–77.
122. Cullen PJ, Sprague GF. Glucose depletion causes haploid invasive growth in yeast. *Proc Natl Acad Sci*. 2000;97(25):13619–24.
123. Buffo J, Herman MA, Soll DR. A characterization of pH-regulated dimorphism in *Candida albicans*. *Mycopathologia*. 1984;85(1–2):21–30.
124. Wongsuk T, Pumeesat P, Luplertlop N. Fungal quorum sensing molecules: Role in fungal morphogenesis and pathogenicity. *J Basic Microbiol*. 2016;56(5):440–7.
125. Domínguez E, Cuartero J, Heredia A. An overview on plant cuticle biomechanics. *Plant Sci*. 2011;181:77–84.
126. Hamel L-P, Nicole M-C, Duplessis S, Ellis BE. Mitogen-Activated Protein Kinase Signaling in Plant-Interacting Fungi: Distinct Messages from Conserved Messengers. *Plant Cell*. 2012;24(4):1327–51.
127. Fuller KK, Rhodes JC. Protein kinase A and fungal virulence A sinister side to a conserved nutrient sensing pathway. *Virulence*. 2012;3(2):109–21.
128. Bölker M, Urban M, Kahmann R. The a mating type locus of *Ustilago maydis* specifies cell signaling components. *Cell*. 1992;68(3):441–50.
129. Smith DG, Garcia-Pedrajas MD, Gold SE, Perlin MH. Isolation and characterization from pathogenic fungi of genes encoding ammonium permeases and their roles in dimorphism. *Mol Microbiol*. 2003;50(1):259–75.
130. Regenfelder E, Spellig T, Hartmann A, Lauenstein S, Bölker M, Kahmann R. G proteins in *Ustilago maydis*: transmission of multiple signals? *EMBO J*. 1997;16(8):1934–42.

131. Müller P, Leibbrandt A, Teunissen H, Cubasch S, Aichinger C, Kahmann R. The G β -subunit-encoding gene *Bpp1* controls cyclic-AMP signaling in *Ustilago maydis*. *Eukaryot Cell*. 2004;3(3):806–14.
132. Gold S, Duncan G, Barrett K, Kronstad J. cAMP regulates morphogenesis in the fungal pathogen *Ustilago maydis*. *Genes Dev*. 1994;8(23):2805–16.
133. Gold SE, Brogdon SM, Mayorga ME, Kronstad JW. The *Ustilago maydis* regulatory subunit of a cAMP-dependent protein kinase is required for gall formation in maize. *Plant Cell*. 1997;9(9):1585–94.
134. Dürrenberger F, Wong K, Kronstad JW. Identification of a cAMP-dependent protein kinase catalytic subunit required for virulence and morphogenesis in *Ustilago maydis*. *Proc Natl Acad Sci*. 1998;95(10):5684–9.
135. Agarwal C, Aulakh KB, Edelen K, Cooper M, Wallen RM, Adams S, et al. *Ustilago maydis* phosphodiesterases play a role in the dimorphic switch and in pathogenicity. *Microbiology*. 2013;159:857–68.
136. Egan JD, García-pedrajas MD, Andrews DL, Gold SE. Calcineurin Is an Antagonist to PKA Protein Phosphorylation Required for Postmating Filamentation and Virulence , While PP2A Is Required for Viability in *Ustilago maydis*. *Mol Plant-Microbe Interact*. 2009;22(10):1293–301.
137. Klosterman SJ, Martinez-Espinoza AD, Andrews DL, Seay JR, Gold SE. Ubc2, an ortholog of the yeast Ste50p adaptor, possesses a basidiomycete-specific carboxy terminal extension essential for pathogenicity independent of pheromone response. *Mol plant-microbe Interact*. 2008;21(1):110–21.
138. Mayorga ME, Gold SE. The *ubc2* gene of *Ustilago maydis* encodes a putative novel adaptor protein required for filamentous growth, pheromone response and virulence. *Mol Microbiol*. 2001;41(6):1365–79.
139. Müller P, Aichinger C, Feldbrügge M, Kahmann R. The MAP kinase *kpp2* regulates mating and pathogenic development in *Ustilago maydis*. *Mol Microbiol*. 1999;34(5):1007–17.
140. Mayorga ME, Gold SE. A MAP kinase encoded by the *ubc3* gene of *Ustilago maydis* is required for filamentous growth and full virulence. *Mol Microbiol*. 1999;34(3):485–97.

141. Brachmann A, Schirawski J, Müller P, Kahmann R. An unusual MAP kinase is required for efficient penetration of the plant surface by *Ustilago maydis*. *EMBO J.* 2003;22(9):2199–210.
142. Banuett F, Herskowitz I. Identification of *fuz7*, a *Ustilago maydis* MEK/MAPKK homolog required for *a* locus-dependent and independent steps in the fungal life cycle. *Genes Dev.* 1994;8(12):1367–78.
143. Andrews DL, Egan JD, Mayorga ME, Gold SE. The *Ustilago maydis* *ubc4* and *ubc5* genes encode members of a MAP kinase cascade required for filamentous growth. *Mol plant-microbe Interact.* 2000;13(7):781–6.
144. Di Stasio M, Brefort T, Mendoza-Mendoza A, Münch K, Kahmann R. The dual specificity phosphatase *Rok1* negatively regulates mating and pathogenicity in *Ustilago maydis*. *Mol Microbiol.* 2009;73(1):73–88.
145. Lee N, Kronstad JW. *ras2* controls morphogenesis, pheromone response, and pathogenicity in the fungal pathogen *Ustilago maydis*. *Eukaryot Cell.* 2002;1(6):954–66.
146. Müller P, Katzenberger D, Loubradou G, Kahmann R. Guanyl Nucleotide Exchange Factor *Sql2* and *Ras2* Regulate Filamentous Growth in *Ustilago maydis*. 2003;2(3):609–17.
147. Pham CD, Yu Z, Bolker M, Gold SE, Perlin MH. *Ustilago maydis* *Rho1* and 14-3-3 Homologues Participate in Pathways Controlling Cell Separation and Cell Polarity. *Eukaryot Cell.* 2009;8(7):977–89.
148. García-pedrajas MD, Nadal M, Bölker M, Gold SE, Perlin MH. Sending mixed signals : Redundancy vs . uniqueness of signaling components in the plant pathogen *Ustilago maydis*. *Fungal Genet Biol.* 2008;45:S22–30.
149. Leveleki L, Mahlert M, Sandrock B, Bölker M. The PAK family kinase *Cla4* is required for budding and morphogenesis in *Ustilago maydis*. *Mol Microbiol.* 2004;54(2):396–406.
150. Mahlert M, Leveleki L, Hlubek A, Sandrock B, Bölker M. *Rac1* and *Cdc42* regulate hyphal growth and cytokinesis in the dimorphic fungus *Ustilago maydis*. *Mol Microbiol.* 2006;59(2):567–78.
151. Flor-Parra I, Vranes M, Kämper J, Pérez-Martín J. *Biz1*, a zinc finger protein required for plant invasion by *Ustilago maydis*, regulates the levels of a mitotic cyclin. *Plant Cell.* 2006;18(9):2369–87.

152. Mendoza-Mendoza A, Eskova A, Weise C, Czajkowski R, Kahmann R. Hap2 regulates the pheromone response transcription factor *prf1* in *Ustilago maydis*. *Mol Microbiol*. 2009;72(3):683–98.
153. Brefort T, Müller P, Kahmann R. The high-mobility-group domain transcription factor *Rop1* is a direct regulator of *prf1* in *Ustilago maydis*. *Eukaryot Cell*. 2005;4(2):379–91.
154. Hartmann HA, Krüger J, Lottspeich F, Kahmann R. Environmental signals controlling sexual development of the corn smut fungus *Ustilago maydis* through the transcriptional regulator *Prf1*. *Plant Cell*. 1999;11(7):1293–305.
155. Heimel K, Scherer M, Vranes M, Wahl R, Pothiratana C, Schuler D, et al. The Transcription Factor *Rbf1* Is the Master Regulator for b-Mating Type Controlled Pathogenic Development in *Ustilago maydis*. *PLoS Pathog* [Internet]. 2010 Aug 5;6(8):e1001035. Available from: <https://doi.org/10.1371/journal.ppat.1001035>
156. Heimel K, Scherer M, Schuler D, Kämper J. The *Ustilago maydis* *Clp1* protein orchestrates pheromone and b-dependent signaling pathways to coordinate the cell cycle and pathogenic development. *Plant Cell* [Internet]. 2010 Aug 1 [cited 2015 Oct 17];22(8):2908–22. Available from: <http://www.plantcell.org/content/22/8/2908.short>
157. González-prieto JM, Rosas-quijano R, Domínguez A, Ruiz-herrera J. The *UmGcn5* gene encoding histone acetyltransferase from *Ustilago maydis* is involved in dimorphism and virulence. *Fungal Genet Biol*. 2014;71:86–95.
158. Elías-Villalobos A, Fernández-Alvarez A, Moreno-Sánchez I. The *Hos2* Histone Deacetylase Controls *Ustilago maydis* Virulence through Direct Regulation of Mating-Type Genes. *PLoS Pathog*. 2015;11(8):e1005134.
159. Elías-Villalobos A, Fernández-Álvarez A, Ibeas JI. The general transcriptional repressor *Tup1* is required for dimorphism and virulence in a fungal plant pathogen. *PLoS Pathog*. 2011;7(9):e1002235.
160. Tollot M, Assmann D, Becker C, Altmüller J. The WOPR Protein *Ros1* Is a Master Regulator of Sporogenesis and Late Effector Gene Expression in the Maize Pathogen *Ustilago maydis*. *PLoS Pathog*. 2016;12(6):e1005697.

161. Chacko N, Gold S. Deletion of the *Ustilago maydis* ortholog of the *Aspergillus* sporulation regulator *medA* affects mating and virulence through pheromone response. *Fungal Genet Biol* [Internet]. 2012;49(6):426–32. Available from: <http://dx.doi.org/10.1016/j.fgb.2012.04.002>
162. Dürrenberger F, Laidlaw RD, Kronstad JW. The *hgl1* gene is required for dimorphism and teliospore formation in the fungal pathogen *Ustilago maydis*. *Mol Microbiol* [Internet]. 2001;41(2):337–48. Available from: <http://www.ncbi.nlm.nih.gov/pubmed/11489122>
163. Wang L, Berndt P, Xia X, Kahnt J, Kahmann R. A seven-WD40 protein related to human RACK1 regulates mating and virulence in *Ustilago maydis*. *Mol Microbiol*. 2011;81(6):1484–98.
164. Weber I, Gruber C, Steinberg G. A class-V myosin required for mating, hyphal growth, and pathogenicity in the dimorphic plant pathogen *Ustilago maydis*. *Plant Cell*. 2003;15(12):2826–42.
165. Schuchardt I, Aßmann D, Thines E, Schuberth C, Steinberg G. Myosin-V, Kinesin-1, and Kinesin-3 cooperate in hyphal growth of the fungus *Ustilago maydis*. *Mol Biol Cell*. 2005;16(11):5191–201.
166. Becht P, Vollmeister E, Feldbrügge M. Role for RNA-Binding Proteins Implicated in Pathogenic Development of *Ustilago maydis*. *Eukaryot Cell*. 2005;4(1):121–33.
167. Vollmeister E, Haag C, Zarnack K, Baumann S, König J, Mannhaupt G, et al. Tandem KH domains of *Khd4* recognize AUACCC and are essential for regulation of morphology as well as pathogenicity in *Ustilago maydis*. *RNA*. 2009;15(12):2206–18.
168. García-Muse T, Steinberg G, Pérez-Martín J. Characterization of B-type cyclins in the smut fungus *Ustilago maydis*: roles in morphogenesis and pathogenicity. *J Cell Sci*. 2004;117(3):487–506.
169. Weber I, Thines E, Steinberg G. Polar Localizing Class V Myosin Chitin Synthases Are Essential during Early Plant Infection in the Plant Pathogenic Fungus *Ustilago maydis*. *Plant Cell*. 2006;18(January):225–42.
170. Valinluck M, Woraratanadharm T, Lu C yu, Quintanilla RH, Banuett F. The cell end marker *Tea4* regulates morphogenesis and pathogenicity in the basidiomycete fungus *Ustilago maydis*. *Fungal Genet Biol* [Internet]. 2014;66:54–68. Available from: <http://dx.doi.org/10.1016/j.fgb.2014.02.010>

171. Woraratanadharm T, Kmosek S, Banuett F. UmTea1, a Kelch and BAR domain-containing protein, acts at the cell cortex to regulate cell morphogenesis in the dimorphic fungus *Ustilago maydis*. *Fungal Genet Biol* [Internet]. 2018;121(August):10–28. Available from: <https://doi.org/10.1016/j.fgb.2018.09.002>
172. Krüger J, Loubradou G, Regenfelder E, Hartmann A, Kahmann R. Crosstalk between cAMP and pheromone signalling pathways in *Ustilago maydis*. *Mol Gen Genet*. 1998;260(2–3):193–8.
173. Martínez-Espinoza AD, Ruiz-Herrera J, León-Ramírez CG, Gold SE. MAP kinase and cAMP signaling pathways modulate the pH-induced yeast-to-mycelium dimorphic transition in the corn smut fungus *Ustilago maydis*. *Curr Microbiol*. 2004;49(4):274–81.
174. Müller P, Weinzierl G, Brachmann A, Feldbrügge M, Kahmann R. Mating and pathogenic development of the smut fungus *Ustilago maydis* are regulated by one mitogen-activated protein kinase cascade. *Eukaryot Cell*. 2003;2(6):1187–99.
175. Garrido E, Voß U, Müller P, Castillo-lluva S, Kahmann R. The induction of sexual development and virulence in the smut fungus *Ustilago maydis* depends on Crk1 , a novel MAPK protein. 2004;7:3117–30.
176. Strudwick N, Brown M, Parmar VM, Schroder M. Ime1 and Ime2 Are Required for Pseudohyphal Growth of *Saccharomyces cerevisiae* on Nonfermentable Carbon Sources. *Mol Cell Biol*. 2010;30(23):5514–30.
177. Castillo-Lluva S, Alvarez-Tabares I, Weber I, Steinberg G, Perez-Martin J. Sustained cell polarity and virulence in the phytopathogenic fungus *Ustilago maydis* depends on an essential cyclin-dependent kinase from the Cdk5/Pho85 family. *J Cell Sci*. 2007;120(9):1584–95.
178. Campos CBL, Di Benedette JPT, Morais F V., Ovalle R, Nobrega MP. Evidence for the role of calcineurin in morphogenesis and calcium homeostasis during mycelium-to-yeast dimorphism of *Paracoccidioides brasiliensis*. *Eukaryot Cell*. 2008;7(10):1856–64.
179. Lee SC, Li A, Calo S, Heitman J. Calcineurin Plays Key Roles in the Dimorphic Transition and Virulence of the Human Pathogenic Zygomycete *Mucor circinelloides*. *PLoS Pathog*. 2013;9(9).

180. Lee SC, Li A, Calo S, Inoue M, Tonthat NK, Bain JM, et al. Calcineurin orchestrates dimorphic transitions , antifungal drug responses and host – pathogen interactions of the pathogenic mucoralean fungus *Mucor circinelloides*. *Mol Microbiol*. 2015;97(5):844–65.
181. Paul JA, Wallen RM, Zhao C, Shi T, Perlin MH. Coordinate regulation of *Ustilago maydis* ammonium transporters and genes involved in mating and pathogenicity. *Fungal Biol* [Internet]. 2018;122(7):639–50. Available from: <https://doi.org/10.1016/j.funbio.2018.03.011>
182. Bakkeren G, Kämper J, Schirawski J. Sex in smut fungi: Structure, function and evolution of mating-type complexes. *Fungal Genet Biol* [Internet]. 2008 Aug [cited 2014 Feb 19];45 Suppl 1:S15-21. Available from: <http://www.ncbi.nlm.nih.gov/pubmed/18501648>
183. Kaffarnik F, Müller P, Leibundgut M, Kahmann R, Feldbrügge M. PKA and MAPK phosphorylation of Prf1 allows promoter discrimination in *Ustilago maydis*. *EMBO J*. 2003;22(21):5817–26.
184. Brachmann A, Weinzierl G. Identification of genes in the bW / bE regulatory cascade in *Ustilago maydis*. *Mol Microbiol*. 2001;42(4):1047–63.
185. Klose J, De Sá MM, Kronstad JW. Lipid-induced filamentous growth in *Ustilago maydis*. *Mol Microbiol*. 2004;52(3):823–35.
186. Bölker M, Genin S, Lehmler C, Kahmann R. Genetic regulation of mating and dimorphism in *Ustilago maydis* . *Can J Bot*. 1995;73(S1):320–5.
187. Scherer M, Heimel K, Starke V, Kämper J. The Clp1 Protein Is Required for Clamp Formation and Pathogenic Development of *Ustilago maydis*. *Plant Cell* [Internet]. 2006 Sep 1;18(9):2388 LP – 2401. Available from: <http://www.plantcell.org/content/18/9/2388.abstract>
188. Hibbett DS, Stajich JE, Spatafora JW. Toward genome-enabled mycology. *Mycologia* [Internet]. 2013 [cited 2014 Feb 27];105(6):1339–49. Available from: <http://www.ncbi.nlm.nih.gov/pubmed/23928422>
189. Grigoriev I V., Nikitin R, Haridas S, Kuo A, Ohm R, Otillar R, et al. MycoCosm portal: Gearing up for 1000 fungal genomes. *Nucleic Acids Res*. 2014;42(D1):699–704.
190. Nguyen TA, Cissé OH, Yun Wong J, Zheng P, Hewitt D, Nowrousian M, et al. Innovation and constraint leading to complex multicellularity in the Ascomycota. *Nat Commun*. 2017;8.

191. Nantel A, Dignard D, Bachewich C, Harcus D, Marcil A, Bouin A-P, et al. Transcription profiling of *Candida albicans* cells undergoing the yeast-to-hyphal transition. *Mol Biol Cell*. 2002;13(10):3452–65.
192. Azadmanesh J, Gowen AM, Creger PE, Schafer ND, Blankenship JR. Filamentation Involves Two Overlapping , but Distinct , Programs of Filamentation in the Pathogenic Fungus *Candida albicans*. *G3 Genes, Genomes, Genet*. 2017;7(November):3797–808.
193. Hwang CS, Rhie GE, Oh JH, Huh WK, Yim HS, Kang SO. Copper- and zinc-containing superoxide dismutase (Cu/ZnSOD) is required for the protection of *Candida albicans* against oxidative stresses and the expression of its full virulence. *Microbiology*. 2002;148(11):3705–13.
194. Edwards JA, Chen C, Kemski MM, Hu J, Mitchell TK, Rappleye CA. *Histoplasma* yeast and mycelial transcriptomes reveal pathogenic-phase and lineage-specific gene expression profiles. *BMC Genomics*. 2013;14:695.
195. Martínez-Soto D, Ruiz-Herrera J. Transcriptomic analysis of the dimorphic transition of *Ustilago maydis* induced in vitro by a change in pH. *Fungal Genet Biol*. 2013;58–59:116–25.
196. Lanver D, Berndt P, Tollot M, Naik V, Vranes M, Warmann T, et al. Plant Surface Cues Prime *Ustilago maydis* for Biotrophic Development. *PLoS Pathog*. 2014;10(7).
197. Nigg M, Laroche J, Landry CR, Bernier L. RNAseq Analysis Highlights Specific Transcriptome Signatures of Yeast and Mycelial Growth Phases in the Dutch Elm Disease Fungus *Ophiostoma novo-ulmi*. *G3 Genes, Genomes, Genet*. 2015;5(11):2487–95.
198. Nigg M, Bernier L. From yeast to hypha : defining transcriptomic signatures of the morphological switch in the dimorphic fungal pathogen *Ophiostoma novo-ulmi*. *BMC Genomics* [Internet]. 2016;1–16. Available from: <http://dx.doi.org/10.1186/s12864-016-3251-8>
199. Nigg M, Bernier L. Large-scale genomic analyses of in vitro yeast-mycelium dimorphism in human, insect and plant pathogenic fungi: From ESTs to RNAseq experiments. *Fungal Biol Rev* [Internet]. 2017;31(3):131–42. Available from: <http://dx.doi.org/10.1016/j.fbr.2017.04.001>
200. Gancedo JM. Control of pseudohyphae formation in *Saccharomyces cerevisiae*. *FEMS Microbiol Rev*. 2001;25:107–23.

201. Borges-Walmsley MI, Walmsley AR. cAMP signalling in pathogenic fungi: Control of dimorphic switching and pathogenicity. *Trends Microbiol.* 2000;8(3):133–41.
202. Wanchoo A, Lewis MW, Keyhani NO. Lectin mapping reveals stage-specific display of surface carbohydrates in in vitro and haemolymph- derived cells of the entomopathogenic fungus *Beauveria bassiana*. *Microbiology.* 2009;155:3121–33.
203. Evans HC, Elliot SL, Hughes DP, Evans HC, Elliot SL, *Ophiocordyceps* DPH. *Ophiocordyceps unilateralis*: A keystone species for unraveling ecosystem functioning and biodiversity of fungi in tropical forests? *Commun Integr Biol.* 2011;4(5):598–602.
204. Holliday R. *Ustilago maydis*. In: King RC, editor. *Handbook of Genetics, Vol 1 Bacteria, Bacteriophages and Fungi*. New York: Plenum: Springer US; 1997. p. 575–95.
205. Manning M, Mitchell TG. Strain variation and morphogenesis of yeast- and mycelial-phase *Candida albicans* in low-sulfate, synthetic medium. *J Bacteriol.* 1980;142(2):714–9.
206. Wickham H. *ggplot2: elegant graphics for data analysis*. Springer; 2016.
207. Naruzawa ES, Bernier L. Control of yeast-mycelium dimorphism invitro in Dutch elm disease fungi by manipulation of specific external stimuli. *Fungal Biol [Internet]*. 2014;118(11):872–84. Available from: <http://dx.doi.org/10.1016/j.funbio.2014.07.006>
208. Naruzawa ES, Malagnac F, Bernier L. Effect of linoleic acid on reproduction and yeast-mycelium dimorphism in the Dutch elm disease pathogens. *Botany.* 2016;96(November 2015):31–9.
209. Rush TA, Aime MC. The genus *Meira*: Phylogenetic placement and description of a new species. *Antonie Van Leeuwenhoek.* 2013;103:1097–106.
210. Kijpornyongpan T, Aime MC. Taxonomic revisions in the Microstromatales: two new yeast species, two new genera, and validation of *Jaminaea* and two *Sympodiomyces* species. *Mycol Prog.* 2017;16(5):495–505.
211. Liu W, Zhou X, Li G, Li L, Kong L, Wang C, et al. Multiple plant surface signals are sensed by different mechanisms in the rice blast fungus for appressorium formation. *PLoS Pathog.* 2011;7(1).
212. Zabka V, Stangl M, Bringmann G, Vogg G, Riederer M, Hildebrandt U. Host surface properties affect prepenetration processes in the barley powdery mildew fungus. *New Phytol.* 2008;177(1):251–63.

213. Joo H, Choi Y, Cho S, Choi J, Lee D, Kim H, et al. *Pseudozyma aphidis* fungaemia with invasive fungal pneumonia in a patient with acute myeloid leukaemia: case report and literature review. *Mycoses*. 2016;59(1):56–61.
214. Krizsán K, Almási É, Merényi Z, Sahu N, Virágh M, Kószó T, et al. Transcriptomic atlas of mushroom development reveals conserved genes behind complex multicellularity in fungi. *Proc Natl Acad Sci*. 2019;116(15):7409–18.
215. Nyland G. The genus *Tilletiopsis*. *Mycologia*. 1950;42(4):487–96.
216. Brasier CM. *Ophiostoma novo-ulmi* sp. nov., causative agent of current Dutch elm disease pandemics. *Mycopathologia*. 1991;115(3):151–61.
217. Forgetta V, Leveque G, Dias J, Grove D, Lyons Jr R, Genik S, et al. Sequencing of the Dutch elm disease fungus genome using the Roche/454 GS-FLX Titanium System in a comparison of multiple genomics core facilities. *J Biomol Tech JBT*. 2013;24(1):39.
218. Emms DM, Kelly S. OrthoFinder: solving fundamental biases in whole genome comparisons dramatically improves orthogroup inference accuracy. *Genome Biol* [Internet]. 2015;16:157. Available from: <http://dx.doi.org/10.1186/s13059-015-0721-2>
219. Huerta-cepas J, Szklarczyk D, Forslund K, Cook H, Heller D, Walter MC, et al. eggNOG 4.5: a hierarchical orthology framework with improved functional annotations for eukaryotic, prokaryotic and viral sequences. *Nucleic Acids Res*. 2016;44(November 2015):286–93.
220. Martin M. Cutadapt removes adapter sequences from high-throughput sequencing reads. *EMBnet J*. 2011;17(1):pp-10.
221. Bolger AM, Lohse M, Usadel B. Trimmomatic: a flexible trimmer for Illumina sequence data. *Bioinformatics*. 2014;30(15):2114–20.
222. Andrews S. FastQC: a quality control tool for high throughput sequence data. 2010.
223. Trapnell C, Pachter L, Salzberg SL. TopHat: discovering splice junctions with RNA-Seq. *Bioinformatics*. 2009;25(9):1105–11.
224. Anders S, Pyl PT, Huber W. HTSeq—a Python framework to work with high-throughput sequencing data. *Bioinformatics*. 2015;31(2):166–9.
225. Love MI, Huber W, Anders S. Moderated estimation of fold change and dispersion for RNA-seq data with DESeq2. *Genome Biol*. 2014;15(12):550.

226. Smyth GK. Limma: linear models for microarray data. In: Bioinformatics and computational biology solutions using R and Bioconductor. New York, NY: Springer; 2005. p. 397–420.
227. Falcon S, Gentleman R. Hypergeometric Testing Used for Gene Set Enrichment Analysis. In: Hahne F, Huber W, Gentleman R, Falcon S, editors. Bioconductor Case Studies. 1st ed. New York: Springer; 2008. p. 207–20.
228. Hu J, Shibata Y, Zhu PP, Voss C, Rismanchi N, Prinz WA, et al. A Class of Dynamin-like GTPases Involved in the Generation of the Tubular ER Network. Cell [Internet]. 2009;138(3):549–61. Available from: <http://dx.doi.org/10.1016/j.cell.2009.05.025>
229. Vijayakrishnapillai LMK, Desmarais JS, Groeschen MN, Perlin MH. Deletion of *ptn1*, a PTEN/TEP1 orthologue, in *Ustilago maydis* reduces pathogenicity and teliospore development. J Fungi. 2019;5(1).
230. Shin ME, Ogburn KD, Varban OA, Gilbert PM, Burd CG. FYVE Domain Targets Pib1p Ubiquitin Ligase to Endosome and Vacuolar Membranes. J Biol Chem. 2001;276(44):41388–93.
231. Foti M, Audhya A, Emr SD. Sac1 lipid phosphatase and Stt4 phosphatidylinositol 4-kinase regulate a pool of phosphatidylinositol 4-phosphate that functions in the control of the actin cytoskeleton and vacuole morphology. Mol Biol Cell. 2001;12(8):2396–411.
232. Baird D, Stefan C, Audhya A, Weys S, Emr SD. Assembly of the PtdIns 4-kinase Stt4 complex at the plasma membrane requires Ypp1 and Efr3. J Cell Biol. 2008;183(6):1061–74.
233. Riquelme M. Tip Growth in Filamentous Fungi: A Road Trip to the Apex. Annu Rev Microbiol. 2013;67(1):587–609.
234. Chesarone M, Gould CJ, Moseley JB, Goode BL. Displacement of Formins from Growing Barbed Ends by Bud14 Is Critical for Actin Cable Architecture and Function. Dev Cell [Internet]. 2009;16(2):292–302. Available from: <http://dx.doi.org/10.1016/j.devcel.2008.12.001>
235. Audhya A, Foti M, Emr SD. Distinct roles for the yeast phosphatidylinositol 4-Kinases, Stt4p and Pik1p, in secretion, cell growth, and organelle membrane dynamics. Mol Biol Cell. 2000;11(8):2673–89.

236. Epp E, Walther A, Lépine G, Leon Z, Mullick A, Raymond M, et al. Forward genetics in *Candida albicans* that reveals the Arp2/3 complex is required for hyphal formation, but not endocytosis. *Mol Microbiol.* 2010;75(5):1182–98.
237. Dienstmann R, Rodon J, Serra V, Tabernero J. Picking the point of inhibition: a comparative review of PI3K/AKT/mTOR pathway inhibitors. *Mol Cancer Ther.* 2014;13(5):1021–31.
238. Ghugtyal V, Garcia-Rodas R, Seminara A, Schaub S, Bassilana M, Arkowitz RA. Phosphatidylinositol-4-phosphate-dependent membrane traffic is critical for fungal filamentous growth. *Proc Natl Acad Sci U S A.* 2015;112(28):8644–9.
239. Heitman J, Sun S, James TY. Evolution of fungal sexual reproduction. *Mycologia.* 2013;105(1):1–27.
240. Dujon B. Yeasts illustrate the molecular mechanisms of eukaryotic genome evolution. *Trends Genet.* 2006;22(7):375–87.
241. Dujon B. Yeast evolutionary genomics. *Nat Rev Genet* [Internet]. 2010 Jul [cited 2014 Mar 24];11(7):512–24. Available from: <http://www.ncbi.nlm.nih.gov/pubmed/20559329>
242. Collins C, Keane TTM, Turner DJ, O’Keeffe G, Fitzpatrick D a, Doyle S. Genomic and proteomic dissection of the ubiquitous plant pathogen, *Armillaria mellea*: toward a new infection model system. *J Proteome Res* [Internet]. 2013;12(6):2552–70. Available from: <http://www.pubmedcentral.nih.gov/articlerender.fcgi?artid=3679558&tool=pmcentrez&rendertype=abstract%5Cnhttp://pubs.acs.org/doi/abs/10.1021/pr301131t>
243. Firrincieli A, Otilar R, Salamov A, Schmutz J, Khan Z, Redman RS, et al. Genome sequence of the plant growth promoting endophytic yeast *Rhodotorula graminis* WP1. *Front Microbiol* [Internet]. 2015 Jan [cited 2016 Feb 19];6:978. Available from: <http://www.ncbi.nlm.nih.gov/pubmed/26441909>
244. Goordial J, Raymond-Bouchard I, Riley R, Ronholm J, Shapiro N, Woyke T, et al. Improved high-quality draft genome sequence of the Eurypsychrophile *Rhodotorula* sp. JG1b, isolated from permafrost in the hyperarid upper-elevation McMurdo dry Valleys, Antarctica. *Genome Announc.* 2016;4(2):e00069-16.
245. Zhu Z, Zhang S, Liu H, Shen H, Lin X, Yang F, et al. A multi-omic map of the lipid-producing yeast *Rhodospiridium toruloides*. *Nat Commun.* 2012;3:1112.
246. Goffeau A, Barrell BG, Bussey H, Davis RW, Dujon B, Feldmann H, et al. Life with 6000 Genes. *Science* (80-). 1996;274(5287):546–67.

247. Ohm RA, De Jong JF, Lugones LG, Aerts A, Kothe E, Stajich JE, et al. Genome sequence of the model mushroom *Schizophyllum commune*. *Nat Biotechnol.* 2010;28(9):957.
248. Rhind N, Chen Z, Yassour M, Thompson DA, Haas BJ, Habib N, et al. Comparative functional genomics of the fission yeasts. *Science.* 2011;1203357.
249. Wood V, Gwilliam R, Rajandream M-A, Lyne M, Lyne R, Stewart A, et al. The genome sequence of *Schizosaccharomyces pombe*. *Nature.* 2002;415(6874):871.
250. Amselem J, Cuomo CA, van Kan JAL, Viaud M, Benito EP, Couloux A, et al. Genomic analysis of the necrotrophic fungal pathogens *Sclerotinia sclerotiorum* and *Botrytis cinerea*. *PLoS Genet [Internet].* 2011 Aug [cited 2016 Feb 19];7(8):e1002230. Available from: <http://journals.plos.org/plosgenetics/article?id=10.1371/journal.pgen.1002230>
251. Eastwood DC, Floudas D, Binder M, Majcherczyk A, Schneider P, Aerts A, et al. The plant cell wall-decomposing machinery underlies the functional diversity of forest fungi. *Science [Internet].* 2011 Aug 5 [cited 2016 Feb 19];333(6043):762–5. Available from: <http://science.sciencemag.org/content/333/6043/762.abstract>
252. Schirawski J, Mannhaupt G, Münch K, Brefort T, Schipper K, Doehlemann G, et al. Pathogenicity determinants in smut fungi revealed by genome comparison. *Science [Internet].* 2010 Dec 10 [cited 2014 Feb 26];330(6010):1546–8. Available from: <http://www.ncbi.nlm.nih.gov/pubmed/21148393>
253. Pan Z, Yang XB, Pivonia S, Xue L, Pasken R, Roads J. Long-Term Prediction of Soybean Rust Entry into the Continental United States. *Plant Dis.* 2006;90(7):840–6.
254. Hane JK, Lowe RGT, Solomon PS, Tan K-C, Schoch CL, Spatafora JW, et al. Dothideomycete plant interactions illuminated by genome sequencing and EST analysis of the wheat pathogen *Stagonospora nodorum*. *Plant Cell [Internet].* 2007 Nov 1 [cited 2016 Feb 19];19(11):3347–68. Available from: <http://www.plantcell.org/content/19/11/3347.abstract>
255. Franco MEE, López S, Medina R, Saparrat MCN, Balatti P. Draft genome sequence and gene annotation of *Stemphylium lycopersici* strain CIDEFI-216. *Genome Announc.* 2015;3(5):e01069-15.
256. Nierman WC, Fedorova-Abrams ND, Andrianopoulos A. Genome sequence of the AIDS-associated pathogen *Penicillium marneffei* (ATCC18224) and its near taxonomic relative *Talaromyces stipitatus* (ATCC10500). *Genome Announc.* 2015;3(1):e01559-14.

257. Cissé OH, Almeida JMGCF, Fonseca A, Kumar AA, Salojärvi J, Overmyer K, et al. Genome sequencing of the plant pathogen *Taphrina deformans*, the causal agent of peach leaf curl. *MBio* [Internet]. 2013 [cited 2016 Aug 23];4(3):e00055-13. Available from: <http://www.ncbi.nlm.nih.gov/pubmed/23631913>
258. Berka RM, Grigoriev I V, Otilar R, Salamov A, Grimwood J, Reid I, et al. Comparative genomic analysis of the thermophilic biomass-degrading fungi *Myceliophthora thermophila* and *Thielavia terrestris*. *Nat Biotechnol*. 2011;29(10):922.
259. Bushley KE, Raja R, Jaiswal P, Cumbie JS, Nonogaki M, Boyd AE, et al. The genome of *Tolypocladium inflatum*: evolution, organization, and expression of the cyclosporin biosynthetic gene cluster. *PLoS Genet*. 2013;9(6):e1003496.
260. Kourist R, Bracharz F, Lorenzen J, Kracht ON, Chovatia M, Daum C, et al. Genomics and Transcriptomics Analyses of the Oil-Accumulating Basidiomycete Yeast *Trichosporon oleaginosus*: Insights into Substrate Utilization and Alternative Evolutionary Trajectories of Fungal Mating Systems. *MBio* [Internet]. 2015 [cited 2016 Aug 23];6(4):e00918. Available from: <http://www.ncbi.nlm.nih.gov/pubmed/26199329>
261. Jourdier E, Baudry L, Poggi-Parodi D, Vicq Y, Koszul R, Margeot A, et al. Proximity ligation scaffolding and comparison of two *Trichoderma reesei* strains genomes. *Biotechnol Biofuels*. 2017;10(1):151.
262. Martin F, Kohler A, Murat C, Balestrini R, Coutinho PM, Jaillon O, et al. Périgord black truffle genome uncovers evolutionary origins and mechanisms of symbiosis. *Nature*. 2010;464(7291):1033.
263. Laurie JD, Ali S, Linning R, Mannhaupt G, Wong P, Güldener U, et al. Genome comparison of barley and maize smut fungi reveals targeted loss of RNA silencing components and species-specific presence of transposable elements. *Plant Cell*. 2012;tpc-112.
264. Yang J, Wang L, Ji X, Feng Y, Li X, Zou C, et al. Genomic and proteomic analyses of the fungus *Arthrobotrys oligospora* provide insights into nematode-trap formation. *PLoS Pathog*. 2011;7(9):e1002179.
265. Kumagai T, Ishii T, Terai G, Umemura M, Machida M, Asai K. Genome sequence of *Ustilaginoidea virens* IPU010, a rice pathogenic fungus causing false smut. *Genome Announc*. 2016;4(3):e00306-16.

266. Deng CH, Plummer KM, Jones DAB, Mesarich CH, Shiller J, Taranto AP, et al. Comparative analysis of the predicted secretomes of Rosaceae scab pathogens *Venturia inaequalis* and *V. pirina* reveals expanded effector families and putative determinants of host range. *BMC Genomics*. 2017;18(1):339.
267. Klosterman SJ, Subbarao K V, Kang S, Veronese P, Gold SE, Thomma BPHJ, et al. Comparative genomics yields insights into niche adaptation of plant vascular wilt pathogens. *PLoS Pathog* [Internet]. 2011 Jul [cited 2016 Jan 21];7(7):e1002137. Available from: <http://journals.plos.org/plospathogens/article?id=10.1371/journal.ppat.1002137>
268. Bao D, Gong M, Zheng H, Chen M, Zhang L, Wang H, et al. Sequencing and comparative analysis of the straw mushroom (*Volvariella volvacea*) genome. *PLoS One* [Internet]. 2013 Jan [cited 2016 Feb 19];8(3):e58294. Available from: <http://journals.plos.org/plosone/article?id=10.1371/journal.pone.0058294>
269. Padamsee M, Kumar TKA, Riley R, Binder M, Boyd A, Calvo AM, et al. The genome of the xerotolerant mold *Wallemia sebi* reveals adaptations to osmotic stress and suggests cryptic sexual reproduction. *Fungal Genet Biol* [Internet]. 2012 Mar [cited 2014 Jan 24];49(3):217–26. Available from: <http://www.ncbi.nlm.nih.gov/pubmed/22326418>
270. Gazis R, Kuo A, Riley R, LaButti K, Lipzen A, Lin J, et al. The genome of *Xylona heveae* provides a window into fungal endophytism. *Fungal Biol*. 2016;120(1):26–42.
271. Souciet J-L, Dujon B, Gaillardin C, Johnston M, Baret P V, Cliften P, et al. Comparative genomics of protoploid Saccharomycetaceae. *Genome Res*. 2009;
272. Grandaubert J, Bhattacharyya A, Stukenbrock EH. RNA-seq based gene annotation and comparative genomics of four fungal grass pathogens in the genus *Zymoseptoria* identify novel orphan genes and species-specific invasions of transposable elements. *G3 Genes, Genomes, Genet*. 2015;g3-115.
273. Dietrich FS, Voegeli S, Brachat S, Lerch A, Gates K, Steiner S, et al. The *Ashbya gossypii* genome as a tool for mapping the ancient *Saccharomyces cerevisiae* genome. *Science*. 2004;304(5668):304–7.
274. Kunze G, Gaillardin C, Czernicka M, Durrens P, Martin T, Böer E, et al. The complete genome of *Blastobotrys (Arxula) adenivorans* LS3-a yeast of biotechnological interest. *Biotechnol Biofuels*. 2014;7(1):66.

275. Verma S, Gazara RK, Nizam S, Parween S, Chattopadhyay D, Verma PK. Draft genome sequencing and secretome analysis of fungal phytopathogen *Ascochyta rabiei* provides insight into the necrotrophic effector repertoire. *Sci Rep*. 2016;6:24638.
276. Riley R, Haridas S, Wolfe KH, Lopes MR, Hittinger CT, Göker M, et al. Comparative genomics of biotechnologically important yeasts. *Proc Natl Acad Sci [Internet]*. 2016;113(35):9882–7. Available from: <http://www.pnas.org/lookup/doi/10.1073/pnas.1603941113>
277. Gianoulis TA, Griffin MA, Spakowicz DJ, Dunican BF, Sboner A, Sismour AM, et al. Genomic analysis of the hydrocarbon-producing, cellulolytic, endophytic fungus *Ascocoryne sarcoides*. *PLoS Genet*. 2012;8(3):e1002558.
278. de Vries RP, Riley R, Wiebenga A, Aguilar-Osorio G, Amillis S, Uchima CA, et al. Comparative genomics reveals high biological diversity and specific adaptations in the industrially and medically important fungal genus *Aspergillus*. [Internet]. Vol. 18, *Genome biology*. 2017. 28 p. Available from: <http://www.ncbi.nlm.nih.gov/pubmed/28196534> <http://www.pubmedcentral.nih.gov/articlerender.fcgi?artid=PMC5307856>
279. Moore GG, Mack BM, Beltz SB, Gilbert MK. Draft genome sequence of an aflatoxigenic *Aspergillus* species, *A. bombycis*. *Genome Biol Evol*. 2016;8(11):3297–300.
280. Arnaud MB, Cerqueira GC, Inglis DO, Skrzypek MS, Binkley J, Chibucos MC, et al. The *Aspergillus* Genome Database (AspGD): recent developments in comprehensive multispecies curation, comparative genomics and community resources. *Nucleic Acids Res*. 2011;40(D1):D653–9.
281. Fedorova ND, Khaldi N, Joardar VS, Maiti R, Amedeo P, Anderson MJ, et al. Genomic islands in the pathogenic filamentous fungus *Aspergillus fumigatus*. *PLoS Genet*. 2008;4(4):e1000046.
282. Gostinčar C, Ohm RA, Kogej T, Sonjak S, Turk M, Zajc J, et al. Genome sequencing of four *Aureobasidium pullulans* varieties: biotechnological potential, stress tolerance, and description of new species. *BMC Genomics*. 2014;15(1):549.
283. Ohm RA, Feau N, Henrissat B, Schoch CL, Horwitz BA, Barry KW, et al. Diverse lifestyles and strategies of plant pathogenesis encoded in the genomes of eighteen Dothideomycetes fungi. *PLoS Pathog*. 2012;8(12):e1003037.

284. Xiao G, Ying S-H, Zheng P, Wang Z-L, Zhang S, Xie X-Q, et al. Genomic perspectives on the evolution of fungal entomopathogenicity in *Beauveria bassiana*. *Sci Rep*. 2012;2:483.
285. Muñoz JF, Gauthier GM, Desjardins CA, Gallo JE, Holder J, Sullivan TD, et al. The dynamic genome and transcriptome of the human fungal pathogen *Blastomyces* and close relative *Emmonsia*. *PLoS Genet*. 2015;11(10):e1005493.
286. Spanu P, Kämper J. Genomics of biotrophy in fungi and oomycetes--emerging patterns. *Curr Opin Plant Biol* [Internet]. 2010 Aug [cited 2014 Mar 20];13(4):409–14. Available from: <http://www.ncbi.nlm.nih.gov/pubmed/20430688>
287. Staats M, van Kan J a L. Genome update of *Botrytis cinerea* strains B05.10 and T4. *Eukaryot Cell*. 2012;11(11):1413–4.
288. Oka T, Ekino K, Fukuda K, Nomura Y. Draft genome sequence of the formaldehyde-resistant fungus *Byssochlamys spectabilis* no. 5 (anamorph *Paecilomyces variotii* no. 5)(NBRC109023). *Genome Announc*. 2014;2(1):e01162-13.
289. Nagy LG, Riley R, Tritt A, Adam C, Daum C, Floudas D, et al. Comparative Genomics of Early-Diverging Mushroom-Forming Fungi Provides Insights into the Origins of Lignocellulose Decay Capabilities. *Mol Biol Evol* [Internet]. 2015 Dec 10 [cited 2016 Feb 18];msv337. Available from: <http://mbe.oxfordjournals.org/content/early/2016/01/20/molbev.msv337.full>
290. Jones T, Federspiel NA, Chibana H, Dungan J, Kalman S, Magee BB, et al. The diploid genome sequence of *Candida albicans*. *Proc Natl Acad Sci*. 2004;101(19):7329–34.
291. Wohlbach DJ, Kuo A, Sato TK, Potts KM, Salamov AA, LaButti KM, et al. Comparative genomics of xylose-fermenting fungi for enhanced biofuel production. *Proc Natl Acad Sci* [Internet]. 2011 Aug 9;108(32):13212 LP – 13217. Available from: <http://www.pnas.org/content/108/32/13212.abstract>
292. Teixeira M de M, Moreno LF, Stielow BJ, Muszewska A, Hainaut M, Gonzaga L, et al. Exploring the genomic diversity of black yeasts and relatives (Chaetothyriales, Ascomycota). *Stud Mycol*. 2017;86:1–28.
293. Peter M, Kohler A, Ohm RA, Kuo A, Krützmann J, Morin E, et al. Ectomycorrhizal ecology is imprinted in the genome of the dominant symbiotic fungus *Cenococcum geophilum*. *Nat Commun*. 2016;7:12662.

294. Fernandez-Fueyo E, Ruiz-Dueñas FJ, Ferreira P, Floudas D, Hibbett DS, Canessa P, et al. Comparative genomics of *Ceriporiopsis subvermispora* and *Phanerochaete chrysosporium* provide insight into selective ligninolysis. *Proc Natl Acad Sci*. 2012;109(14):5458–63.
295. Cuomo CA, Untereiner WA, Ma L-J, Grabherr M, Birren BW. Draft genome sequence of the cellulolytic fungus *Chaetomium globosum*. *Genome Announc*. 2015;3(1):e00021-15.
296. De Wit PJGM, Van Der Burgt A, Ökmen B, Stergiopoulos I, Abd-Elsalam KA, Aerts AL, et al. The genomes of the fungal plant pathogens *Cladosporium fulvum* and *Dothistroma septosporum* reveal adaptation to different hosts and lifestyles but also signatures of common ancestry. *PLoS Genet*. 2012;8(11):e1003088.
297. Butler G, Rasmussen MD, Lin MF, Santos MAS, Sakthikumar S, Munro CA, et al. Evolution of pathogenicity and sexual reproduction in eight *Candida* genomes. *Nature*. 2009;459(7247):657.
298. Condon BJ, Leng Y, Wu D, Bushley KE, Ohm RA, Otiillar R, et al. Comparative genome structure, secondary metabolite, and effector coding capacity across *Cochliobolus* pathogens. *PLoS Genet*. 2013;9(1):e1003233.
299. Sharpton TJ, Stajich JE, Rounsley SD, Gardner MJ, Wortman JR, Jordar VS, et al. Comparative genomic analyses of the human fungal pathogens *Coccidioides* and their relatives. *Genome Res* [Internet]. 2009 Oct [cited 2016 Aug 23];19(10):1722–31. Available from: <http://www.ncbi.nlm.nih.gov/pubmed/19717792>
300. O’Connell RJ, Thon MR, Hacquard S, Amyotte SG, Kleemann J, Torres MF, et al. Lifestyle transitions in plant pathogenic *Colletotrichum* fungi deciphered by genome and transcriptome analyses. *Nat Genet*. 2012;44(9):1060.
301. Mondo SJ, Dannebaum RO, Kuo RC, Louie KB, Bewick AJ, LaButti K, et al. Widespread adenine N6-methylation of active genes in fungi. *Nat Genet*. 2017;49(6):964.
302. Jiménez DJ, Hector RE, Riley R, Lipzen A, Kuo RC, Amirebrahimi M, et al. Draft genome sequence of *Coniochaeta ligniaria* NRRL 30616, a lignocellulolytic fungus for bioabatement of inhibitors in plant biomass hydrolysates. *Genome Announc*. 2017;5(4):e01476-16.
303. Floudas D, Binder M, Riley R, Barry K, Blanchette R a., Henrissat B, et al. The Paleozoic Origin of Enzymatic Lignin Decomposition Reconstructed from 31 Fungal Genomes. *Science* (80-). 2012;336(6089):1715–9.

304. Muraguchi H, Umezawa K, Niikura M, Yoshida M, Kozaki T, Ishii K, et al. Strand-specific RNA-seq analyses of fruiting body development in *Coprinopsis cinerea*. PLoS One. 2015;10(10):e0141586.
305. Zheng P, Xia Y, Xiao G, Xiong C, Hu X, Zhang S, et al. Genome sequence of the insect pathogenic fungus *Cordyceps militaris*, a valued traditional Chinese medicine. Genome Biol. 2012;12(11):R116.
306. Pendleton AL, Smith KE, Feau N, Martin FM, Grigoriev I V, Hamelin R, et al. Duplications and losses in gene families of rust pathogens highlight putative effectors. Front Plant Sci. 2014;5:299.
307. Loftus BJ, Fung E, Roncaglia P, Rowley D, Amedeo P, Bruno D, et al. The genome of the basidiomycetous yeast and human pathogen *Cryptococcus neoformans*. Science. 2005;307:1321-4.
308. Wu W, Davis RW, Tran-Gyamfi MB, Kuo A, LaButti K, Mihaltcheva S, et al. Characterization of four endophytic fungi as potential consolidated bioprocessing hosts for conversion of lignocellulose into advanced biofuels. Appl Microbiol Biotechnol. 2017;101(6):2603–18.
309. Sacerdot C, Casaregola S, Lafontaine I, Tekaiia F, Dujon B, Ozier-Kalogeropoulos O. Promiscuous DNA in the nuclear genomes of hemiascomycetous yeasts. FEMS Yeast Res. 2008;8(6):846–57.
310. Piškur J, Ling Z, Marcet-Houben M, Ishchuk OP, Aerts A, LaButti K, et al. The genome of wine yeast *Dekkera bruxellensis* provides a tool to explore its food-related properties. Int J Food Microbiol. 2012;157(2):202–9.
311. Morales-Cruz A, Amrine KCH, Blanco-Ulate B, Lawrence DP, Travadon R, Rolshausen PE, et al. Distinctive expansion of gene families associated with plant cell wall degradation, secondary metabolism, and nutrient uptake in the genomes of grapevine trunk pathogens. BMC Genomics. 2015;16(1):469.
312. Mosier AC, Miller CS, Frischkorn KR, Ohm RA, Li Z, LaButti K, et al. Fungi contribute critical but spatially varying roles in nitrogen and carbon cycling in acid mine drainage. Front Microbiol. 2016;7:238.
313. Bininda-Emonds ORP, Cardillo M, Jones KE, Macphee RDE, Beck RMD, Grenyer R, et al. The delayed rise of present-day mammals. Nature. 2007;446(March):507–12.

314. Jones L, Riaz S, Morales-Cruz A, Amrine KCH, McGuire B, Gubler WD, et al. Adaptive genomic structural variation in the grape powdery mildew pathogen, *Erysiphe necator*. *BMC Genomics*. 2014;15(1):1081.
315. Tang JD, Perkins AD, Sonstegard TS, Schroeder SG, Burgess SC, Diehl S V. Short-read sequencing for genomic analysis of the brown rot fungus *Fibroporia radiculosa*. *Appl Environ Microbiol* [Internet]. 2012 Apr [cited 2016 Aug 23];78(7):2272–81. Available from: <http://www.ncbi.nlm.nih.gov/pubmed/22247176>
316. Costa FF, de Hoog S, Raittz RT, Weiss VA, Leão ACR, Bombassaro A, et al. Draft genome sequence of *Fonsecaea nubica* strain CBS 269.64, causative agent of human chromoblastomycosis. *Genome Announc*. 2016;4(4):e00735-16.
317. Cuomo CA, Güldener U, Xu J-R, Trail F, Turgeon BG, Di Pietro A, et al. The *Fusarium graminearum* genome reveals a link between localized polymorphism and pathogen specialization. *Science* [Internet]. 2007 Sep 7 [cited 2015 Dec 24];317(5843):1400–2. Available from: <http://science.sciencemag.org/content/317/5843/1400.abstract>
318. Ma L-J, Van Der Does HC, Borkovich KA, Coleman JJ, Daboussi M-J, Di Pietro A, et al. Comparative genomics reveals mobile pathogenicity chromosomes in *Fusarium*. *Nature*. 2010;464(7287):367.
319. Okagaki LH, Nunes CC, Sailsbery J, Clay B, Brown D, John T, et al. Genome sequences of three phytopathogenic species of the Magnaporthaceae family of fungi. *G3 Genes, Genomes, Genet*. 2015;g3-115.
320. Chen L, Yue Q, Zhang X, Xiang M, Wang C, Li S, et al. Genomics-driven discovery of the pneumocandin biosynthetic gene cluster in the fungus *Glarea lozoyensis*. *BMC Genomics*. 2013;14(1):339.
321. DiGuistini S, Wang Y, Liao NY, Taylor G, Tanguay P, Feau N, et al. Genome and transcriptome analyses of the mountain pine beetle-fungal symbiont *Grosmannia clavigera*, a lodgepole pine pathogen. *Proc Natl Acad Sci*. 2011;201011289.
322. Olson Å, Aerts A, Asiegbu F, Belbahri L, Bouzid O, Broberg A, et al. Insight into trade-off between wood decay and parasitism from the genome of a fungal forest pathogen. *New Phytol*. 2012;194(4):1001–13.

323. Terfehr D, Dahlmann TA, Specht T, Zadra I, Kürsteiner H, Kück U. Genome sequence and annotation of *Acremonium chrysogenum*, producer of the β -lactam antibiotic cephalosporin C. *Genome Announc.* 2014;2(5):e00948-14.
324. Lenassi M, Gostinčar C, Jackman S, Turk M, Sadowski I, Nislow C, et al. Whole genome duplication and enrichment of metal cation transporters revealed by de novo genome sequencing of extremely halotolerant black yeast *Hortaea werneckii*. *PLoS One.* 2013;8(8):e71328.
325. Gordon JL, Armisén D, Proux-Wéra E, ÓhÉigeartaigh SS, Byrne KP, Wolfe KH. Evolutionary erosion of yeast sex chromosomes by mating-type switching accidents. *Proc Natl Acad Sci.* 2011;108(50):20024–9.
326. Dujon B, Sherman D, Fischer G, Durrens P, Casaregola S, Lafontaine I, et al. Genome evolution in yeasts. *Nature.* 2004;430(6995):35.
327. Morales L, Noel B, Porcel B, Marcet-Houben M, Hullo M-F, Sacerdot C, et al. Complete DNA sequence of *Kuraishia capsulata* illustrates novel genomic features among budding yeasts (Saccharomycotina). *Genome Biol Evol.* 2013;5(12):2524–39.
328. Martin F, Aerts A, Ahrén D, Brun A, Danchin EGJ, Duchaussoy F, et al. The genome of *Laccaria bicolor* provides insights into mycorrhizal symbiosis. *Nature* [Internet]. 2008 Mar 6 [cited 2016 Feb 20];452(7183):88–92. Available from: <http://dx.doi.org/10.1038/nature06556>
329. Islam MS, Haque MS, Islam MM, Emdad EM, Halim A, Hossen QMM, et al. Tools to kill: genome of one of the most destructive plant pathogenic fungi *Macrophomina phaseolina*. *BMC Genomics.* 2012;13(1):493.
330. Dean RA, Talbot NJ, Ebbole DJ, Farman ML, Mitchell TK, Orbach MJ, et al. The genome sequence of the rice blast fungus *Magnaporthe grisea*. *Nature* [Internet]. 2005 Apr 21 [cited 2015 Dec 24];434(7036):980–6. Available from: <http://dx.doi.org/10.1038/nature03449>
331. Xu J, Saunders CW, Hu P, Grant R a, Boekhout T, Kuramae EE, et al. Dandruff-associated *Malassezia* genomes reveal convergent and divergent virulence traits shared with plant and human fungal pathogens. *Proc Natl Acad Sci U S A* [Internet]. 2007 Nov 20;104(47):18730–5. Available from: <http://www.pubmedcentral.nih.gov/articlerender.fcgi?artid=2141845&tool=pmcentrez&rendertype=abstract>

332. Gioti A, Nystedt B, Li W. Genomic Insights into the Atopic Eczema-Associated Skin Commensal Yeast *Malassezia sympodialis*. *MBio*. 2013;4(1):1–16.
333. Zhu S, Cao Y-Z, Jiang C, Tan B-Y, Wang Z, Feng S, et al. Sequencing the genome of *Marssonina brunnea* reveals fungus-poplar co-evolution. *BMC Genomics*. 2012;13(1):382.
334. Zeiner CA, Purvine SO, Zink EM, Paša-Tolić L, Chaput DL, Haridas S, et al. Comparative analysis of secretome profiles of manganese (II)-oxidizing Ascomycete fungi. *PLoS One*. 2016;11(7):e0157844.
335. Nemri A, Saunders DGO, Anderson C, Upadhyaya NM, Win J, Lawrence G, et al. The genome sequence and effector complement of the flax rust pathogen *Melampsora lini*. *Front Plant Sci*. 2014;5:98.
336. Gao Q, Jin K, Ying S-H, Zhang Y, Xiao G, Shang Y, et al. Genome sequencing and comparative transcriptomics of the model entomopathogenic fungi *Metarhizium anisopliae* and *M. acridum*. *PLoS Genet*. 2011;7(1):e1001264.
337. Goodwin SB, M'barek S Ben, Dhillon B, Wittenberg AHJ, Crane CF, Hane JK, et al. Finished genome of the fungal wheat pathogen *Mycosphaerella graminicola* reveals dispensome structure, chromosome plasticity, and stealth pathogenesis. *PLoS Genet* [Internet]. 2011 Jun [cited 2016 Aug 23];7(6):e1002070. Available from: <http://www.ncbi.nlm.nih.gov/pubmed/21695235>
338. Martinez DA, Oliver BG, Gräser Y, Goldberg JM, Li W, Martinez-Rossi NM, et al. Comparative genome analysis of *Trichophyton rubrum* and related dermatophytes reveals candidate genes involved in infection. *MBio* [Internet]. 2012 [cited 2016 Aug 23];3(5):e00259-12. Available from: <http://www.ncbi.nlm.nih.gov/pubmed/22951933>
339. Perlin MH, Amselem J, Fontanillas E, Toh SS, Chen Z, Goldberg J, et al. Sex and parasites: genomic and transcriptomic analysis of *Microbotryum lychnidis-dioicae*, the biotrophic and plant-castrating anther smut fungus. *BMC Genomics* [Internet]. 2015;16(1):461. Available from: <http://www.biomedcentral.com/1471-2164/16/461>
340. Toome M, Ohm RA, Riley RW, James TY, Lazarus KL, Henrissat B, et al. Genome sequencing provides insight into the reproductive biology, nutritional mode and ploidy of the fern pathogen *Mixia osmundae*. *New Phytol* [Internet]. 2014 Dec 1;202:554–64. Available from: <http://dx.doi.org/10.1111/nph.12653>

341. Lorenz S, Guenther M, Grumaz C, Rupp S, Zibek S, Sohn K. Genome sequence of the basidiomycetous fungus *Pseudozyma aphidis* DSM70725, an efficient producer of biosurfactant mannosylerythritol lipids. *Genome Announc.* 2014;2(1):e00053-14.
342. Gabaldón T, Martin T, Marcet-Houben M, Durrens P, Bolotin-Fukuhara M, Lespinet O, et al. Comparative genomics of emerging pathogens in the *Candida glabrata* clade. *BMC Genomics.* 2013;14(1):623.
343. Galagan JE, Calvo SE, Borkovich KA, Selker EU, Read ND, Jaffe D, et al. The genome sequence of the filamentous fungus *Neurospora crassa*. *Nature* [Internet]. 2003 Apr 24 [cited 2016 Aug 23];422(6934):859–68. Available from: <http://www.ncbi.nlm.nih.gov/pubmed/12712197>
344. Desjardins CA, Champion MD, Holder JW, Muszewska A, Goldberg J, Bailão AM, et al. Comparative genomic analysis of human fungal pathogens causing paracoccidioidomycosis. *PLoS Genet.* 2011;7(10):e1002345.
345. Kohler A, Kuo A, Nagy LG, Morin E, Barry KW, Buscot F, et al. Convergent losses of decay mechanisms and rapid turnover of symbiosis genes in mycorrhizal mutualists. *Nat Genet* [Internet]. 2015 Apr [cited 2016 Feb 11];47(4):410–5. Available from: <http://dx.doi.org/10.1038/ng.3223>
346. Van Den Berg MA, Albang R, Albermann K, Badger JH, Daran J-M, Driessen AJM, et al. Genome sequencing and analysis of the filamentous fungus *Penicillium chrysogenum*. *Nat Biotechnol.* 2008;26(10):1161.
347. Banani H, Marcet-Houben M, Ballester A-R, Abbruscato P, González-Candelas L, Gabaldón T, et al. Genome sequencing and secondary metabolism of the postharvest pathogen *Penicillium griseofulvum*. *BMC Genomics.* 2016;17(1):19.
348. Nielsen JC, Grijseels S, Prigent S, Ji B, Dainat J, Nielsen KF, et al. Global analysis of biosynthetic gene clusters reveals vast potential of secondary metabolite production in *Penicillium* species. *Nat Microbiol* [Internet]. 2017 Apr 3;2:17044. Available from: <https://doi.org/10.1038/nmicrobiol.2017.44>
349. Blanco-Ulate B, Rolshausen P, Cantu D. Draft genome sequence of the ascomycete *Phaeoacremonium aleophilum* strain UCR-PA7, a causal agent of the esca disease complex in grapevines. *Genome Announc.* 2013;1(3):e00390-13.

350. Suzuki H, MacDonald J, Syed K, Salamov A, Hori C, Aerts A, et al. Comparative genomics of the white-rot fungi, *Phanerochaete carnosus* and *P. chrysosporium*, to elucidate the genetic basis of the distinct wood types they colonize. *BMC Genomics* [Internet]. 2012 Jan 2 [cited 2016 Feb 2];13(1):444. Available from: <http://bmcgenomics.biomedcentral.com/articles/10.1186/1471-2164-13-444>
351. Walker AK, Frasz SL, Seifert KA, Miller JD, Mondo SJ, LaButti K, et al. Full genome of *Phialocephala scopiformis* DAOMC 229536, a fungal endophyte of spruce producing the potent anti-insectan compound rugulosin. *Genome Announc.* 2016;4(1):e01768-15.
352. Binder M, Justo A, Riley R, Salamov A, Lopez-Giraldez F, Sjökvist E, et al. Phylogenetic and phylogenomic overview of the Polyporales. *Mycologia* [Internet]. 2013;105(6):1350–73. Available from: <http://www.ncbi.nlm.nih.gov/pubmed/23935031>
353. De Schutter K, Lin Y-C, Tiels P, Van Hecke A, Glinka S, Weber-Lehmann J, et al. Genome sequence of the recombinant protein production host *Pichia pastoris*. *Nat Biotechnol.* 2009;27(6):561.
354. Zuccaro A, Lahrmann U, Güldener U, Langen G, Pfiffi S, Biedenkopf D, et al. Endophytic Life Strategies Decoded by Genome and Transcriptome Analyses of the Mutualistic Root Symbiont *Piriformospora indica*. Howlett BJ, editor. *PLoS Pathog* [Internet]. 2011 Oct 13 [cited 2016 Aug 23];7(10):e1002290. Available from: <http://dx.plos.org/10.1371/journal.ppat.1002290>
355. Cissé OH, Pagni M, Hauser PM. De novo assembly of the *Pneumocystis jirovecii* genome from a single bronchoalveolar lavage fluid specimen from a patient. *MBio.* 2013;4(1):e00428-12.
356. Martino E, Morin E, Grelet G, Kuo A, Kohler A, Daghino S, et al. Comparative genomics and transcriptomics depict ericoid mycorrhizal fungi as versatile saprotrophs and plant mutualists. *New Phytol.* 2018;217(3):1213–29.
357. Espagne E, Lespinet O, Malagnac F, Da Silva C, Jaillon O, Porcel BM, et al. The genome sequence of the model ascomycete fungus *Podospora anserina*. *Genome Biol.* 2008;9(5):R77.
358. Morita T, Koike H, Koyama Y, Hagiwara H, Ito E, Fukuoka T, et al. Genome sequence of the basidiomycetous yeast *Pseudozyma antarctica* T-34, a producer of the glycolipid biosurfactants mannosylerythritol lipids. *Genome Announc.* 2013;1(2):e00064-13.

359. Konishi M, Hatada Y, Horiuchi J-I. Draft Genome Sequence of the Basidiomycetous Yeast-Like Fungus *Pseudozyma hubeiensis* SY62, Which Produces an Abundant Amount of the Biosurfactant Mannosylerythritol Lipids. *Genome Announc* [Internet]. 2013;1(4):e00409-13. Available from: <http://genomea.asm.org/content/1/4/e00409-13.full>
360. Drees KP, Palmer JM, Sebra R, Lorch JM, Chen C, Wu C-C, et al. Use of multiple sequencing technologies to produce a high-quality genome of the fungus *Pseudogymnoascus destructans*, the causative agent of bat white-nose syndrome. *Genome Announc*. 2016;4(3):e00445-16.
361. Jeffries TW, Grigoriev I V, Grimwood J, Laplaza JM, Aerts A, Salamov A, et al. Genome sequence of the lignocellulose-bioconverting and xylose-fermenting yeast *Pichia stipitis*. *Nat Biotechnol* [Internet]. 2007 Mar 4;25:319. Available from: <http://dx.doi.org/10.1038/nbt1290>
362. Duplessis S, Cuomo C a., Lin Y-C, Aerts A, Tisserant E, Veneault-Fourrey C. Obligate biotrophy features unraveled by the genomic analysis of rust fungi. *Proc Natl Acad Sci U S A*. 2011;108(22):9166–71.
363. Cuomo CA, Bakkeren G, Khalil HB, Panwar V, Joly D, Linning R, et al. Comparative analysis highlights variable genome content of wheat rusts and divergence of the mating loci. *G3 Genes, Genomes, Genet*. 2017;7(2):361–76.
364. Ellwood SR, Liu Z, Syme RA, Lai Z, Hane JK, Keiper F, et al. A first genome assembly of the barley fungal pathogen *Pyrenophora teres* f. *teres*. *Genome Biol*. 2010;11(11):R109.
365. Wibberg D, Jelonek L, Rupp O, Hennig M, Eikmeyer F, Goesmann A, et al. Establishment and interpretation of the genome sequence of the phytopathogenic fungus *Rhizoctonia solani* AG1-IB isolate 7/3/14. *J Biotechnol* [Internet]. 2013 Aug 20 [cited 2016 Feb 19];167(2):142–55. Available from: <http://www.sciencedirect.com/science/article/pii/S0168165612007584>
366. Mujic AB, Kuo A, Tritt A, Lipzen A, Chen C, Johnson J, et al. Comparative Genomics of the Ectomycorrhizal Sister Species *Rhizopogon vinicolor* and *Rhizopogon vesiculosus* (Basidiomycota: Boletales) Reveals a Divergence of the Mating Type B Locus. *G3 Genes, Genomes, Genet*. 2017;g3-117.
367. Oksanen J, Blanchet FG, Kindt R, Legendre P, Minchin PR, O'hara RB, et al. Package 'vegan.' Vol. 2, Community ecology package, version. 2013.

368. Fox J, Weisberg S. Multivariate linear models in R. 2nd ed. An R Companion to Applied Regression. Thousand Oaks, California: Sage publications; 2011.
369. Signorell A. DescTools: Tools for descriptive statistics. Vol. 18, R package version 0.99. 2016.
370. De Caceres M, Jansen F. Package 'indicspecies'. Relationship between species and groups of sites [Internet]. 2016. Available from: <ftp://r-project.org/pub/R/web/packages/indicspecies/indicspecies.pdf>
371. Revell LJ. phytools: an R package for phylogenetic comparative biology (and other things). *Methods Ecol Evol.* 2012;3(2):217–23.
372. Duf rene M, Legendre P. Species assemblages and indicator species: the need for a flexible asymmetrical approach. *Ecol Monogr.* 1997;67(3):345–66.
373. Elliott TA, Gregory TR. What’s in a genome? The C-value enigma and the evolution of eukaryotic genome content. *Philos Trans R Soc B Biol Sci.* 2015;370(1678).
374. Shinohara ML, Correa A, Bell-Pedersen D, Dunlap JC, Loros JJ. *Neurospora* clock-controlled gene 9 (ccg-9) encodes trehalose synthase: Circadian regulation of stress responses and development. *Eukaryot Cell.* 2002;1(1):33–43.
375. Lee BN, Adams TH. The *Aspergillus nidulans* fluG gene is required for production of an extracellular developmental signal and is related to prokaryotic glutamine synthetase I. *Genes Dev.* 1994;8(6):641–51.
376. D’Souza CA, Lee BN, Adams TH. Characterization of the role of the FluG protein in asexual development of *Aspergillus nidulans*. *Genetics.* 2001;158(3):1027–36.
377. Tudzynski P, Heller J, Siegmund U. Reactive oxygen species generation in fungal development and pathogenesis. *Curr Opin Microbiol* [Internet]. 2012;15(6):653–9. Available from: <http://dx.doi.org/10.1016/j.mib.2012.10.002>
378. Takemoto D, Tanaka A, Scott B. NADPH oxidases in fungi: Diverse roles of reactive oxygen species in fungal cellular differentiation. *Fungal Genet Biol.* 2007;44(11):1065–76.

VITA

Teeratas Kijpornyongpan, with the nickname ‘Tas’, was born and raised in Bangkok, Thailand. He has his original name as Jatuporn Wanichanont before changing to the current name in 2012. His interest in Biology was ignited when he joined the National Biology Olympiad in 2007, and then the 20th International Biology Olympiad at Tsukuba, Japan in 2009. After that, he received a long-term scholarship under the Development and Promotion of Science and Technology Talents project (DPST), supported by the Ministry of Education, to study up to a doctoral degree. During his undergraduate degree at Chulalongkorn University, he allowed himself to expose to various research areas. One of these included an undergraduate research project in Cancer Biology, which Tas got his paper published one year after the completion of the project. Another was an intern experience with Dr. Daniel J. Ebbole at Texas A&M University. This makes Tas confirm his own interest in fungi. After finishing his B.S. in Biology in 2013, he received the Anandamahidol foundation scholarship under the Royal Patronage of King Bhumibol Adulyadej, who passed away in 2016. He came to Purdue University in Fall 2013 as a M.S. student in the Dr. Cathie Aime’s lab. His M.S. research project focused on systematics and phylogenomics of smut fungi. He then continued working with Dr. Aime for his doctoral degree in Fall 2015, with a shifted interest to fungal cell biology and genomics. Throughout Tas’ graduate program, he published six research articles—four of these he served as the first author. Outside a lab bench (or a computer bench), he enjoys cooking and photographing. If a week-long vacation is available, he loves exploring United States with his road trip folks.

PUBLICATIONS

Aime MC, **Kijpornyongpan T**, Abbasi M, Wood KR, Flynn T. A new species of *Cintractiella* (Ustilaginales) from the volcanic island of Kosrae, Caroline Islands, Micronesia. *MycKeys*. 2018;42:1–6.

Kijpornyongpan T, Aime MC. Rare or rarely detected? *Ceraceosorus guamensis* sp. nov.: a second described species of Ceraceosorales and the potential for underdetection of rare lineages with common sampling techniques. *Antonie Van Leeuwenhoek*. 2016;109:1127–39.

Kijpornyongpan T, Aime MC. Taxonomic revisions in the Microstromatales: two new yeast species, two new genera, and validation of *Jaminaea* and two *Sympodiomyopsis* species. *Mycol Prog*. 2017;16(5):495–505.

Kijpornyongpan T, Mondo SJ, Barry K, Sandor L, Lee J, Lipzen A, et al. Broad Genomic Sampling Reveals a Smut Pathogenic Ancestry of the Fungal Clade Ustilaginomycotina. *Mol Biol Evol*. 2018;35(8):1840–54.

Kijpornyongpan T, Urbina H, Suh SO, Luangsa-Ard J, Aime MC, Blackwell M. The *Suhomyces* clade: From single isolate to multiple species to disintegrating sex loci. *FEMS Yeast Res*. 2019;19(2):1–15.

Prasanna AN, Gerber D, **Kijpornyongpan T**, Aime MC, Doyle VP, Nagy LG. Model Choice, Missing Data and Taxon Sampling Impact Phylogenomic Inference of Deep Basidiomycota Relationships. *Syst Biol*. *in press*.